

國立臺灣大學工學院高分子科學與工程學研究所

博士論文

Institute of Polymer Science and Engineering

College of Engineering

National Taiwan University

Doctoral Dissertation

幾何形態影響分散因子之通則性

Generalization of Geometric-Shape Inhomogeneity Factor  
for Dispersion

研究生：藍伊奮

Graduated Student: Yi-Fen Lan

指導教授：林江珍 教授

Advisor: Jiang-Jen Lin, Professor

中華民國 99 年 10 月

October, 2010

國立臺灣大學博士學位論文口試委員會審定書

國立臺灣大學博士學位論文  
口試委員會審定書

幾何形態影響分散因子之通則性  
Generalization of Geometric-Shape Inhomogeneity Factor  
for Dispersion

本論文係藍伊奮君（學號: d95549006）在國立臺灣大學高分子科學與工程學研究所完成之博士學位論文，於民國 99 年 10 月 27 日承下列考試委員審查通過及口試及格，特此證明

口試委員：

林江珍

（簽名）

（指導教授）

謝國煌

蕭見超

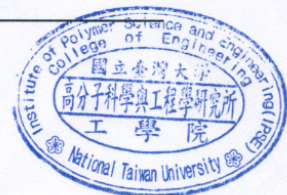
李榮和

邱文英

系主任、所長

陳文章

（簽名）



---

---

## 謝 誌

---

---

我由衷感謝指導老師 林江珍 教授六年的辛苦栽培與指導，在我迷惘困惑之際，老師總以包容的態度與深遠的思維引領我，讓我能夠順利完成學業之路。老師的中心思想：**認真、精緻、前瞻**，是學生這一輩子最受用不盡的六字箴言。

感謝實驗室的學長(曾峰柏、魏寬良、劉唐豪、莊宗原、陳育民、黃智楷、辜政修、劉增達、陳建清、劉耕硯、李坤穆、呂志鋒、詹英楠、邱智璋、許彥琦、余明宏、張裕忠、蘇嘉榮、羅偉舜、黃亭凱、劉天民)以及學姊(李姿蓓)在研究上的協助、感謝同儕(蔣明立、魏郡菽、方彥文、董睿軒)生活上的陪伴、感謝學弟(謝璧任、邱昭諭、廖一驊、許昭博、陳威廷)以及學妹(蘇佑安、林筱筑、張文馨、許如秀、王雅琪、梁凱玲、顏于婷)在實驗上的幫忙，感謝研究助理(吳月仙老師、許譯內、蔡美安、洪鈺惠)在實驗與行政作業上的協助安排。

感謝工研院先進(李宗銘主任、邱國展組長、李巡天、廖如仕、田宏隆、呂奇明、胡志明、林慈婷、陳凱琪、黃淑娟組長、張信真組長)在研究材料的提供與分析上的協助，感謝中國石油煉研所的先進(何永盛、王逸萍、張行)提升我的報告歷練。

感謝口試委員，中正化工蔣見超教授、台大高分子謝國煌教授、台大高分子邱文英教授、中興化工李榮和教授，對本論文的諸多寶貴建議及指正，在此致上十二萬分的謝意。感謝高分子所辦公室學長姊(陳玉岱、高千惠、謝明國)在學務上的協助。

感謝我多年的好友楊勝恩、林政輝、廖俊銘、陳志偉、蔡肇原、李敏輝、尤介彥、方俞傑、林育如、羅小惠、林美君、張瑜珍、陳慧蓉、馬夙璋、許雅婷、郭紓錚、謝進良、陳志彬、鄭香福、江舫進、Toy、阿毛、娃娃、給予精神上的支持與鼓勵。

最後，由衷地感謝我的父親、母親、北貝、已故的親弟(藍伊權)，在求學期間給予精神上的鼓勵、支持及開導，讓我度過低潮與難關，使我得以順利完成學業，取得台大博士學位。

---

---

# Content

---

---

國立臺灣大學博士學位論文口試委員會審定書 .....	I
謝 誌.....	II
CONTENT .....	III
LIST OF TABLES .....	V
LIST OF FIGURES.....	VI
摘 要.....	IX
ABSTRACT .....	X
<b>CHAPTER 1. INTRODUCTION OF DISPERSION TECHNIQUES FOR NANOMATERIALS-</b>	<b>12 -</b>
<b>1.1. HISTORY AND DEVELOPMENT OF NANOTECHNOLOGY AND DISPERSION TECHNIQUES</b> .....	<b>12 -</b>
<i>1.1.1. Dispersion Techniques for Carbon Nanotubes</i> .....	<i>14 -</i>
<i>1.1.2. Dispersion Techniques for Nanoparticles</i> .....	<i>20 -</i>
<i>1.1.2.1. Dispersion Techniques for Carbon Nanoparticles</i> .....	<i>20 -</i>
<i>1.1.2.2. Preparation and Dispersion Techniques for Silver Nanoparticles</i> .....	<i>24 -</i>
<i>1.1.2.3. Preparation and Dispersion Techniques for Iron-Oxide Nanoparticles</i> .....	<i>29 -</i>
<i>1.1.3. Dispersion Techniques for Hydrophobic Conjugated Polymers</i> .....	<i>31 -</i>
<i>1.1.4. Dispersion Techniques for Organic Pigments</i> .....	<i>34 -</i>
<b>1.2. NEW DISPERSION TECHNIQUES OF GEOMETRIC-SHAPE INHOMOGENEITY FACTOR</b> .....	<b>37 -</b>
<b>CHAPTER 2. EXPERIMENTAL SECTION.....</b>	<b>39 -</b>
<b>2.1. MATERIALS.....</b>	<b>39 -</b>
<i>2.1.1. Platelet-Like Clays</i> .....	<i>39 -</i>
<i>2.1.2. Tubular Nanomaterials</i> .....	<i>40 -</i>
<i>2.1.3. Nanoparticles</i> .....	<i>40 -</i>
<i>2.1.4. Hydrophobic Conjugated Polymers</i> .....	<i>41 -</i>
<i>2.1.5. Poly(N-Isopropyl Acrylamide)-Tethered NSP</i> .....	<i>43 -</i>
<i>2.1.6. Organic Pigments</i> .....	<i>44 -</i>
<b>2.2. PREPARATION OF NANOMATERIALS-CLAY HYBRIDS</b> .....	<b>45 -</b>
<b>2.3. AMPHIPHILIC DISPERSION IN ORGANIC SOLVENTS OR WATER</b> .....	<b>45 -</b>
<b>2.4. CHARACTERIZATIONS</b> .....	<b>46 -</b>



2.4.1. Dispersion.....	- 46 -
2.4.2. Thermoresponsive Behavior .....	- 46 -
2.4.3. Luminescence Property.....	- 47 -
2.4.4. Conductivity Property.....	- 47 -
2.4.5. Thermal Degradation, Particle Size and Zeta Potential Properties.....	- 47 -
<b>CHAPTER 3. RESULTS AND DISCUSSION .....</b>	<b>- 49 -</b>
<b>3.1. DISPERSION OF TUBULAR-LIKE NANOMATERIALS BY USING PLATELET-LIKE CLAYS<sup>7</sup> .....</b>	<b>- 49 -</b>
3.1.1. Dispersion of Carbon Nanotubes in the Presence of Clays .....	- 50 -
3.1.2. Amphiphilic Property for Dispersion.....	- 55 -
3.1.3. Explanation for the Formation of Mica-CNT Microstructures.....	- 59 -
3.1.4. Conclusion.....	- 60 -
3.2.1. Dispersion of Carbon Nanocapsules in the Presence of Clays.....	- 62 -
3.2.2. Dispersion of Carbon Black in the Presence of Clays .....	- 70 -
3.2.3. Preparation and Dispersion of Silver Nanoparticles in the Presence of Clays .....	- 72 -
3.2.4. Preparation and Dispersion of Iron-Oxide Nanoparticles in the Presence of Clays .....	- 73 -
<b>3.3. DISPERSION OF HYDROPHOBIC CONJUGATED POLYMERS BY USING PLATELET-LIKE CLAYS AND THEIR THERMORESPONSIVE PROPERTY.....</b>	<b>- 75 -</b>
3.3.1. Dispersion of CP/Clay in the Presence of Clays .....	- 76 -
3.3.2. Optical Performance of CP/Mica Hybrids .....	- 83 -
3.3.3. Explanation for the Dispersion Behavior of CP/Clay.....	- 87 -
3.3.4. Thermoresponsive behavior of conjugated polymer induced by NSP-PNiPAAm .....	- 89 -
3.3.5. Photoluminescence behavior of dispersion solution and solid film .....	- 95 -
3.3.6. Conclusion.....	- 98 -
<b>3.4. DISPERSION OF ORGANIC PIGMENTS BY USING PLATELET-LIKE CLAYS.....</b>	<b>- 100 -</b>
3.4.1. Dispersion of Organic Pigments in the Presence of Clays .....	- 101 -
3.4.2. Conclusion.....	- 114 -
<b>CHAPTER 4. SUMMARY .....</b>	<b>- 115 -</b>
<b>CURRICULUM VITAE.....</b>	<b>- 117 -</b>
<b>REFERENCES .....</b>	<b>- 126 -</b>

---

---

## List of Tables

---

---

<b>Table 1.</b> Summarized of Anionic, Cationic, Non-Ionic, Polymeric Surfactants, Polymers, Copolymers and Proteins for Dispersing Carbon Nanotubes.....	- 17 -
<b>Table 2.</b> Chemical Methods for Improving Solubility of Carbon Nanoparticles.....	- 21 -
<b>Table 3.</b> Utilization of Organic Dispersants for Improving Solubility of Carbon Nanoparticles.....	- 23 -
<b>Table 4.</b> Various Methods for Preparing Silver Structures with Different Morphologies.-	26 -
<b>Table 5.</b> Common Reducing Agents for Converting Silver Salts to Nanoparticles. ...	- 28 -
<b>Table 6.</b> Chemical Syntheses for Improving Solubility of Conjugated Polymers in Organic Solvents.....	- 32 -
<b>Table 7.</b> Chemical Syntheses for Improving Solubility of Conjugated Polymers in Water.....	- 33 -
<b>Table 8.</b> General Properties of Platelet Clays. ....	- 40 -
<b>Table 9.</b> Dispersion of CNT, Mica and the Hybrid in Various Mediums.....	- 55 -
<b>Table 10.</b> Dispersion of CNC and CNC-Mica Hybrid in Various Solvents.....	- 68 -
<b>Table 11.</b> Zeta Potential of Pristine Mica and MEH-PPV/Clay Hybrid.....	- 83 -
<b>Table 12.</b> Particle Size and Zeta Potential of Pigment-Mica Dispersion in Water...-	105 -

---

---

## List of Figures

---

---

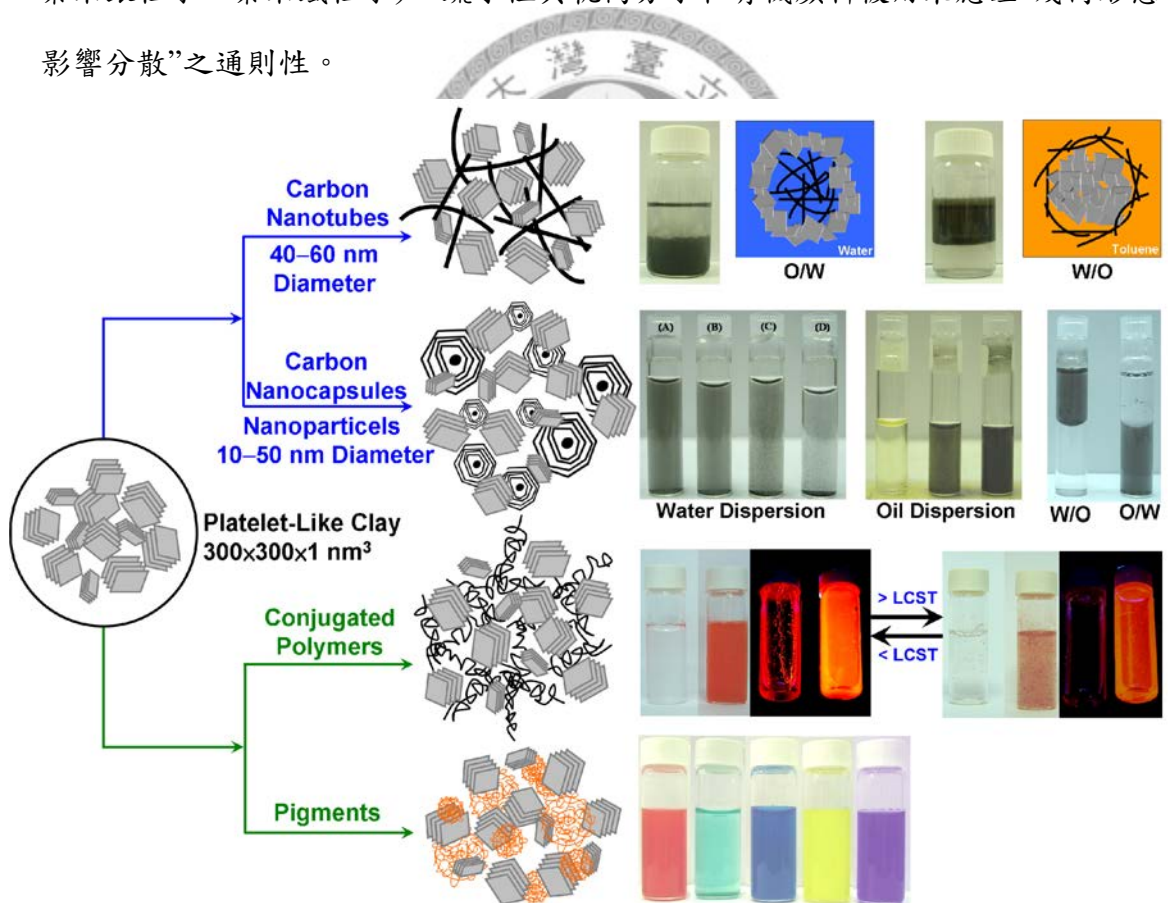
- Figure 1.** Functionalized CNTs through chemical approaches. .... - 15 -
- Figure 2.** Conceptual diagram of iron-oxide nanoparticles dispersed in aqueous solution by surfactants. .... - 30 -
- Figure 3.** Conceptual diagram of disperse pigment by using polymeric dispersant. . - 34 -
- Figure 4.** Development of geometric-shape inhomogeneity factor (GIF) for dispersing nanomaterials. .... - 37 -
- Figure 5.** Scanning electron microscopy of tubular sulfonated polyaniline (a) and polygonal triphenyl phosphine oxide cored polyaniline (b). .... - 41 -
- Figure 6.** Chemical structures of MEH-PPV (a), SPA (b) and TPOPA (c). .... - 42 -
- Figure 7.** Chemical structures of pigments and their color appearances. .... - 44 -
- Figure 8.** FE-SEM of CNTs and Mica under pulverizing for (a) 1 min and (b) 5 min. Visual observation of the dispersion of clay-CNT hybrids in water: (c) Mica-CNT, (d) MMT-CNT and (e) LDH-CNT, under varied  $\alpha$  value ( $\alpha$  = clay/CNT weight ratio). Each sample contained 1 mg CNTs in 20 g water. .... - 51 -
- Figure 9.** (a) UV-vis absorbance of clay-CNT at different  $\alpha$  value of hybrids in water. (b) Three standard curves of clay-CNT hybrids at different CNT content. The increase of UV-vis absorbance in (a) indicated the dispersing ability of the clay species improvement of CNT dispersion in reference to the standard curves in (b) of absorbance vs. CNT in water. .... - 53 -
- Figure 10.** Irreversible dispersion phenomenon of Mica-CNT at  $\alpha = 2$ : (a) Grinding procedure of Mica-CNT hybrid. Hybrid was dispersed in either water (d) or toluene (e), both dispersions remained in the original solvent after adding the other solvent (f and g). After vigorously shaking, the dispersion settled into distinct layers in an irreversible manner (h and i). .... - 56 -
- Figure 11.** TEM images of Mica-CNT hybrid dispersed in water (a and b) and in toluene (c and d). Mica-CNT hybrid was obtained from the same batch, however, hybrid has completely different microstructures when exposing to water or toluene. In water, hybrid shows more Mica appearance, on the contrary, more hairy CNT composition was observed. Conceptual presentation of amphiphilic dispersion with oil-in-water (O/W) and water-in-oil (W/O) microstructures (e), representing CNT-in-Mica and Mica-in-CNT, respectively. .... - 57 -
- Figure 12.** TGA patterns for the pristine CNT, Mica and their hybrid ( $\alpha = 2$ ). Mica-CNT (pulverized powder); Mica-CNT (O/W): the hybrid being dispersed in

water and dried; Mica-CNT (W/O): the hybrid being dispersed in toluene and dried.-	59 -
<b>Figure 13.</b> Conceptual Diagram of dispersion nanoparticles by geometric-shape inhomogeneity factor. ....	62 -
<b>Figure 14.</b> Visual observation of dispersing CNCs by different clays. (a) pristine CNCs (b) Mica (c) MMT (d) SWN (e) LDH (1 mg CNCs/5 g water; weight ratio of CNCs/clay = 1/1). ....	63 -
<b>Figure 15.</b> UV-vis adsorbance of CNC-Clay hybrid in water. ....	64 -
<b>Figure 16.</b> Visual observation of CNC-Mica hybrid in water at weight ratio of Mica/CNC = 0.5/1 (a), 1/1 (b), 2/1 (c) and 3/1 (d). (1 mg CNCs/5 g water) .....	65 -
<b>Figure 17.</b> UV-vis absorbance of CNC-Mica hybrid in water and the standard curves of absorbance against concentration (insert). ....	66 -
<b>Figure 18.</b> SEM image of CNC-Mica hybrid powder (a–d) and TEM morphology of dispersion of hybrid (e) and pristine CNCs (f). ....	67 -
<b>Figure 19.</b> Amphiphilic dispersion of CNC-Mica hybrid in water (a) and toluene (b).-	69 -
<b>Figure 20.</b> SEM morphology of CB-MMT hybrid at weight ratio of CB/MMT = 100/0 (a), 85/15 (b), 67/33 (c), and their hydrophilic property (insert). ....	71 -
<b>Figure 21.</b> Preparation of AgNPs in the presence of clays and the melting behavior.-	72 -
<b>Figure 22.</b> Preparation of FeNPs in the presence of organoclays and the magnetic behavior. ....	73 -
<b>Figure 23.</b> Dispersion of CP/Clay in water (1 mg CPs in 5 g water): (a) MEH-PPV/Mica at 3/1, 2/1, 1/1 and 1/2 weight ratios, (b) MEH-PPV/Mica (1/1) under UV light, (c) MEH-PPV/Clay (1/1), Clay=Mica, MMT, SWN and LDH, (d) SPA/Mica at 2/1, 1/1 and 1/2 ratios, and (e) TPOPA/Mica at 2/1, 1/1 and 1/2 ratios. ....	78 -
<b>Figure 24.</b> UV-vis absorbance of CP/clay in water: MEH-PPV dispersed by Mica, MMT, SWN or LDH, at weight ratio of 1/1. ....	79 -
<b>Figure 25.</b> UV-vis absorbance of CP/clay in water: MEH-PPV, SPA and TPOPA polymers dispersed by Mica at different weight ratio. ....	80 -
<b>Figure 26.</b> TEM images of CP/Mica dispersion (at 1/1 weight ratio) in water: MEH-PPV (a,b), SPA (c,d), and TPOPA (e,f). ....	81 -
<b>Figure 27.</b> Particle Size of Mica/MEH-PPV hybrids. ....	82 -
<b>Figure 28.</b> PL spectra of CP/clay solution with different clay. ....	84 -
<b>Figure 29.</b> PL spectra of CP/clay solution with Mica but different weight ratio. ....	85 -
<b>Figure 30.</b> UV-vis and PL spectra of hybrid film of MEH-PPV/Mica (a). ....	86 -
<b>Figure 31.</b> UV-vis and PL spectra of hybrid film of SPA/Mica (b). ....	86 -
<b>Figure 32.</b> UV-vis and PL spectra of hybrid film of TPOPA/Mica (c). ....	87 -
<b>Figure 33.</b> Conceptual illustration of homogeneous distribution between clay and CP through re-distribution of non-covalent bonding forces of the CP coils and rigid clay units. ....	88 -

<b>Figure 34.</b> (a) Conceptual illustration of thermoresponsive NSP-PNiPAAm/MEH-PPV in water. (b) Thermoresponsive dispersion of NSP-PNiPAAm/MEH-PPV in water (1 mg MEH-PPV in 5 g water) at weight ratio of NSP-PNiPAAm/MEH-PPV = 1/0, 0/1, 1/1, 2/1, 3/1 and 4/1 weight ratios under temperature cycle and UV exposure.....	- 90 -
<b>Figure 35.</b> NSP-PNiPAAm/MEH-PPV dispersed in water at different weight ratio for UV-vis absorbance (a,b) and transmittance (c,d).....	- 92 -
<b>Figure 36.</b> FE-SEM images of NSP-PNiPAAm/MEH-PPV dispersed in water and then dried at 25 °C (a,b) and 80 °C (c,d), and surface of NSP-PNiPAAm coating at 25 °C (e,f) and 80 °C (g,h). .....	- 94 -
<b>Figure 37.</b> NSP-PNiPAAm/MEH-PPV dispersed in water at different weight ratio for PL emission (a,b), and their corresponding films at weight ratio of NSP-PNiPAAm/MEH-PPV = 3/1 and their optical properties (c,d). .....	- 96 -
<b>Figure 38.</b> Conceptual diagram of dispersion organic pigment through GIF. ....	- 101 -
<b>Figure 39.</b> Visual pictures of dispersing pigments red 177 and green 36 and their control experiments. Pristine pigment directly added into water (a,b). Pristine pigment with grinding treatment and then added into water (c,d). The pigment grinding with Mica powder at weight ratio of 1/1 and the mixture powder is dispersible in water (e,f).-	102 -
<b>Figure 40.</b> Visual observation of dispersing pigment blue 15 (a) and red 177 (b) at various amounts of Mica presence and their UV-vis absorbance at wavelength of 337 nm (c) and 558 nm (d). .....	- 103 -
<b>Figure 41.</b> Particle size and zeta potential analysis of dispersing pigment blue 15 (a) and red 177 (b) in water. ....	- 107 -
<b>Figure 42.</b> Size distribution of blue (a) and red (b) pigments dispersion in water. .-	109 -
<b>Figure 43.</b> TEM morphology of dispersing pigment red 177, green 36, blue 15, yellow 138, violet 23 and pristine Mica in water (weight ratio of Mica/pigment = 1/1). ....	- 110 -
<b>Figure 44.</b> Visual observation of mixture solution of pigment-PVA: blue-PVA (a) and red-PVA (b) at various amounts of Mica presence and their UV-vis absorbance of blue (c) and red (d). .....	- 112 -
<b>Figure 45.</b> Visual observation of composite films of pigment-PVA: blue-PVA (a) and red-PVA (b) at various amounts of Mica presence and their UV-vis absorbance of blue (c) and red (d). .....	- 113 -
<b>Figure 46.</b> Generalization of Geometric-Shape Inhomogeneity Factor for dispersing Nanomaterials. ....	- 115 -

## 摘要

奈米技術發展數十年，各式各樣的奈米材料已被發現或製備，為了應用這些奈米材料，分散技術是關鍵點。在文獻中已提出各種化學或物理的分散方法，然而，這些技術仍無法配合分散和應用間的需求。因此，我們建立了一個新式的分散系統—幾何形態分散，其分散概念為利用材料在幾何形態上的高度差異性，可提升材料的分散性。在本研究中，各種奈米材料(奈米碳管、奈米碳球、奈米炭黑、奈米銀粒子、奈米鐵粒子)、疏水性共軛高分子和有機顏料被用來應證“幾何形態影響分散”之通則性。



**關鍵詞:**分散、奈米碳管、碳黑、奈米碳球、共軛高分子、顏料



---

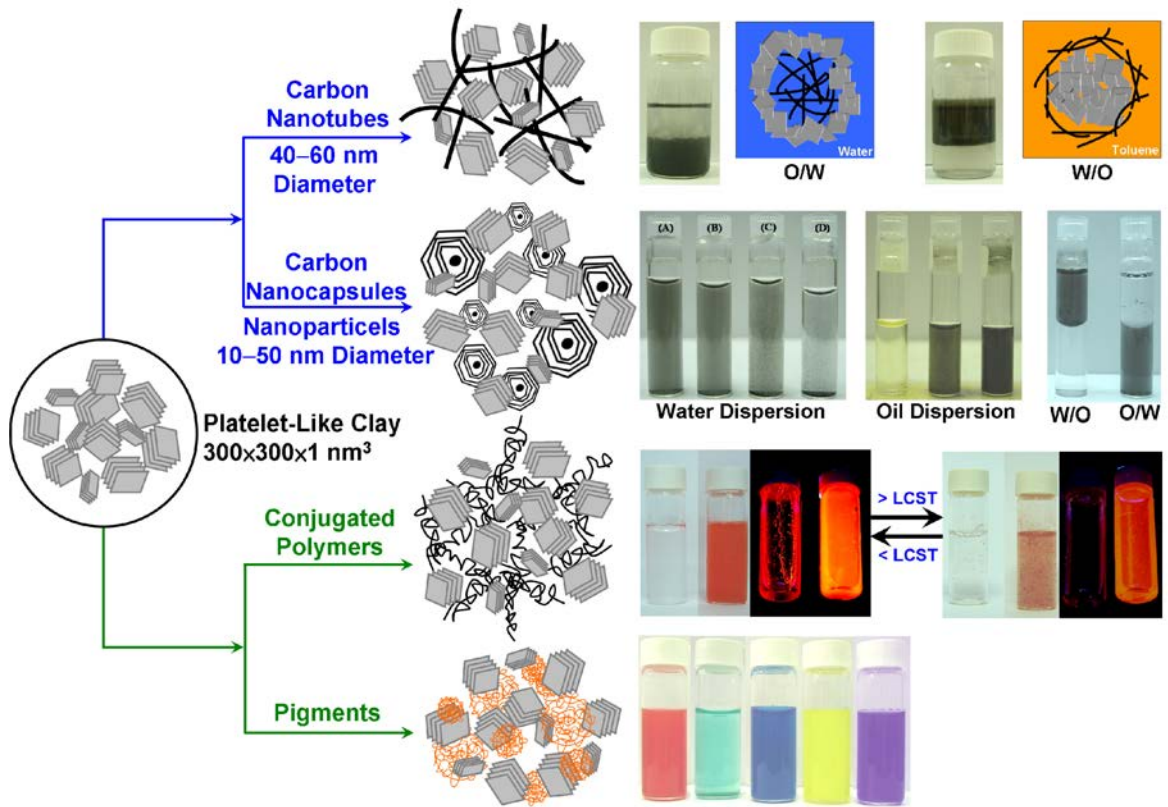
---

## Abstract

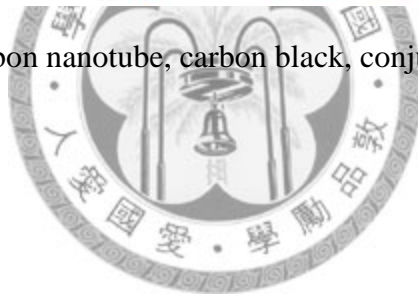
---

---

Nanotechnology has been developed for decades and various nanomaterials were created and discovered. To apply these nanomaterials in advanced applications, dispersion techniques are the key issue for utilizing the novel nanomaterials. In the literatures, a variety of dispersion methods involving chemical and physical approaches were proposed. However, these techniques are still not meeting the requirements for the applications. Therefore, we established a new dispersion method based on the concept of using the distinct difference of geometric shapes of nanomaterials namely, “Geometric-Shape Inhomogeneity Factor” (GIF) for Dispersion. Various nanomaterials, including carbon nanotubes, carbon blacks, carbon nanocapsules, silver nanoparticles, iron-oxide nanoparticles, hydrophobic conjugated polymers and organic pigments were selected to generalize the GIF. All practical applications have been successfully improved on utilizing GIF for dispersing nanomaterials.



**Keywords:** dispersion, carbon nanotube, carbon black, conjugated polymer, pigment



---

---

# Chapter 1. Introduction of Dispersion Techniques for Nanomaterials

---

---

## 1.1. History and Development of Nanotechnology and Dispersion Techniques

Nanotechnology has been widely developed since the special-analytical microscopes were invented such as scanning electron microscopy (SEM),<sup>1</sup> transmission electron microscopy (TEM)<sup>2</sup> and atom force microscopy (AFM).<sup>3</sup> By using these advanced instruments, various nanomaterials were discovered, created and synthesized including silver nanoparticles (AgNPs),<sup>4</sup> iron-oxide nanoparticles (FeNPs), carbon blacks (CBs),<sup>5</sup> carbon nanocapsules (CNCs),<sup>6</sup> carbon nanotubes (CNTs),<sup>7</sup> graphenes,<sup>8</sup> clays,<sup>9</sup> organic pigments (OPs),<sup>10</sup> self-assembly of polymers,<sup>11</sup> proteins<sup>12</sup> and surfactants,<sup>13</sup> etc. These new materials have excellent physical and chemical properties and many creative applications were proposed, for example, antimicrobials,<sup>14</sup> superhydrophobic surfaces,<sup>15</sup> electromagnetic interferences,<sup>16</sup> mode-locking laser absorbers,<sup>17</sup> flame retardant materials,<sup>18</sup> nanocomposites,<sup>19</sup> nanocarriers,<sup>20</sup> etc. However, the nanomaterials easily formed aggregation and hindered their advanced applications. The strong aggregation between nanomaterials are due to the higher aspect-ratio, large surface area and strong interaction forces of van der Waal attraction, hydrophobic entanglement,  $\pi$ - $\pi$  stacking, ionic absorption.

In the literatures, various ideas and approaches were proposed and applied in dispersing nanomaterials. These dispersion techniques can be classified into two sorts, one is chemical surface modification (*By Covalent Bonding*), and the other is physical absorption surface modification (*By Noncovalent Bonding*). The chemical surface modification on nanomaterials showed effectively promotion in dispersion. Physical absorption surface modification is the alternative approach to reduce the aggregation and enhance the dispersed stability through noncovalent bonding such as ionic forces, hydrophobic attractions, hydrogen bonding, van der Waal and hydrophilic interactions, etc. The chemical and physical methods applied in dispersion of CNTs, CBs, CNCs, AgNPs, FeNPs, CPs and OPs were described in the following sections.



### *1.1.1. Dispersion Techniques for Carbon Nanotubes*

CNTs have superior chemical and physical properties because of their high aspect-ratio dimension and the conjugated character of individual tubes.<sup>21</sup> Due to their unique conducting properties, numerous applications have been reported, for examples flat panel field-emission displays, nanoelectronic devices, chemical sensors, batteries, and so forth.<sup>22</sup> However, the CNTs tend to aggregate through their lengthy geometric shape and strong van der Waals force attraction, which may consequently hinder their uses in many applications.

To overcome these problems, covalent functionalization was proposed to improve the dispersibility (**Figure 1**). Up to the present, there are various chemical methods for CNT modification, including strong oxidation (**Figure 1a**),<sup>23</sup> Bingel reaction (**Figure 1b**),<sup>24</sup> cyclo addition (**Figure 1c**)<sup>25</sup> and anionic polymerization (**Figure 1d**),<sup>26</sup> etc. Among those chemical methods, strong oxidation is the most useful and studied widely (**Figure 1e**<sup>27</sup> and **1f**<sup>28</sup>). Recently, both atom transfer radical polymerization (**Figure 1g**)<sup>28,29</sup> and free radical polymerization (**Figure 1h**)<sup>30</sup> also are applied in CNT modification. Most of the approaches have been involved in functionalized the surface of CNTs and effectively improved their solubility in polymeric mediums or organic solvents.<sup>31</sup>

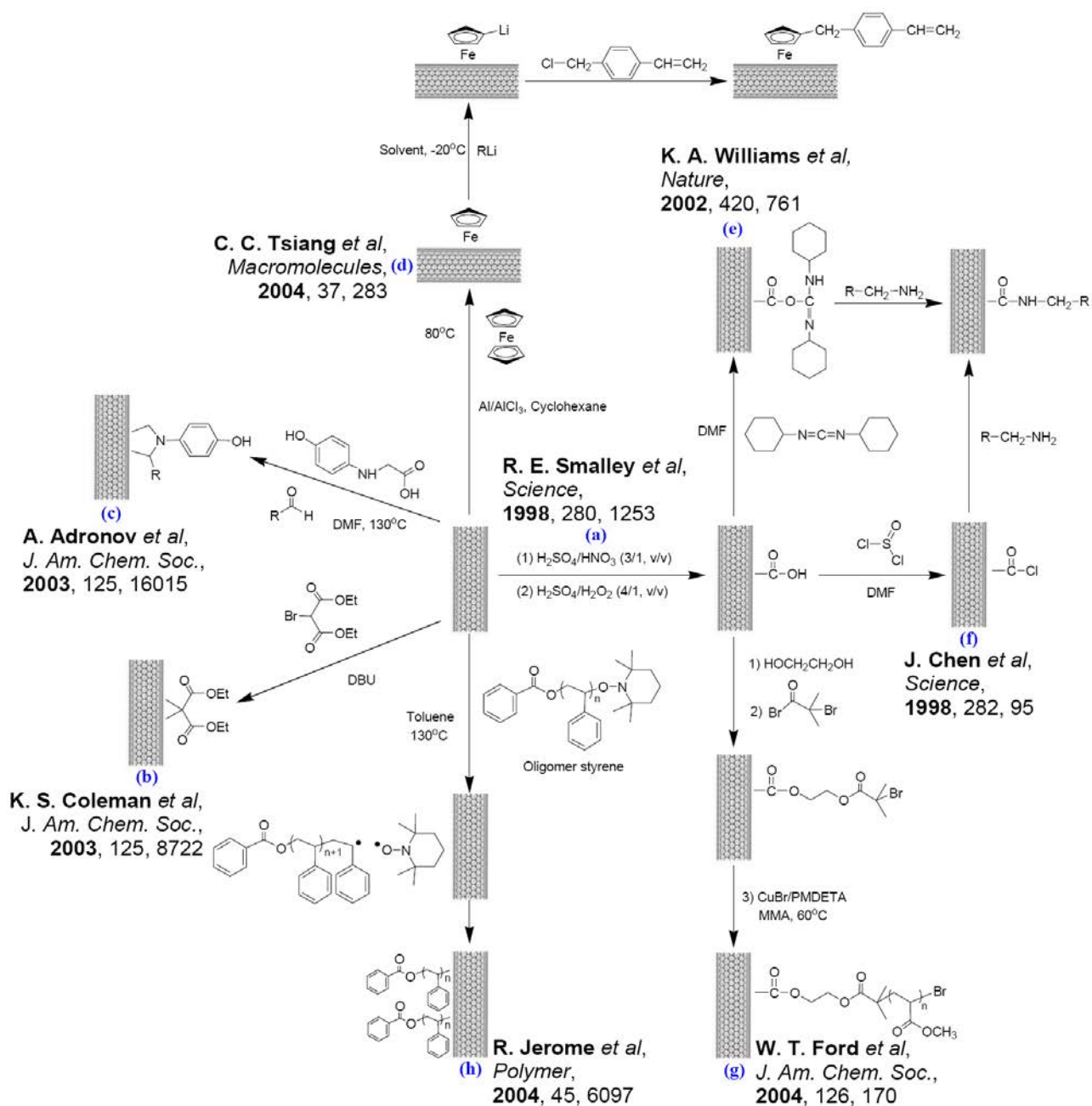


**Figure 1.** Functionalized CNTs through chemical approaches.

Nevertheless, most of these processes involve an organic covalent bonding reaction which consequently destroys the  $sp^2$  structure in the graphite sheet. Hence, the covalent-bonding modification may be disadvantageous due to the possible destruction of the unique tubular-like structure. Alternative methods by using non-covalent bonding modifications are desired. Suitable surfactants,<sup>32-42</sup> polymers,<sup>35,44-53</sup> and



bio-molecules<sup>54-60</sup> are commonly applied for the purpose of easy dispersion through  $\pi$ - $\pi$  stacking, van der Waals force or hydrophobic interactions. All the organic dispersants utilizing for improved dispersion of CNTs were listed in **Table 1**. Among organic surfactants, the anionic-type molecules are most suitable for dispersing CNTs, particularly sodium dodecyl sulfate (SDS)<sup>33</sup> and sodium dodecyl benzene sulfonic acid (SDBS).<sup>32</sup> For cationic surfactants, the amine-type dispersants with primary amine and long alkyl chain are more prefer to disperse CNTs due to the strong interaction between amine moiety and CNT surface.<sup>36-39</sup> The polymeric wrapping CNTs offer an alternative methods to increase the compatibility with polymers such as polyethylene, polypropylene and polymethylmethacrylate.<sup>35,44-53</sup> The hydrophobicity within molecular chains of DNAs, proteins and nucleotides showed strong attraction with CNTs and enhanced biocompatibility of CNTs *in vitro*.<sup>55-61</sup> Various di- and tri-block copolymers were designed and synthesis for dispersing CNTs, however, the results did not have great improvement for practical applications. More recently, room-temperature ionic liquids were found to be effective for dispersing CNTs by physical grinding to form gels through the cation- $\pi$  interaction.<sup>61-64</sup>

**Table 1.** Summarized of Anionic, Cationic, Non-Ionic, Polymeric Surfactants, Polymers, Copolymers and Proteins for Dispersing Carbon Nanotubes.

<b>Classifications</b>	<b>Organic Dispersants</b>	<b>Ref.</b>
<b>Anionic Surfactants</b>	Sodium Octanoic Acid	32a
	Sodium Octylsulfate	32a
	Sodium Dodecyl Sulfate (SDS)	32d,33,35a
	Lithium Dodecyl Sulfate	34
	Sodium Dodecyl Benzene Sulfonic Acid (SDBS)	32a,c–e,35a
	Sodium Octadecylsulfate	32a
	Sodium n-Lauroylsarcosinate (Sarkosyl)	35
	Sodium Lauroylsulfosuccinate (TREM, Cognis Co.)	35
	Poly(styrene sulfonate)	35
<b>Cationic Surfactants</b>	Ethylenediamine (C <sub>2</sub> )	36
	Propylamine (C <sub>3</sub> )	37a
	Propylenediamine (C <sub>3</sub> )	36
	Butylamine (C <sub>4</sub> )	37a,b
	Hexylamine (C <sub>6</sub> )	32a
	Triethylamine (C <sub>6</sub> )	32a
	Octylamine (C <sub>8</sub> )	38
	Nonylamine (C <sub>9</sub> )	36
	Decylamine (C <sub>10</sub> )	32a
	Dipentylamine (C <sub>10</sub> )	36
	Dodecylamine (C <sub>12</sub> )	32a
	Dodecyltrimethylammonium Bromide (C <sub>15</sub> )	32d
	Hexadecylamine (C <sub>16</sub> )	32a
	Octadecylamine (C <sub>18</sub> )	32a,b
	Cetyltrimethylammonium Bromide (C <sub>19</sub> )	35
	Benzalkonium Chloride	39
	3-Aminopropyl Triethoxysilane	37b
<b>Non-Ionic Surfactants</b>	Pentanol (C <sub>5</sub> )	32a
	Octanol (C <sub>8</sub> )	32a
	Polyoxyethylene 8 Lauryl	40
	Octyl-Phenol-Ethoxylate (Triton X-100)	35d,41
	Sorbitan Mono-Oleate (Tween 80)	32d
	Sorbitan Mono-Oleate (Tween 85)	35a
	Disodium Dodecylphenoxybenzene Disulfonate (Dowfax 8390)	32d
	Brij 78	35a

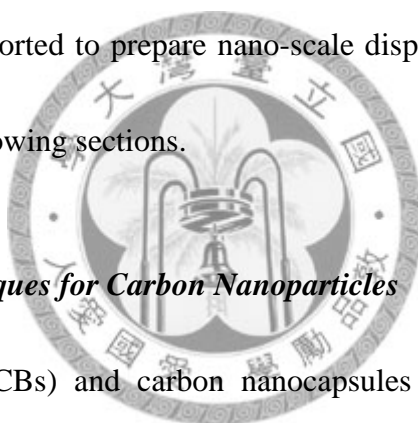
<b>Classifications</b>	<b>Organic Dispersants</b>	<b>Ref.</b>
<b>Non-Ionic Surfactants</b>	Brij 700	35a
	Pluronic P103 (PEO-PPO-PEO Triblock Polymer, BASF)	35a
	Pluronic P104	35a
	Pluronic P105	35a
	Pluronic F108	35a
	Pluronic F98	35a
	Pluronic F68	35a
	Pluronic F127	35a
	Pluronic F87	35a
	Pluronic F77	35a
Pluronic F85	35a	
	Tergitol NP 7	42
<b>Benzene Molecules</b>	Anthracene	43
	1,4-Terphenyl	43
<b>Polymers</b>	Poly(vinylpyrrolidone)	35c
	Polystyrene Sulfonate	35c
	Polyethylene	44
	Polyethylene Glycol (PEG 20,000)	35b
	Poly(metaphenylenevinylene)	45
	Poly(methylmethacrylate)	46
	poly(aryleneethynylene)	47
<b>Copolymers</b>	Poly(styrene- <i>alt</i> -maleic anhydride)	48
	Poly(styrene- <i>co</i> -acrylic acid)	49
	Poly(methylmethacrylate- <i>co</i> -pyrene)	50
	Poly(vinylidene fluoride- <i>co</i> -trifluoroethylene)	51
	Poly(ethylene oxide- <i>co</i> -butylene oxide- <i>co</i> -ethylene oxide)	35
	Poly(vinylpyridinium bromide- <i>co</i> -vinylpyridine)	52
	Poly(vinylpyrrolidone- <i>co</i> -allylamine)	52
	Poly(isopropylacrylamide- <i>co</i> -styrene- <i>co</i> -isopropylacrylamide)	53
<b>Proteins or DNAs</b>	Streptavidin	54
	DNA oligomer	55
	$\alpha$ -Helical Peptide	56
	Cyclic Peptides	57
	Phospholipids	58
	Bovine Serum Albumin (BSA)	59
<b>Nucleotides</b>	Adenosine 5'-Monophosphate (AMP)	60
	Adenosine 5'-Diphosphate (ADP)	60

<b>Classifications</b>	<b>Organic Dispersants</b>	<b>Ref.</b>
<b>Nucleotides</b>	Adenosine 5'-Triphosphate (ATP)	60
	Guanosine 5'-Monophosphate (GMP)	60
	Cytidine 5'-Monophosphate (CMP)	60
	Uridine 5'-Monophosphate (UMP)	60
	Ribose 5-Phosphate	60
<b>Ionic Liquids</b>	1-Ethyl-3-Methylimidazolium Tetrafluoroborate (C <sub>6</sub> )	61
	1-Ethyl-3-Methylimidazolium Hexafluorophosphate (C <sub>6</sub> )	61
	1-Butyl-3-Methylimidazolium Tetrafluoroborate (C <sub>8</sub> )	62
	1-Butyl-3-Methylimidazolium Hexafluorophosphate (C <sub>8</sub> )	63
	1-Hexyl-3-Methylimidazolium Tetrafluoroborate (C <sub>10</sub> )	61
	1-Hexyl-3-Methylimidazolium Hexafluorophosphate (C <sub>10</sub> )	61
	1-Octyl-3-Methylimidazolium Tetrafluoroborate	64
<b>Others</b>	Starch	65
	Saturated Sodium Hydroxide (aq.)	66
	Gum Arabic	67
	Amylose	68
	Pyrenebutanoic Acid,	69
	Cyclodextrin	70



### ***1.1.2. Dispersion Techniques for Nanoparticles***

Recent studies have put more attention on nanoparticles, particularly carbon blacks (CBs), carbon nanocapsules (CNCs), silver nanoparticles (AgNPs) and iron-oxide nanoparticles (FeNPs) due to they have nano-scale sizes in three dimensions. With large surface area and zero dimensions in nano-scale, various applications were proposed. However, the strong interaction in the nanoparticles materials caused severe aggregation and hindered their applications. In the literatures, both chemical and physical methods were reported to prepare nano-scale dispersion and we summarized these researches in the following sections.



#### ***1.1.2.1. Dispersion Techniques for Carbon Nanoparticles***

Both carbon black (CBs) and carbon nanocapsules (CNCs) are the common nanomaterials preparing from carbon sources. Owing to the advantage in nano geometric shape and carbon matrix, the diversified practical applications were reported such as oil lubrication,<sup>71</sup> electromagnetic interference,<sup>72</sup> fuel cell,<sup>73</sup> thermal dissipation<sup>74</sup> and carbon nanocomposites of rubber,<sup>75</sup> epoxy resin,<sup>76</sup> poly(lactic acid),<sup>77</sup> polypropylene,<sup>78</sup> poly(vinyl chloride),<sup>79</sup> poly(vinyl alcohol)<sup>80</sup> and poly(vinyl pyrrolidone),<sup>81</sup> etc. However, the use of carbon nanoparticles required a finely dispersed system which is difficult to achieve due to the large aggregation of CBs and CNCs. Nowadays the fine dispersing carbon nanoparticles of CBs or CNCs can be

obtained by using chemical surface modification and the surface grafting of polymers onto carbon black provided new functional carbon materials which have the excellent properties. The grafting of polymers onto the surface was achieved by (1) grafting onto process, (2) grafting from process, (3) polymer reaction process, and (4) stepwise growth by dendrimer synthesis methodology.<sup>82-97</sup> All the chemical methodologies for improved dispersion of carbon nanoparticles were summarized in **Table 2**.

**Table 2.** Chemical Methods for Improving Solubility of Carbon Nanoparticles.

<b>Methods</b>	<b>Materials</b>	<b>Ref.</b>
<b>Oxidation</b>	Nitric Acid (> 60 wt%)	82
<b>Grafting Polymers by Initiator</b>	Potassium Carboxylate Groups	83
	Azo Groups	84
	Peroxy carbonate Groups	85
	Trichloroacetyl Groups on Mo(CO) <sub>6</sub>	86
	Carboxyl Groups	87
<b>Grafting Polymers by Radical Trapping</b>	Peroxide Groups	88
	Decomposition of Macro-Initiators	89
<b>Grafting Polymers by Functional Groups</b>	$\gamma$ -Ray Irradiation	90
	Functional Polymers	91
<b>Grafting Polymers by Ligand Exchange</b>	Living Polymers	92
	Polymer with Ferrocene Moieties	93
<b>Grafting Polymers by Dendrimer Synthesis</b>	Poly(amido amine)	94
<b>Sol-Gel Reactions</b>	Silica Gel	95
	Alumina Gel	96
<b>Atom Transfer Radical Polymerization</b>	Poly(n-butyl acrylate)	97

Alternated approaches were proposed to increase the solubility of carbon nanoparticles through non-covalent bonding interactions.<sup>98-109</sup> Compared to the chemical modifications, the physical absorption methods are more convenient and



simple to decrease the aggregated size of carbon nanoparticles. The methods used for dispersing carbon materials were listed in **Table 3**. By using non-ionic surfactants, the molecules content amine groups are more suitable to interaction with carbon nanoparticles and those containing primary amines are more effectively improved the stability to aggregation of carbon black dispersions.<sup>101</sup> It is suggested that this is due to proton exchange reactions occurring at the surface, which can lead to surface charge, and, hence, long-range electrostatic repulsion between the particles. The dispersion behavior of carbon nanoparticles is similar to the CNTs due to the same chemical compositions with different geometric shapes.

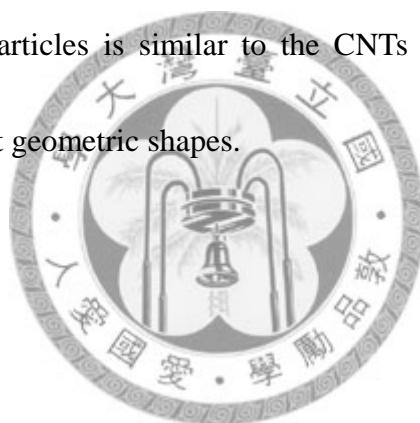


**Table 3.** Utilization of Organic Dispersants for Improving Solubility of Carbon Nanoparticles.

<b>Classifications</b>	<b>Organic Dispersants</b>	<b>Ref.</b>
<b>Anionic Surfactants</b>	bis-2-Ethylhexyl Sodium Sulfosuccinate	98
	Sodium Polystyrene Sulfonates	99
<b>Cationic Surfactants</b>	Cetyltrimethylammonium Chloride	100
	Polymeric Siloxane Surfactant	101
<b>Non-Ionic Surfactants</b>	Ethoxylated Nonylphenols	99
	Polyoxyethylene Cetyl Ether	99
	Polyisobutylene-Phenol	102
	Polyisobutylene-Phenol-Dimethylamine	102
	Polyisobutylene-Phenol-(ethylene diamine)	102
	Polyisobutylene-Phenol-(N,N-diethylthylenediamine)	102
	Polyisobutylene-Phenol-(N,N-diethyl-N'-methylthylenediamine)	102
	Polyisobutylene-Phenol-bis-(N,N-diethyl-N'-methyl-enthylenediamine)	102
<b>Polymers</b>	Polystyrene-Polyethylene Oxide	100
	Poly(vinyl alcohol)	103
<b>Copolymers</b>	Poly(1-nonylphenyloxy-2-decaoxyethylene-3-allyloxypropane ammonium sulfate- <i>co</i> -acrylonitrile)	104
	Poly(ester of hydroxy-carboxylic acid)	105
	Poly(alkyl ester- <i>co</i> -caprolactone)	105
	Diblock Polymers	106
	Triblock Polymers	107
	Graft Polymers	108
	Star Polymers	109

### ***1.1.2.2. Preparation and Dispersion Techniques for Silver Nanoparticles***

Several approaches have been reported for synthesizing silver nanoparticles (AgNPs) including chemical methods (electrochemical reduction,<sup>110</sup> ultrasonic-assisted reduction,<sup>111</sup> photoinduced or photocatalytic reduction,<sup>112</sup> microwave-assisted synthesis,<sup>113</sup> irradiation reduction,<sup>114</sup> microemulsion,<sup>115</sup> biochemical reduction<sup>116</sup> and, reduction in aqueous solutions<sup>117</sup> and non-aqueous solutions,<sup>118</sup>) and physical methods (metal ablation using a laser<sup>119</sup> and metal vapor deposition<sup>120</sup>). Among the approaches, metal vapor deposition was an efficient process, and it has been extensively employed in combination with the evaporation and sputtering of metals with plasma as well as with magnetron sputtering. The advantages of physical over chemical processes are the uniformity of nanoparticle distribution and the relative absence of solvent contamination in the prepared thin films. However, in the case of polymeric substrates, the adhesion between the deposited metal and polymer matrix is generally poor.

In general, by using a wet chemical process, AgNPs can be made into different shapes. The mechanism involves initial interactions of silver ions with organic stabilizers before their reduction into nanoparticles. Further aggregation leads to optimal sizes as well as the generation of a repelling layer. On the surface of small particles, the absorbed silver ions can be further reduced forming larger silver

crystallites. However, the inherent problems of nanoparticle aggregation or coalescence might still be encountered. One of the key issues for synthesizing AgNPs is the stabilization and prevention of particle agglomeration. The presence of surfactants comprising functionalities such as amines, thiols, acids, and alcohols<sup>121</sup> for interactions with the particle surface can stabilize the particle growth. Polymeric compounds such as poly(vinylpyrrolidone),<sup>110c,113b,114c,117cde</sup> poly(vinyl alcohol),<sup>122</sup> poly(ethylene glycol),<sup>118a</sup> and various block copolymers<sup>123</sup> have been found to be effective stabilizers. These organic surfactants or functional polymers enable the protection of small particles from agglomeration or losing their surface properties. In addition, the presence of surfactants might also affect the growth process of nanocrystallites and allow control of AgNP shapes and sizes. By controlling the stability, size distribution, and shape, the surface activity and performance in the targeted applications can be influenced. Recent literature reports on various synthetic methods with different process parameters, solvents, stabilizers, and organic templates were summarized in **Table 4**. Various morphologies including spherical, triangular, wire, cubic, and dendritic shapes have been reported.

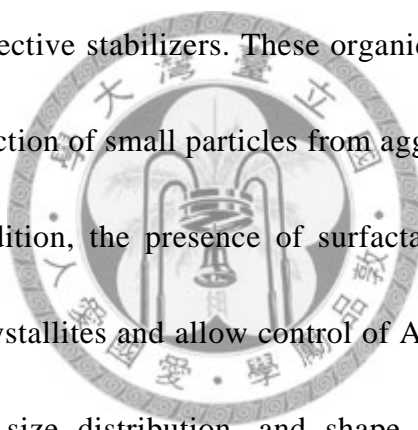
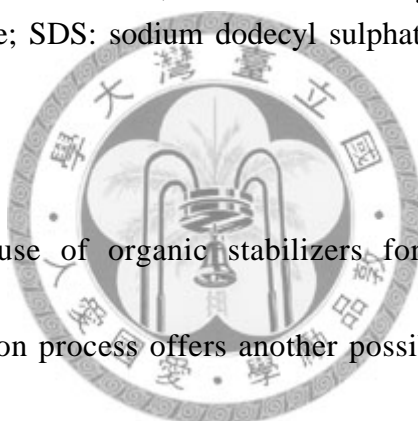


**Table 4.** Various Methods for Preparing Silver Structures with Different Morphologies.

<b>Synthetic Methods</b>	<b>Reducing agents</b>	<b>Organic Stabilizers</b>	<b>Morphologies</b>	<b>Ref.</b>
Chemical Reduction (water-system)	Sodium Citrate	Citrate	Nanowire Spheroid	117a,b
	NaBH <sub>4</sub>	PVP, PVA	Nanospheroids (7–20 nm)	117c
	Polyol	PVP	Nanowire Nanocubes	117d
	Ethylene Glycol	PVP	Nanocubes	117e
Chemical Reduction (organic solvents)	Dimethyl Acetamide	PEG	Nanospheroids	118a
	Acetonitrile	TTF	Dendritic	118b
Electrochemical Reduction	Cyclic Voltammetry	Polyphenylpyrrole	Nanospheroids (3–20 nm)	110a
	Rotating Platinum Cathode	PVP	Nanospheroids (10–20 nm)	110c
	Zeolite Film- Modified Electrodes	Zeolites	Nanospheroids (1–18 nm)	110b
Ultrasonic-Assisted Reduction	Sonoelectro- Deposition	PVA	Nanosphere Nanowire Dendrite	111a
	Sonoelectro- Chemistry Reduction	NTA	Nanosphere	111b
Photoinduced or Photocatalytic Reduction	Dual-Beam Illumination	Citrate, PSS	Triangular Nanoprisms (3–120 nm)	112a
	PSS, Polychromatic Irradiation	PSS	Nanospheroids ( <i>ca.</i> 8 nm)	112b
Microwave-Assisted Synthesis	Sodium Citrate	Citrate	Nanorods Spheroids	113a
	Ethylene Glycol	PVP	Nanospheroids	113b
	Formaldehyde	Citrate	Nanospheroids	113c
Irradiation Reduction	$\gamma$ -Irradiation	Mesoporous Silica	Nanospheroids (1–4 nm)	114a
	$\gamma$ -Irradiation	PVP	Nanospheroids (5–20 nm)	114b
	feto and nano sec. Laser Ablation	No	Nanospheroids (20–50 nm)	114c

Synthetic Methods	Reducing agents	Organic Stabilizers	Morphologies	Ref.
Microemulsion Method	V <sub>c</sub>	CTAB	Nanowires	115a
		SDS	Dendrites	
	KBH <sub>4</sub>	Ellipsoidal Micelles	Needle-Shaped Wire-Shaped	115b
	NaBH <sub>4</sub>	PFPE-NH <sub>4</sub>	Nanospheroids	115c
Biochemical Reduction	Peptide	Peptide	Hexagonal Spherical	116a
	Yeast Strain	Proteins	Nanospheres (2–5 nm)	116b
	Neem Leaf	Flavanones	Spheres	116c
	Extension	Terpenoids	(5–35 nm)	

PVA: poly(vinylalcohol); PVP: poly(vinylpyrrolidone); PEG: polyethyleneglycol; TTF: tetrathiafulvalene; NTA: nitrilotriacetate; PSS: Poly(styrene sulfonate); CTAB: cetyltrimethylammonium bromide; SDS: sodium dodecyl sulphate; PFPE: ammonium carboxylate perfluoropolyether



In addition to the use of organic stabilizers for controlling the particle morphologies, the reduction process offers another possibility—tailoring of particle characteristics. Reducing agents such as sodium borohydride,<sup>117c</sup> sodium citrate,<sup>117a,b</sup> *N,N*-dimethylformamide (DMF),<sup>124</sup> polyols,<sup>125</sup> ascorbate,<sup>126</sup> Tollens reagent,<sup>127</sup> and poly(ethylene glycol)-block copolymers<sup>113b,117e</sup> are popular. In general, strong reducing agents such as sodium borohydride can often afford fine particle sizes, as demonstrated by studies conducted with sodium citrate<sup>117b</sup> and sodium borohydride.<sup>117c</sup> Systematic studies were performed by varying the reductant/AgNO<sub>3</sub> ratios. The resultant colloids were characterized by UV-vis spectroscopy immediately after the preparation as well as during its long-term

stability studies. The AgNPs generated by the citrate method were large particles with diameters of around 40–60 nm; they were stable during storage. In contrast, the borohydride reduction afforded smaller AgNPs (3–10 nm). DMF is another example of a strong reducing agent for the silver ion reduction; it achieves fast reaction rate and nanoprism morphology.<sup>125</sup> AgNPs having diameters in the range of *ca.* 40 nm were prepared by using weak reducing agents such as polyols at elevated temperatures.<sup>125</sup> Large colloidal silver particles using ascorbic acid as the reducing agent have also been prepared in aqueous media.<sup>127</sup> The Tollens process has been recently recognized as a simple one-pot synthetic route for AgNPs with a narrow size distribution.<sup>128</sup> The basic reaction involves the reduction of silver solution from glucose. Stable aqueous dispersion of silver colloids having a size of 20–50 nm can be obtained. In this manner, the choice of reducing agents and synthetic conditions can significantly affect the size and stability of AgNPs. In **Table 5**, the commonly used reducing agents given in literatures have been cited.

**Table 5.** Common Reducing Agents for Converting Silver Salts to Nanoparticles.

<b>Reducing agents</b>	<b>References</b>
Sodium Borohydride (NaBH <sub>4</sub> )	117c
<i>N,N</i> -Dimethylformamide (DMF)	124
Polyols	125
Ascorbate	126
Tollens Reagent	127
Poly(ethylene glycol)-Based	113b, 117e

### *1.1.2.3. Preparation and Dispersion Techniques for Iron-Oxide Nanoparticles*

Magnetic iron-oxide nanoparticles (FeNPs) are well known for their wide applications including drug delivery<sup>128</sup> and magnetic resonance imaging (MRI)<sup>129</sup> because of the biocompatibility and high-density for digital storage.<sup>130</sup> Generally, the particle size of FeNPs is 10–50 nm by the water-in-oil (w/o) microemulsion method.<sup>131</sup> Synthesis of magnetite nanoparticles smaller than 10 nm has been carried out in bulk aqueous solution and surfactant systems such coprecipitation,<sup>132</sup> spray pyrolysis,<sup>133</sup> electrochemistry,<sup>134</sup> and hydrothermal synthesis.<sup>135</sup> When the particles are below 10 nm, they are optically transparent and suited for incorporation into ultrathin films of polymers. However, the nano-scale FeNPs are easily formed large aggregations due to the strong hydrophilic attraction.<sup>136</sup> Surfactants such as tetramethylammonium hydroxide,<sup>132</sup> sodium dodecyl benzene sulphonate,<sup>132</sup> polyglycides, polyglycerol isostearate<sup>132</sup> and polyoxyethylene ter-octyl ether (Triton X-100)<sup>132</sup> are dispersion agents for particles in a liquid that work by adhering to the particles and creating a net repulsion between them (steric and/or coulombic), raising the energy required for the particles to agglomerate, and stabilizing the colloid (**Figure 2**).



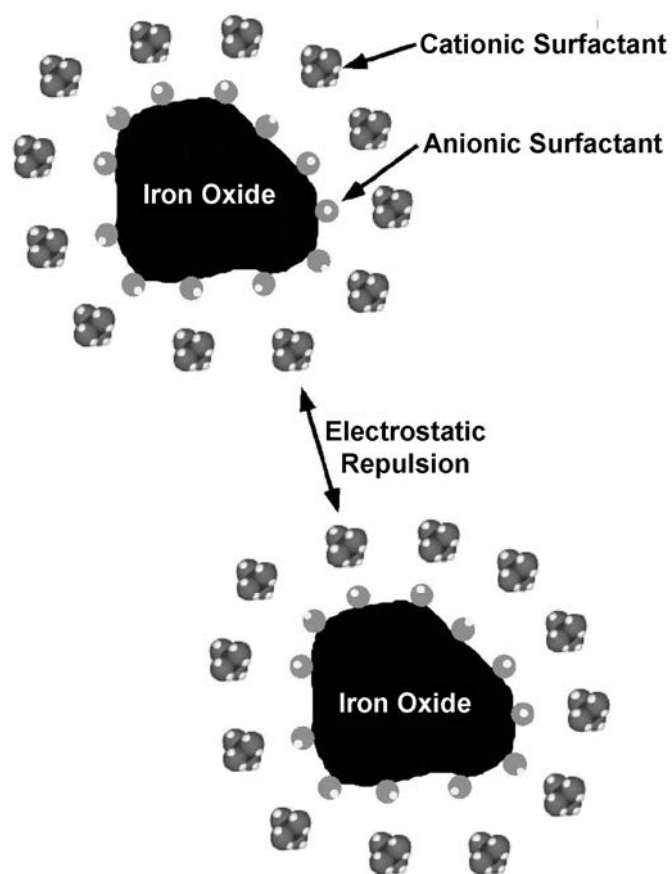


**Figure 2.** Conceptual diagram of iron-oxide nanoparticles dispersed in aqueous solution by surfactants.<sup>132</sup>



### 1.1.3. Dispersion Techniques for Hydrophobic Conjugated Polymers

Hydrophobic conjugated polymers (CPs) with various chemical structures, such as, poly(*p*-phenylene),<sup>137</sup> poly(*p*-phenylene-vinylene),<sup>138</sup> poly(*p*-phenyleneethynylene),<sup>139</sup> polyaniline,<sup>140</sup> poly(triacetylene),<sup>141</sup> poly(acetylene),<sup>142</sup> polythiophene,<sup>143</sup> polycarbazole,<sup>144</sup> and poly(flourene),<sup>145</sup> are well documented for their properties and applications of electronic conductivity<sup>146</sup> and light-emitting devices.<sup>147</sup> Among the diversified applications, the process of fabricating devices may be limited by the inherent physical properties such as insolubility of the rigid-rod CPs. Structural modification by attaching alkoxy or flexible alkyls to the main polymer backbone is the common approach for synthesizing soluble CPs.<sup>148</sup> The synthetic techniques used for improved the dispersion of CPs were collected and showed in **Table 6**. With the enhancement of their solubility in organic mediums, the process may be improved for some applications in optoelectronics, microelectronics,<sup>149</sup> and their devices for sensors.<sup>150</sup>

**Table 6.** Chemical Syntheses for Improving Solubility of Conjugated Polymers in Organic Solvents.

Conjugated Polymers	Synthetic Methods	Grafting Moieties	Ref.
<b>Poly(<i>p</i>-phenylene)s</b>	Reversed Williamson Route	Hexyloxy	148a,b,c,e
	Urethane Route	Hexyloxy	148a,b,c,e
	Macromonomer Route	Hexyloxy	148a,b,c,e
	Esterification	Ethylhexyloxy	148d
<b>Poly(triacetylene)s</b>	Mitsunobu Reaction	Fréchet-type Dendrons	148f
	Coupling Reaction	Hydroxy Methylbutynyl	148g
	Elimination Reaction	<i>tert</i> -Butylphenyl	148g
<b>Polythiophenes</b>	Dehalogenation Polymerization	Alkyl	148h
	Demercuration Polymerization	Alkyl	148h
<b>Polycarbazoles</b>	Copolymerization	Styrene	148i
		Vinyl Acetate,	148i
		Divinyl Benzene	148i
	Friedel-Crafts Reaction	Alkyl Methacrylates	148i
		Cu Phthalocyanine	148i
	Fullerenation	*Carbon Sixty	148i
	Free-Radical Polymerization	<i>N</i> -ethyl	148i
		Methylbutyl	148i
	Cationic Polymerization	Carbazolyl Cyclobutane	148i
	Anionic Polymerization	Methylstyrene	148i

However, the structural modifications could be complicated procedures, have great influence on optical performance and the modified CPs only can be dispersed in hazard-organic solvents, such as chloroform, dichloroform and dichlorobenzene, etc. In the recent literature surveillance, syntheses of water-soluble CPs are found for the applications as fluorescence biosensors.<sup>151</sup> The synthesis generally involves the grafting anionic polar functionalities such as sulfonic, carboxylic, bromo and amine groups on the alkoxy side-chain of the polymers (**Table 7**).<sup>152</sup> One of advantages for

using water-borne CPs is to reduce the use of volatile organic solvents in fabricating devices. This “green process” can be important for advancing these nanomaterial applications.

**Table 7.** Chemical Syntheses for Improving Solubility of Conjugated Polymers in Water.

<b>Conjugated Polymers</b>	<b>Synthetic Methods</b>	<b>Grafting Moieties</b>	<b>Ref.</b>
<b>Polythiophenes</b>	Electropolymerization	Ethanesulfonate	152a
		Butanesulfonate	152a
<b>Polypyrroles</b>	Oxidation	Carboxylic Acid	152b
<b>Poly(<i>p</i>-phenylenevinylene)</b>	Precursor Polymer Approach	Sulfopropoxy	152c
<b>Poly(<i>p</i>-phenylene)</b>	Suzuki Coupling Method	Dicarboxylic Acid	152d
		Sulfonatoalkoxy	152e
		Dibromobenzenes	152f
		Dialkylamino	152g



### 1.1.4. Dispersion Techniques for Organic Pigments

Organic pigments are widely used as colorants for coatings, inks, plastics, and color filters in electronic devices,<sup>153</sup> mainly because of their advantageous performances such as good photosensitivity, brilliance, color strength, transparency, and high thermal stability. Different from dyes, pigment materials are totally insoluble in organic mediums due to the strong intermolecular aggregation. The pigments are required to be finely ground and dispersed in an organic medium to warrant their gloss appearance, lighting efficiency, and maximizing material utilization. Amphiphilic copolymers are suitable for using to stabilize the pigment particles against flocculation during the milling disruption and storage.<sup>154</sup>

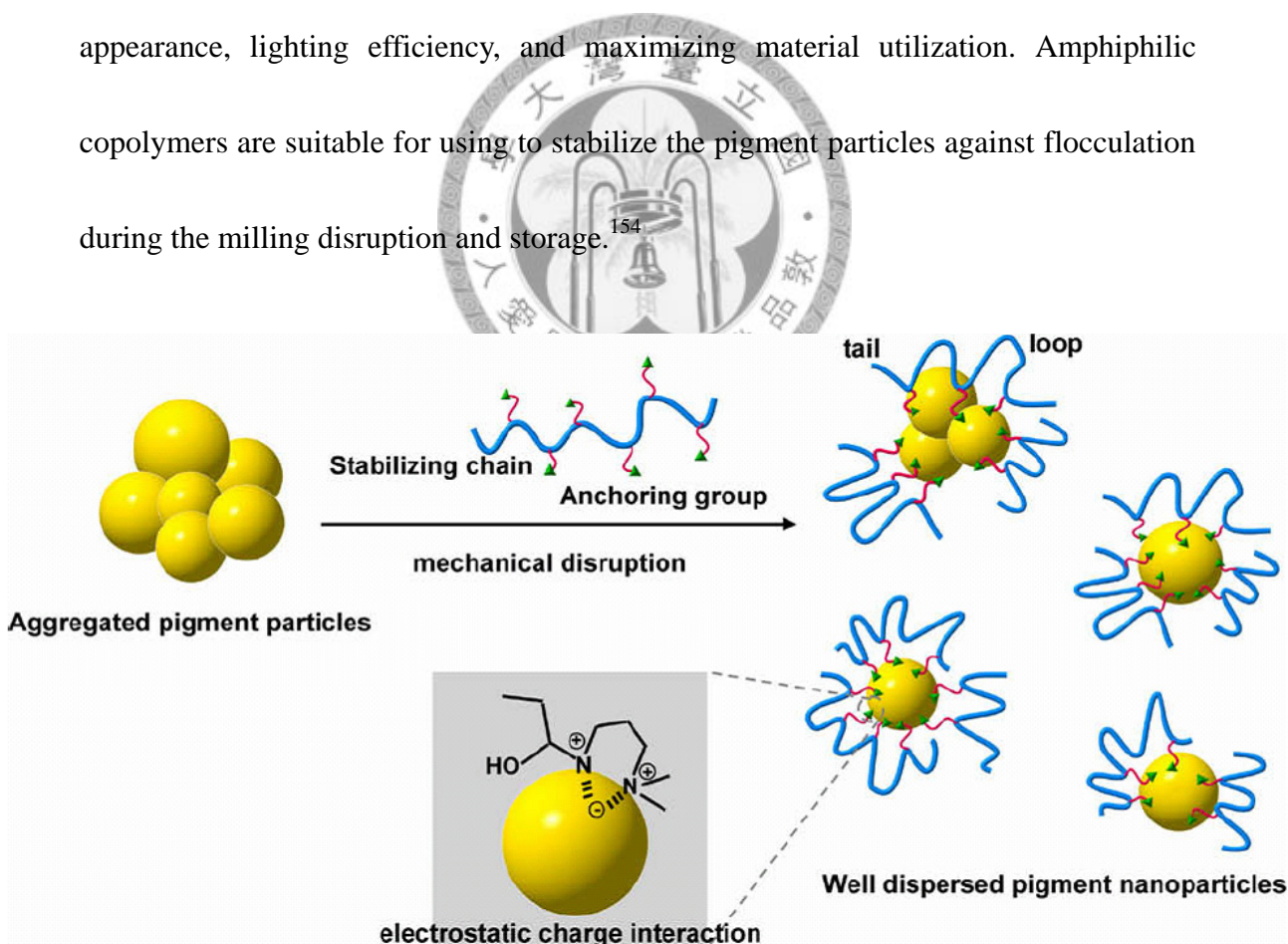


**Figure 3.** Conceptual diagram of disperse pigment by using polymeric dispersant.<sup>10</sup>

The principle for achieving a fine dispersion is a thermodynamically driven interaction among dispersant molecules, pigment particles, and solvents in a collective manner of mutual non-covalent bonding such as electrostatic charge attraction, hydrogen bonding,  $\pi$ - $\pi$  stacking, dipole-dipole interaction, and van der Waals forces (**Figure 3**). For practical applications, the pigment dispersion is optimized to achieve the performance of low viscosity, narrow range of size distribution, and long-term stability.

Low molecular-weight surfactants are conventionally used as dispersants for pigments, but often lacking a high stability for a long-term storage. Amphiphilic copolymers are advantageous for providing multiple anchoring sites toward pigment surface as well as structurally more designable for solvating with the selected solvents.<sup>155</sup> Polymeric structures of random, A-B block, comb-like copolymers prepared by various synthetic techniques had been employed as stabilizers against particle flocculation.<sup>156</sup> However, the methods of anionic and group transfer polymerization are less appropriate since the synthesis of dispersants often involves the monomers with polar functionalities.<sup>157</sup> Recent developments in living/controlled polymerization including nitroxide mediated polymerization (NMP),<sup>158</sup> reversible addition-fragmentation chain transfer (RAFT),<sup>159</sup> and atom transfer radical polymerization (ATRP)<sup>160</sup> are reported. The copolymers with specific functionalities

can be prepared from the monomers with diversified functionalities such as C<sub>1</sub>–C<sub>12</sub> alkyl (meth)acrylate,<sup>161</sup> amine-functionalized (meth)acrylate,<sup>162</sup> and acid-functionalized (meth)acrylate.<sup>163</sup> In addition, polymeric structure can be controlled for their molecular weight distribution and tailored for specific pigment applications.<sup>164</sup>



## 1.2. New Dispersion Techniques of Geometric-Shape Inhomogeneity Factor

These chemical and physical methods which described above are still non-satisfied the requirements between dispersion and applications. In our researches, a novel dispersion method was proposed and named by “Geometric-Shape Inhomogeneity Factor” (GIF). Various nanomaterials (CNTs),<sup>7, 165</sup> nanoparticles (CNCs,<sup>166</sup> CBs,<sup>5</sup> AgNPs,<sup>4</sup> FeNPs<sup>167</sup>), organic materials (pigments)<sup>168</sup> and polymers (conjugated polymers)<sup>169</sup> were systematically studied to generalize the GIF (**Figure 4**).

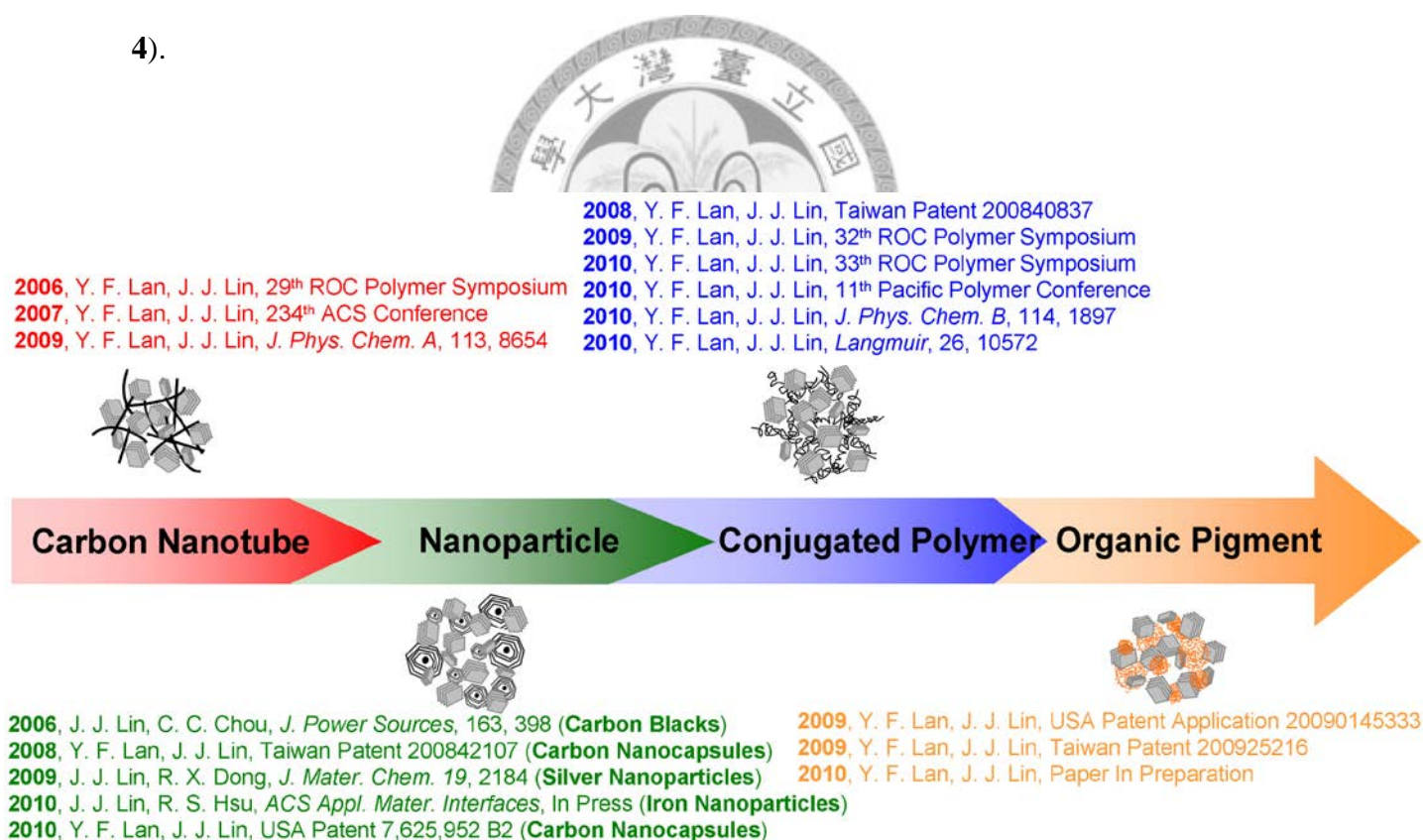


**Figure 4.** Development of geometric-shape inhomogeneity factor (GIF) for dispersing nanomaterials.



A mechanism involving large geometric difference of platelet-like nanomaterials, spherical nanoparticles, hydrophobic polymers and amorphous small molecules is proposed for accounting the dispersion of advanced materials. The interactions between different geometric shapes of nanomaterials revealed significantly improved and enhanced in various applications including nanocomposites,<sup>170</sup> conductive substrate,<sup>171</sup> supercapacitors<sup>172</sup> and photodegradation.<sup>173</sup>



---

---

## Chapter 2. Experimental Section

---

---

### 2.1. Materials

#### 2.1.1. Platelet-Like Clays

Different species of clays, synthetic fluorinated mica (Mica, trade name as SOMASIF ME-100) and synthetic smectite (SWN, trade name as Lucentite™ SWN), were obtained from CO-OP Chemical Co. (Japan). Sodium montmorillonite (Na<sup>+</sup>-MMT), supplied from Nanocor Co., is a Na<sup>+</sup> form of smectite clay with a cationic exchange capacity (CEC) of 1.2 mequiv./g. These anionic clays are irregularly aggregates from their primary units consisting of silicate plates in stacks.<sup>174</sup> The plate-like units are polygonal and polydisperse in geometric shape, carrying ionic charges and counter ions ( $\equiv\text{SiO}^-\text{Na}^+$ ) within the interlayer structure. The average plate dimension is 300×300×1 nm<sup>3</sup> for Mica, 100×100×1 nm<sup>3</sup> for MMT and 80×80×1 nm<sup>3</sup> for SWN. The negative surface charge density of Mica, MMT and SWN are 2.1, 0.708 and 30 (e/nm<sup>2</sup>), respectively.<sup>175</sup> Due to the presence of an intensive ionic charge character, these clays are capable of swelling and gelling in water.<sup>9</sup> With a similar plate-like structure (*ca.* 200×200×1 nm<sup>3</sup>) but with oppositely charged character, the layered double hydroxide (LDH) [Mg<sub>6</sub>Al<sub>2</sub>(OH)<sub>16</sub>]CO<sub>3</sub>•4H<sub>2</sub>O was prepared according

the reported procedures.<sup>176</sup> The cationic LDH clay has the counter-ions of carbonates<sup>177</sup> and positive charge density of 1.5 (e/nm<sup>2</sup>).<sup>178</sup> All properties of clays were summarized in **Table 8**.

**Table 8.** General Properties of Platelet Clays.

<b>Platelet-Like Clay</b>	<b>Composition</b>	<b>Surface Charge (e/nm<sup>2</sup>)</b>	<b>Dimension of one platelet (nm<sup>3</sup>)</b>
Synthetic fluorinated mica	Nature talc+Na <sub>2</sub> SiF <sub>6</sub>	-2.1	300×300×1
Sodium montmorillonite	Nature aluminosilicates	-0.708	100×100×1
Synthetic smectite	Nature talc+Na <sub>2</sub> SiF <sub>6</sub>	-30	80×80×1
Layered double hydroxide	[Mg <sub>6</sub> Al <sub>2</sub> (OH) <sub>16</sub> ]CO <sub>3</sub> •4H <sub>2</sub> O	1.5	200×200×1

### **2.1.2. Tubular Nanomaterials**

Carbon nanotubes was supplied by Seedchem Company Pty., Ltd. and prepared from chemical vapor deposition. The CNTs are 95% pure and 40–60 nm in diameter and 0.5–10 μm in length.



### **2.1.3. Nanoparticles**

Carbon nanocapsules (CNCs) were supplied by Industrial Technology Research Institute (ITRI) of Taiwan. The CNCs are 70% pure (30% carbon black) and 10–50 nm in diameter. Carbon black (CBs, Vulcan<sup>®</sup> XC-72, Cabot) were used as received.

#### 2.1.4. Hydrophobic Conjugated Polymers

The conjugated polymer, poly[2-methoxy-5-(2'-ethylhexyloxy)-1,4-phenylene vinylene] (MEH-PPV) with weight-average molecular weight ( $M_w$ ) of 51,000, was purchased from Aldrich Chemical Co. Two other conjugated polymers, sulfonated polyaniline (SPA) and triphenyl phosphine oxide cored polyaniline (TPOPA), were prepared as previously described.<sup>179</sup> Both SPA and TPOPA are rigid morphology with tubular and polygonal shape (**Figure 5a,b**), and sluggishly dispersible in water. All chemical structures of hydrophobic conjugated polymers are showed in **Figure 6a–c**.

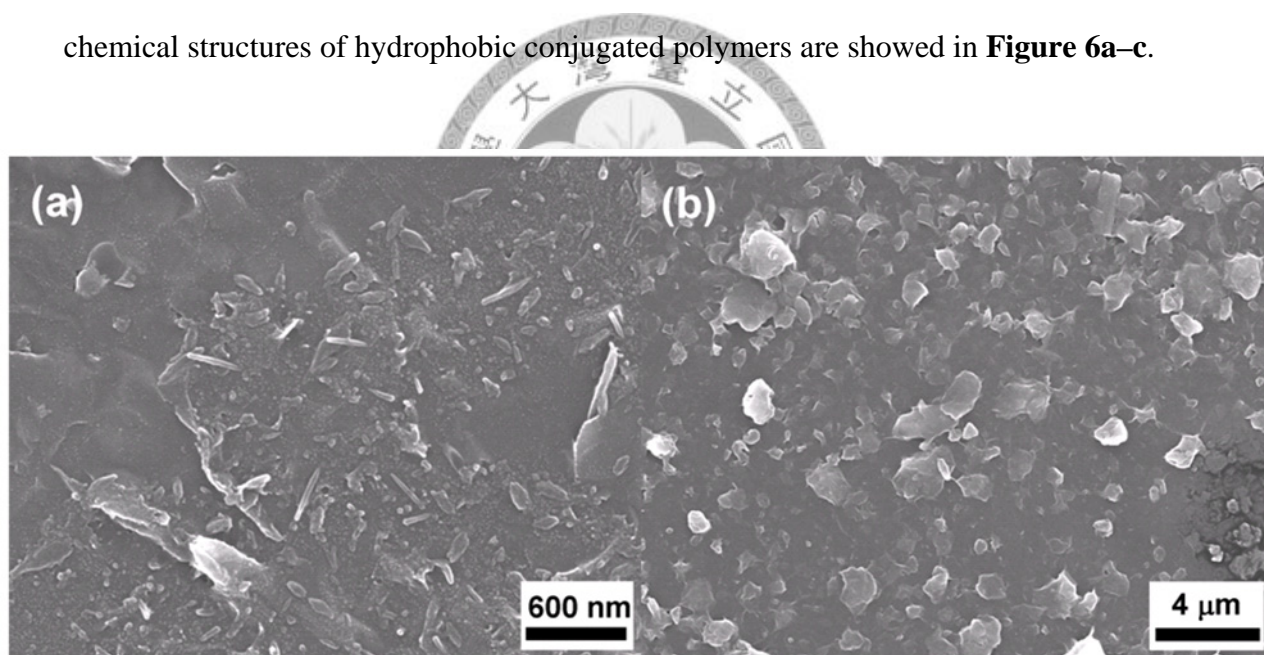


**Figure 5.** Scanning electron microscopy of tubular sulfonated polyaniline (a) and polygonal triphenyl phosphine oxide cored polyaniline (b).

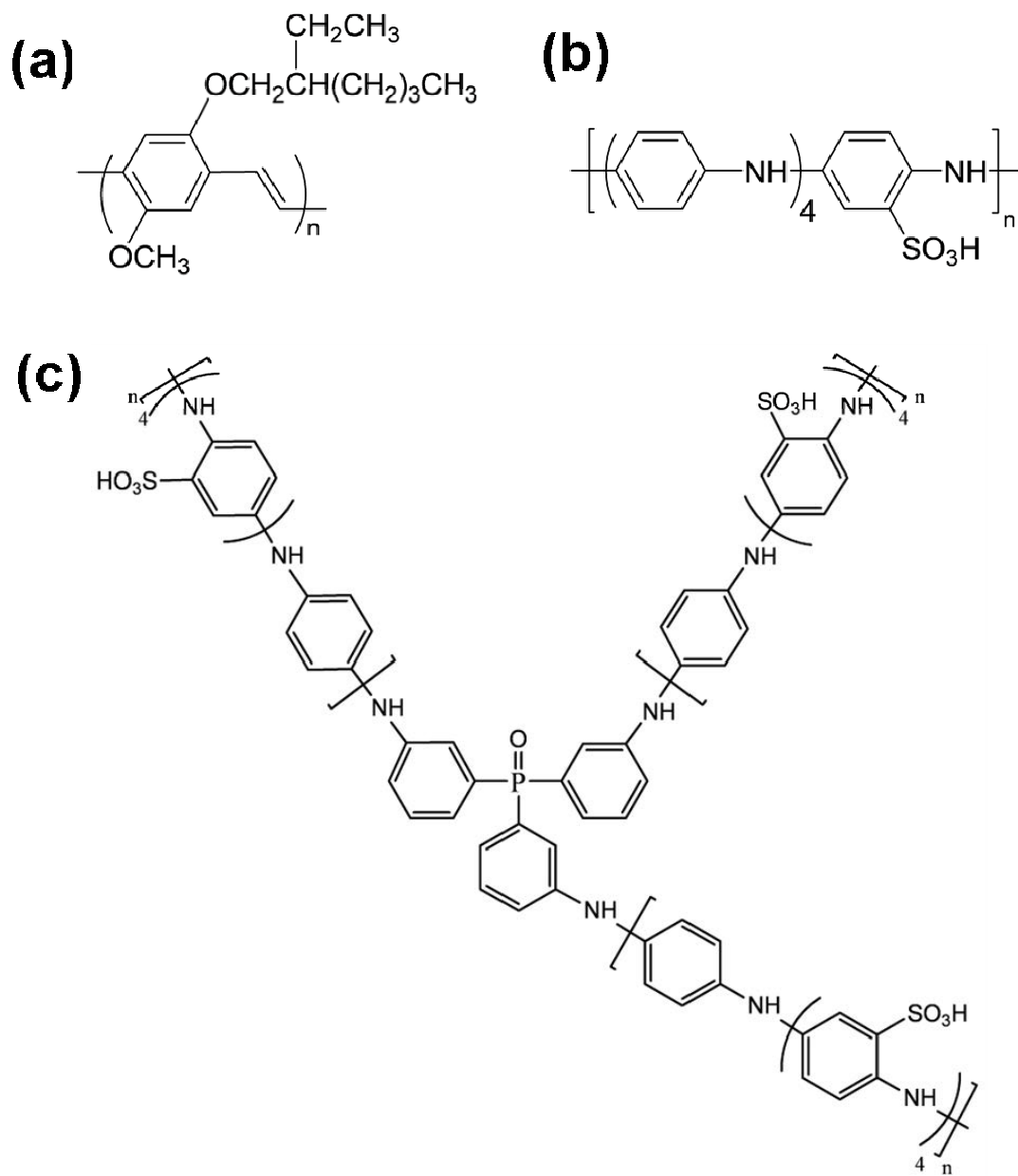
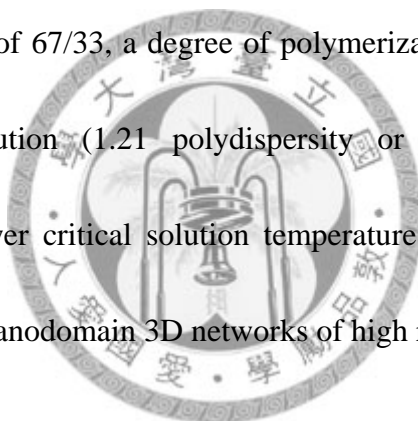


**Figure 6.** Chemical structures of MEH-PPV (a), SPA (b) and TPOPA (c).

### **2.1.5. Poly(*N*-Isopropyl Acrylamide)-Tethered NSP**

NSP were obtained by delaminating the layered Na<sup>+</sup>-MMT using an exfoliation process developed by our research group<sup>180</sup> and NSP-PNiPAAm was prepared according to the reported procedures.<sup>156d</sup> A linker with bromide and triethoxysilane functionalities was grafted onto the NSP clay surfaces at a weight ratio of 1/5 (linker/NSP). Subsequent atom-transfer radical polymerization (ATRP) afforded NSP-PNiPAAm brushes. The product of hybrids of PNiPAAm tethered to NSP had an organic/inorganic fraction of 67/33, a degree of polymerization of 1370 and a narrow molecular weight distribution (1.21 polydispersity or  $M_w/M_n$ ). Moreover, the NSP-PNiPAAm has a lower critical solution temperature (LCST) at 32–33 °C and controllable formation of nanodomain 3D networks of high regularity.



### 2.1.6. Organic Pigments

The organic pigments of red, green, blue, yellow and violet pigments (C.I. Name: Pigment Red 177, Pigment Green 36, Pigment Blue 15, Pigment Yellow 138, Pigment Violet 23) were obtained from BASF in powder form and the chemical structures were showed in **Figure 7**.

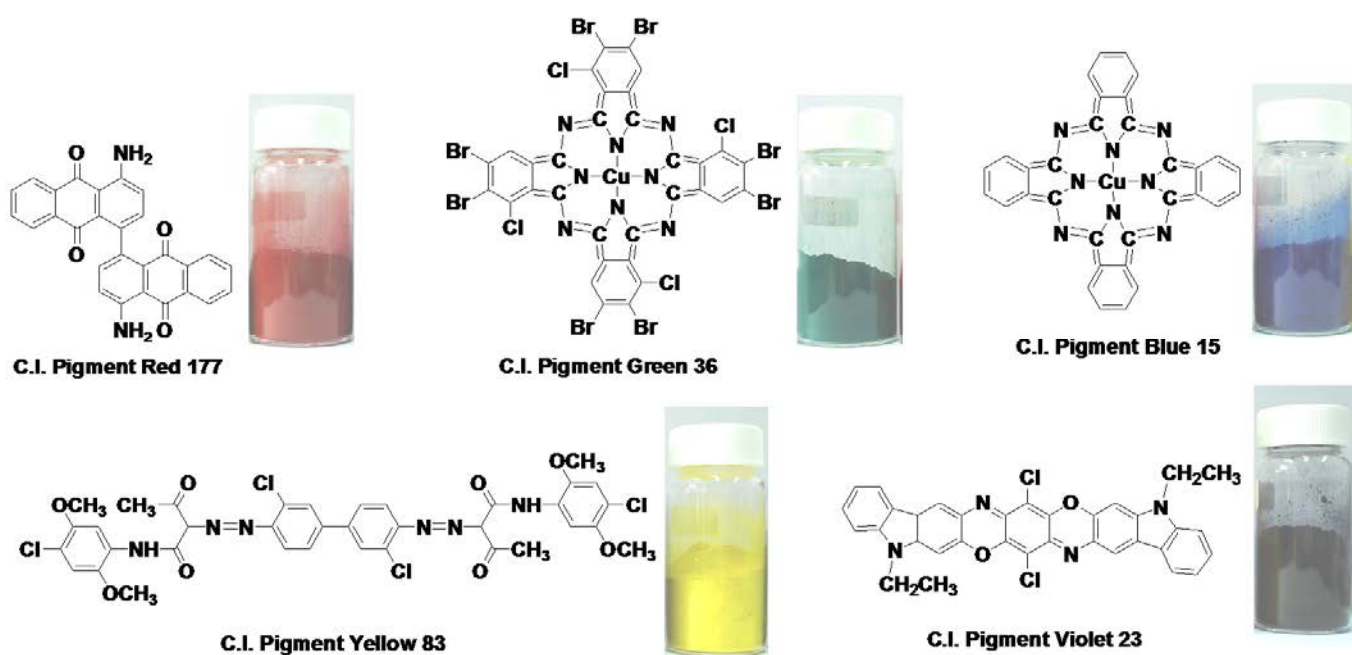
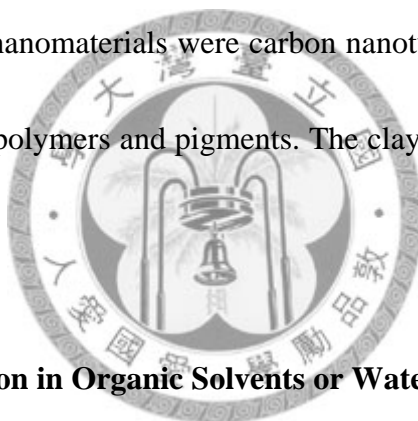


**Figure 7.** Chemical structures of pigments and their color appearances.

## 2.2. Preparation of Nanomaterials-Clay Hybrids

The procedure of mixing nanomaterial-clay hybrids were exemplified below. Nanomaterial (1 mg) and clay (1 mg) were ground adequately in an agate mortar and pestle. The sides of the mortar were occasionally scraped down with the pestle during grinding to ensure a thorough mixing. The mixture was washed from mortar and pestle using deionized water at concentration of 1 mg nanomaterial in 20 g water. The nanomaterial-clay hybrids were prepared at weight ratios of clay/nanomaterial = 1/3, 1/2, 1/1, 2/1 and 3/1. The nanomaterials were carbon nanotubes, carbon nanocapsules, carbon blacks, conjugated polymers and pigments. The clays were Mica, MMT, SWN, LDH and NSP-PNiPAAm.



## 2.3. Amphiphilic Dispersion in Organic Solvents or Water

Ternary mixtures of the Mica-CNT hybrid were examined for the dispersion ability in water and toluene in different orders of addition. In the first example, the hybrid of Mica-CNT (weight ratio of Mica/CNT = 2.0 mg/1.0 mg) was added to 7.5 g water first, thoroughly dispersed and then added to 7.5 g toluene. In the second example, the hybrid was dispersed in toluene, homogeneously mixed and then added to water. During the mixing, ultrasonic vibration was applied for 2 min. Ultrasonication was operated on BRANSON 5510R-DTH (135 W, 42 kHz).



## 2.4. Characterizations

### 2.4.1. Dispersion

The dispersion of nanomaterials was examined by the following instruments. Ultraviolet-visible (UV-vis) absorbance was measured by Perkin-Elmer Lambda 20 UV-vis spectrophotometer at 550 nm. Transmission electron microscopy (TEM) was performed on a Zeiss EM 902A at 120 kV. Samples were prepared by drop-coating sample solution (0.01 wt%) on a copper target and evaporation under vacuum at ambient temperature for 1h. Field emission-scanning electron microscopy (SEM) images were obtained from a JOEL JSM-6700F SEM system. The samples were coated with Au before the SEM measurements. The liquid water contact angle (WCA) at the surface of CB/clay was measured with the sessile-drop method by using a contact angle system FTA 200 (ACIL & First Ten Angstroms Inc.).

### 2.4.2. Thermoresponsive Behavior

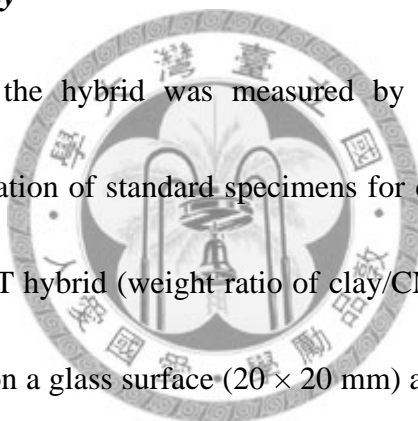
The thermoresponsive behavior was examined by the following instruments. The UV-vis transmittance of nanomaterial solution was monitored at 524 nm. During the measurement of UV-vis transmittance, hybrid solution was controlled in a temperature gradient that ramped from 25 °C to 50 °C. The LCST of NSP-PNiPAAm/MEH-PPV was observed by SEM at 80 kV.

#### ***2.4.3. Luminescence Property***

The CP hybrid films were prepared by dropping 0.1% (w/w) CP/clay solutions on 10×10 mm glass substrate and dried at 80 °C. Both solutions and films of the CP/clay hybrid were analyzed by photoluminescence spectrophotometer LS45/55. The light-emitting phenomenon was observed under the UV light from a handheld ultraviolet (UV) lamp, UVGL-85 (365 nm, 6 watt, 115 V, 60 Hz, 0.12 amps).

#### ***2.4.4. Conductivity Property***

The conductivity of the hybrid was measured by a four-terminal technique (ASTM F390). The preparation of standard specimens for conductivity was described as following. The clay-CNT hybrid (weight ratio of clay/CNT = 2/1) was dispersed in toluene or water, dropped on a glass surface (20 × 20 mm) and then dried in an oven at 80 °C.



#### ***2.4.5. Thermal Degradation, Particle Size and Zeta Potential Properties***

Thermal gravimetric analysis (TGA) was performed on Perkin-Elmer Pyris 1 TGA from 100 °C to 800 °C in air to examine the thermal stability of clay-CNT hybrid. A ZetaPlus zetameter (Brookhaven Instrument Corp., NJ) was used for characterizing the ionic property of the pristine clays and MEH-PPV/clay hybrids. Samples of aqueous suspension at 0.01 and 0.02 wt% were measured. The suspension pH was

adjusted to pH 7 by either adding 0.5 M NaOH or HCl. The zeta potential was measured in the solution with an ionic strength of 0.2. The same instrument was used to estimate the average particle size of the clay particles.



---

---

## Chapter 3. Results and Discussion

---

---

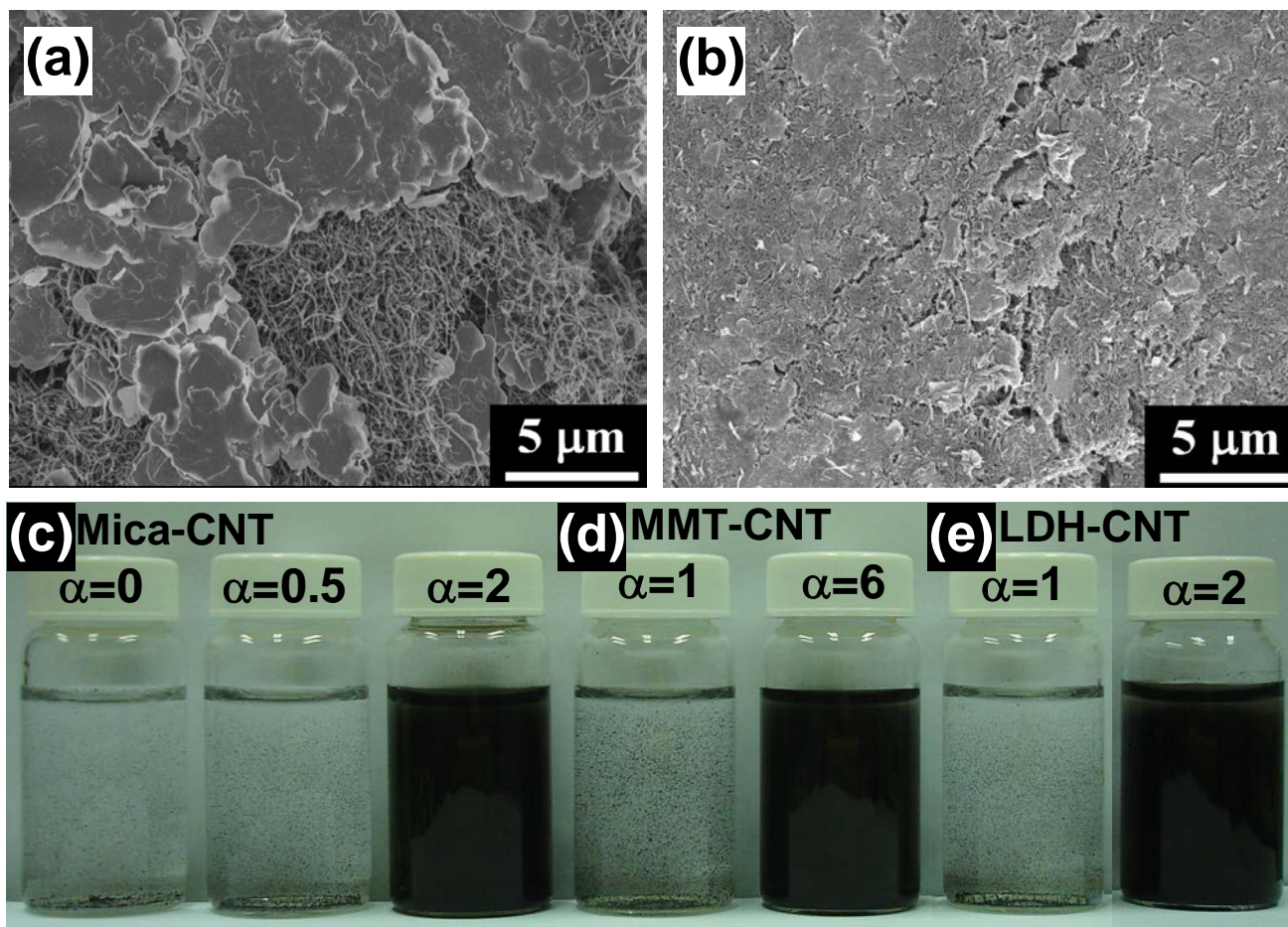
### 3.1. Dispersion of Tubular-Like Nanomaterials by Using Platelet-Like Clays<sup>7</sup>

In this section, we revealed a unique nature of dispersing behavior for the pulverized CNTs with platelet-like silicates and development of a convenient method for dispersing without using organic dispersants. In particular, the synthetic fluorinated mica clay is most effective due to its large plate size and anionic property. Through the simple physical mixing of two nanomaterials of different geometric shapes, tubular-like nanomaterials and plate-like silicate clays, the mutual interaction affects their inherent self-aggregating forces. The CNT-clay hybrid is dispersible in most common organic solvents including water and toluene. The possible formation of micelle-like microstructures of CNT-clay mixture is postulated and indirectly proven their existence by measuring the thermal and electronic properties. A mechanism, involving the factor of geometric-shape difference and mutual exclusion of non-covalent bonding interaction among the pristine nanoparticles, was proposed to account for this dispersion preference.

### 3.1.1. Dispersion of Carbon Nanotubes in the Presence of Clays

The tube-like CNTs are composed of conjugated  $sp^2$  orbital bonds. Due to the high aspect-ratio dimension of 40–60 nm in diameter and 0.5–10  $\mu\text{m}$  in length, the materials tend to aggregate and are difficult for solvating into water or organic solvents. The self-aggregation and entanglement are mainly caused by van der Waals force attraction. However, when CNTs were properly ground with the plate-like clays such as the fluorinated Mica, the pulverized powders as a physical mixture became readily dispersible in water. The grinding procedure for the preparation can be monitored by the FE-SEM image. As shown in **Figure 8**, the heterogeneous mixtures were observed after grinding 1 min (**Figure. 8a**), and the homogeneity was obtained after grinding 5 min (**Figure. 8b**). The dispersion of CNTs was observed by compounding CNT with the clays at varied weight ratios. Initially, it was found that the Mica with CNT at 2:1 weight ratio, or  $\alpha = 2$  (defined as the weight ratio of clay to CNT), could render the mixtures easily dispersible in water to generate a fine slurry. The fine dispersion can be differentiated by naked eyes as a black suspension from solid precipitates in the bottom layer (**Figure 8c**). The controlled experiments showed that the pristine CNTs were not dispersible in water but forming severe aggregates. The efficacy for the CNT dispersion depends on the relative amount of the Mica presence. The black CNTs were mostly precipitated at the bottom of water phase when using a lesser amount of Mica

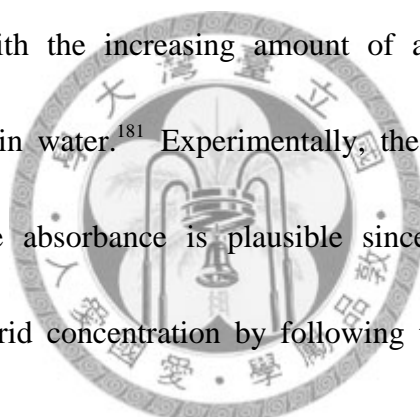
to CNT at  $\alpha = 1-0.5$ . It appears that the presence of Mica may mitigate the formation of CNT aggregates.



**Figure 8.** FE-SEM of CNTs and Mica under pulverizing for (a) 1 min and (b) 5 min. Visual observation of the dispersion of clay-CNT hybrids in water: (c) Mica-CNT, (d) MMT-CNT and (e) LDH-CNT, under varied  $\alpha$  value ( $\alpha = \text{clay/CNT}$  weight ratio). Each sample contained 1 mg CNTs in 20 g water.

In order to understand the nature of Mica-CNT interaction, two other clays including MMT and cationic type of LDH were further examined. The use of different clays in geometric dimension and charges, for examples, Mica ( $300 \times 300 \times 1 \text{ nm}^3$ ), MMT ( $80 \times 80 \times 1 \text{ nm}^3$ ) and LDH ( $200 \times 200 \times 1 \text{ nm}^3$ ), allow the understanding of

their size effect for the CNT dispersion in water. In **Figure 8d,e**, the photographs illustrate the fine CNT dispersion was obtained by the addition of MMT at  $\alpha = 6$  (or 6 times the clay weight to CNTs). For comparison, Mica is more effective than MMT under the same agitating condition of mechanical stirring or shaking. These results indicate that the platelet size may be the dominating factor for the fine dispersion. The dispersion was further measured by analyzing the suspension using a UV-visible spectrometry. As shown in **Figure 9a**, the absorbance at 550 nm for the CNTs becomes more intense with the increasing amount of added Mica, implying the increase of CNT content in water.<sup>181</sup> Experimentally, the comparison of dispersing ability by the UV-visible absorbance is plausible since the absorbance actually correlates well to the hybrid concentration by following the Lambert-Beer's law.<sup>182</sup> The standard curves of absorbance against concentration were established at 550 nm (**Figure 9b**) for the hybrids of using three different clays. According to the UV-vis analysis in **Figure 9a**, the Mica is most effective for enhancing the CNT dispersion in water. The absorbance reached to a maximum when the Mica-CNT weight ratio approached  $\alpha = 2-3$ , but required a higher  $\alpha$  value of 6 for the comparative MMT.



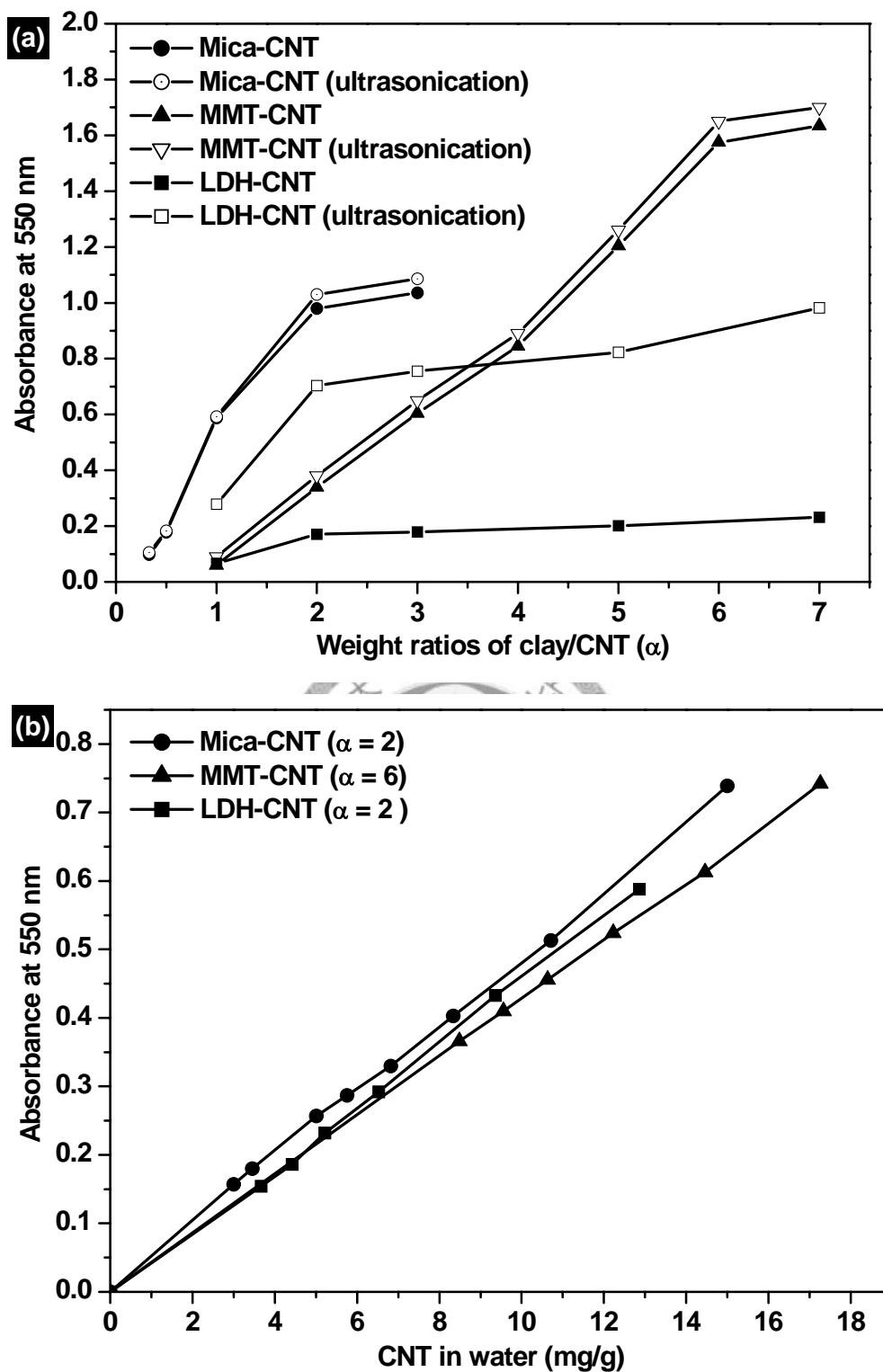
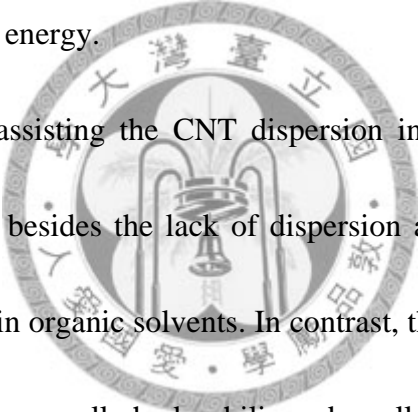


**Figure 9.** (a) UV-vis absorbance of clay-CNT at different  $\alpha$  value of hybrids in water. (b) Three standard curves of clay-CNT hybrids at different CNT content. The increase of UV-vis absorbance in (a) indicated the dispersing ability of the clay species improvement of CNT dispersion in reference to the standard curves in (b) of absorbance vs. CNT in water.



In considering their ionic charges, the LDH is ionic, with cationic charges on the platelet surface and nitrate anionic species as the counter ions. The ionic charge interaction between CNTs and clay, through the clay surface anions ( $\equiv\text{SiO}^-$ ) in MMT and Mica structures or cations in LDH, may be the second reason for affecting the CNT dispersion. The apparent dispersing experiments indicated that the LDH was also effective but requiring an additional ultrasonic agitation during mixing as shown in **Figure 9b** (LDH-CNT). In general, the ultrasonic vibration was found to be able to provide additional agitation energy.



The role of Mica in assisting the CNT dispersion in other mediums was also explored. It is known that, besides the lack of dispersion ability in water, CNTs are only sluggishly dispersible in organic solvents. In contrast, the inorganic clay materials such as MMT and LDH are generally hydrophilic and swollen in water, but lacking the dispersing ability in most organic mediums. However, due to the presence of fluorinated functionality, the synthetic Mica is actually amphiphilic or behaving a dual dispersing property in water as well as in most common solvents, such as ethanol, acetone, dimethyl formamide and toluene. As summarized in **Table 9**, Mica could generally affect the CNTs to dispersion in most organic mediums. For example, the pulverized Mica-CNT hybrid at  $\alpha = 2$ , after thoroughly grounding and ultrasonic agitation, became dispersible for most organic solvents.

**Table 9.** Dispersion of CNT, Mica and the Hybrid in Various Mediums.

Solvents	Mica <sup>a</sup>	MMT <sup>a</sup>	CNT <sup>b</sup>	Clay-CNT <sup>c</sup>
H <sub>2</sub> O	+	+ <sup>d</sup>	- <sup>e</sup>	+
Ethanol	+	-	-	+
Acetone	+	-	-	+
DMF	+	-	+	+
Toluene	+	-	-	+

<sup>a</sup> Clay (Mica or MMT, 2 mg) in 20 g of solvent. <sup>b</sup> CNT (1 mg) in 20 g of solvent.

<sup>c</sup> Clay-CNT hybrid (2.0 mg/1.0 mg or  $\alpha = 2$ ) dispersed in 20 g of solvent. <sup>d</sup> + good dispersion. <sup>e</sup> - poor dispersion or precipitation.

### 3.1.2. Amphiphilic Property for Dispersion

Being dispersible in both of water and toluene, the Mica-CNT hybrid ( $\alpha = 2$ ) is considered to be amphiphilic in nature. This dual hydrophilic/hydrophobic dispersion behavior was further shown to be in an irreversible manner. In **Figure 10a**, it shows the grinding procedure of preparation Mica-CNT hybrid. The hybrid was dispersed in water first and then adding toluene, shaking and allowing settlement, the black Mica-CNT remained in the water phase (**Figure 10b**). In contrast, if the same hybrid powder was dispersed in toluene first, a toluene suspension remained in toluene phase even after vigorously agitated with water (**Figure 10c**). The order of solvent exposure to either water or toluene determined the hybrid's preference in an irreversible manner. The phenomenon is explainable by adopting the concept of stable "micelle-like" microstructures, the formations of water-in-oil (W/O) and oil-in-water (O/W) phases as shows in **Figure 11e**.

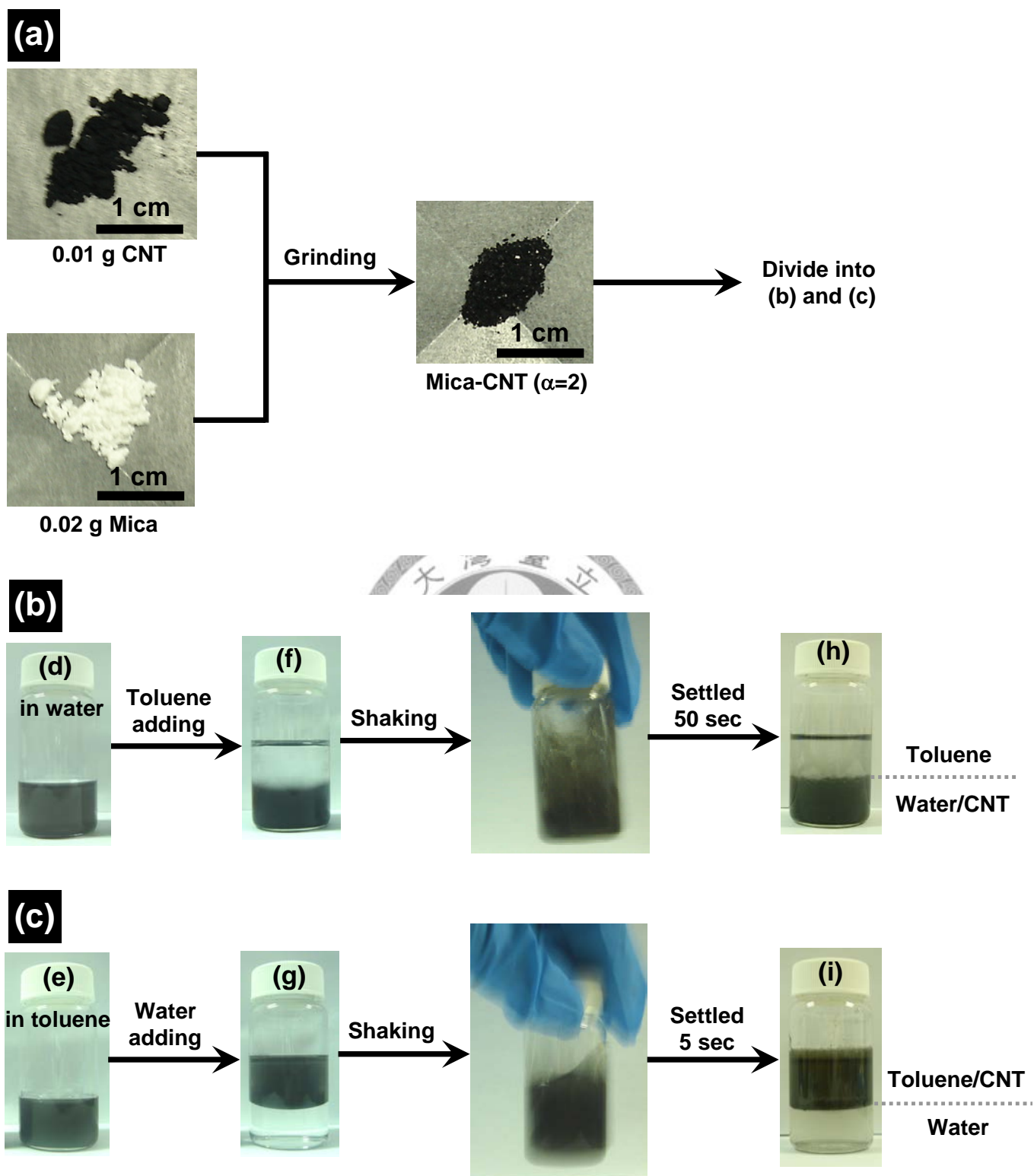


**Figure 10.** Irreversible dispersion phenomenon of Mica-CNT at  $\alpha = 2$ : (a) Grinding procedure of Mica-CNT hybrid. Hybrid was dispersed in either water (d) or toluene (e), both dispersions remained in the original solvent after adding the other solvent (f and g). After vigorously shaking, the dispersion settled into distinct layers in an irreversible manner (h and i).

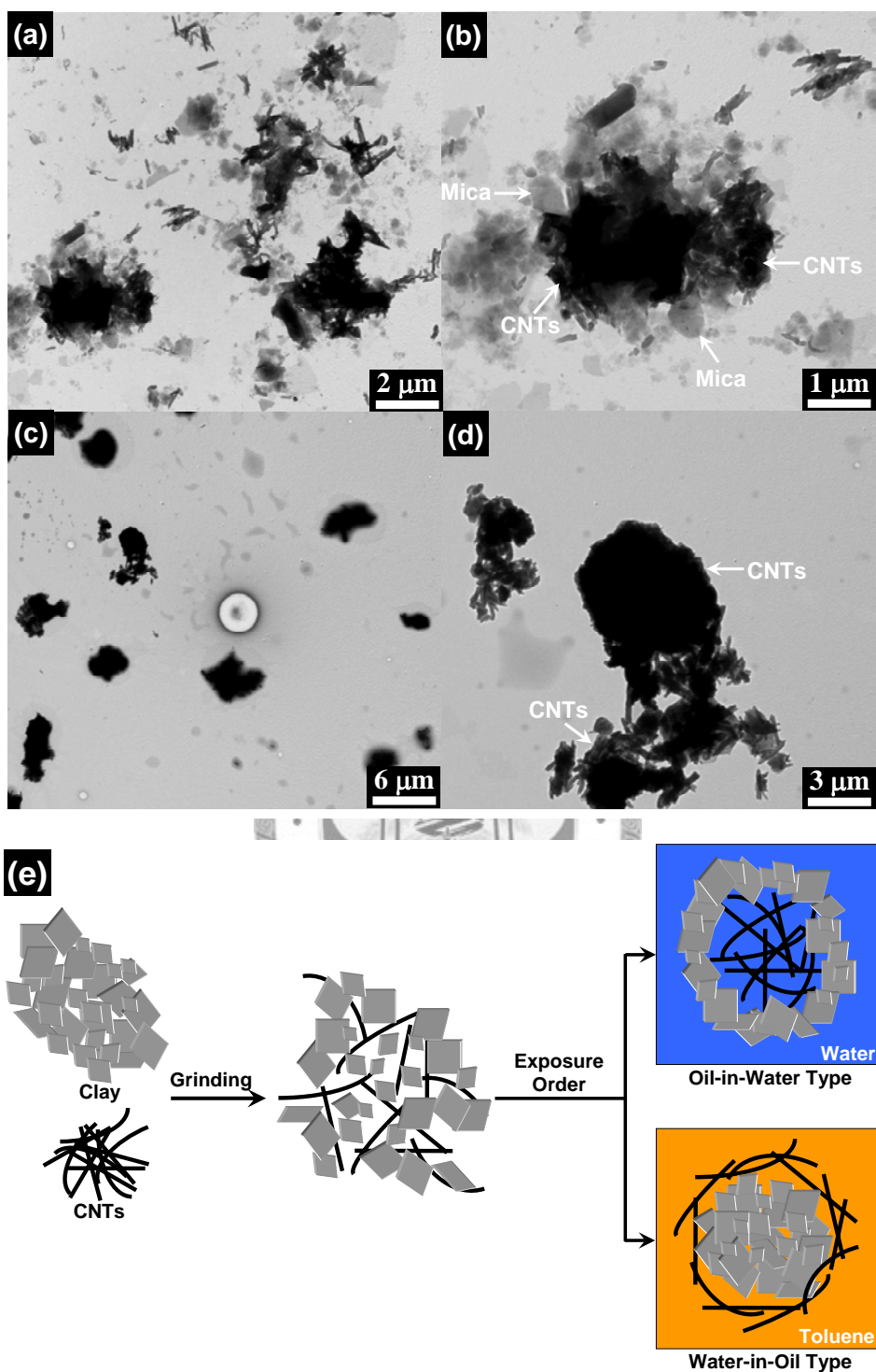


**Figure 11.** TEM images of Mica-CNT hybrid dispersed in water (a and b) and in toluene (c and d). Mica-CNT hybrid was obtained from the same batch, however, hybrid has completely different microstructures when exposing to water or toluene. In water, hybrid shows more Mica appearance, on the contrary, more hairy CNT composition was observed. Conceptual presentation of amphiphilic dispersion with oil-in-water (O/W) and water-in-oil (W/O) microstructures (e), representing CNT-in-Mica and Mica-in-CNT, respectively.

Regarding the nature of “micelle-like” microstructures, both types of dispersions in water and toluene were analyzed by using TEM, TGA and devise of electrical conductivity. The dispersion was spread and evaporated on copper grid for the TEM observation. Different morphologies of microstructures can be differentiated, more visible Mica platelets in micrometer size aggregation are found for the hybrid being exposed with water (**Figure 11a,b**). On the contrary, when the Mica-CNT hybrid was dispersed in toluene, the CNT aggregates appear to be on the surface of microstructures (**Figure 11c,d**). On thermal stability, the Mica-CNT hybrid exhibited different decomposition patterns when being exposed with water or toluene. The hybrid after dispersing in water is thermally more stable than that in toluene. There is a 50 °C difference in the decomposition patterns for delaying the weight loss (**Figure 12**). It appears that the Mica surrounded CNTs in an O/W microstructure may have a shielding effect for the CNT decomposition, in comparison with the naked CNTs in the W/O hybrid. Furthermore, the micelle-like microstructures can be further indirectly evidenced by the performance of conductivity. When the hybrid was coated on the glass substrate, the specimen from toluene suspension had a higher conductivity at  $10^{-4}$  S/cm than that from water suspension, at  $10^{-6}$  S/cm. The result of two-order magnitude difference is derived from the same batch of pulverized powder ( $\alpha = 2$ ). Hence, two

forms of W/O and O/W type or different arrangement of CNT-in-Mica and Mica-in-CNT microstructures are indirectly evidenced.

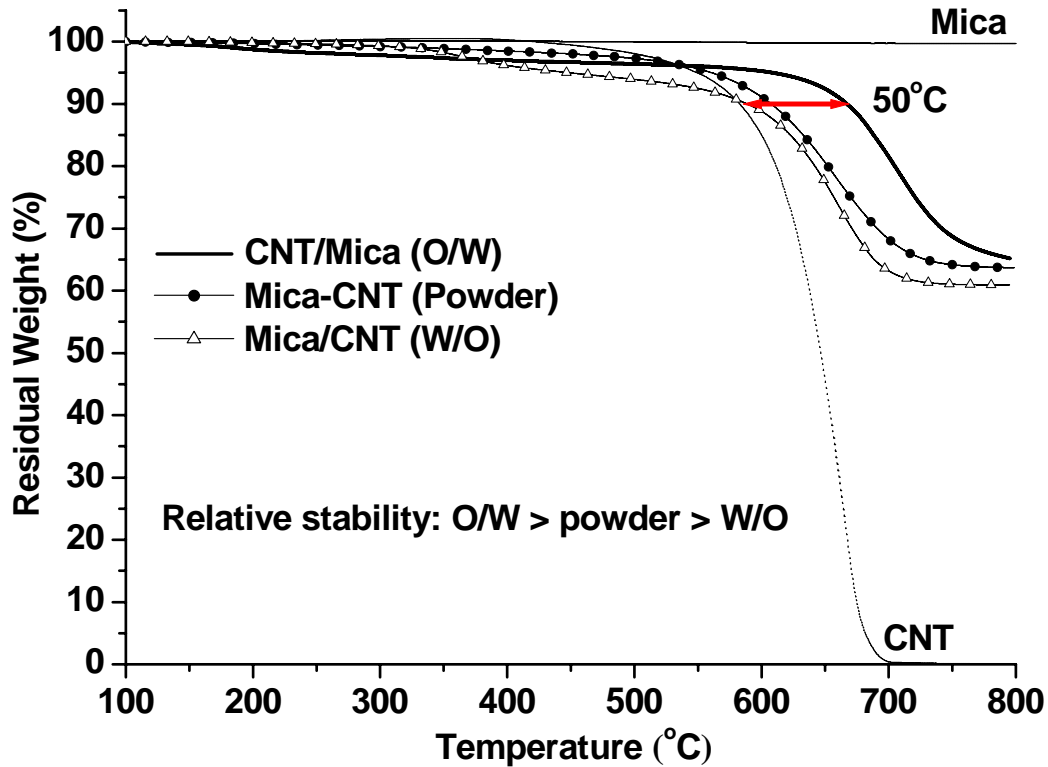


**Figure 12.** TGA patterns for the pristine CNT, Mica and their hybrid ( $\alpha = 2$ ). Mica-CNT (pulverized powder); Mica-CNT (O/W): the hybrid being dispersed in water and dried; Mica-CNT (W/O): the hybrid being dispersed in toluene and dried.

### 3.1.3. Explanation for the Formation of Mica-CNT Microstructures

The formation of two Mica-CNT microstructures is attributed to the randomization of the non-covalent bonding forces among individual CNTs and clays in different hydrophilic water or hydrophobic toluene medium. The initial grinding of two nanomaterials, tube-like CNTs and plate-like clay, could largely redistribute the original CNT self-aggregation. Their CNT entanglement force may be mitigated or blocked by the neighboring platelets due to the difference in their geometric shapes.

Furthermore, since the clay is hydrophilic, the contact with water could render the hybrid to form an O/W microstructure, comprising CNTs as the core and Mica as the surrounding corolla. Similarly, the opposite water-in-oil (W/O) or Mica-in-CNT microstructures is possibly generated since the CNTs favored the toluene in the continuous phase. Two different types of microstructures could be generated and stabilized through the vigorous agitation in the selected solvent.

#### **3.1.4. Conclusion**

The dispersion ability of CNTs in various organic mediums or in water was significantly improved by simply grinding CNTs with clays into fine powder. In particular, the CNT dispersion in water and toluene was significantly enhanced by Mica that was more effective than MMT or LDH because of its high aspect-ratio geometric shape and anionic character. A mechanism involving the formation of CNT-Mica and Mica-CNT micelle-like microstructures, resembling the organic surfactants in oil-in-water and water-in-oil forms, is proposed. The existence of two different microstructures was indirectly evidenced by observing the differences in thermal stability due to the Mica shielding in CNT-in-Mica microstructure and variable electrical conductivity ( $10^{-4}$  vs.  $10^{-6}$  S/cm). The clay-assisted CNT dispersion in water without using an organic dispersant may offer a significant advances for the CNT applications.

### 3.2. Dispersion of Spherical-Like Nanoparticles by Using Platelet-Like Clays

In **Section 3.2.**, we applied the GIF for dispersing spherical nanoparticles (i.e. CNCs, CBs, AgNPs and FeNPs) in the presence of platelet-like silicates and development of a convenient method for dispersing without using organic dispersants or covalent bonding approaches. Various platelet-like silicates including sodium montmorillonite (MMT), synthetic fluorinated mica (Mica), synthetic smectite (SWN) and layered double hydroxide (LDH) were used to generalize the GIF in spherical nanoparticles. A mechanism, involving the factor of geometric-shape difference between spherical particles and platelet-like materials was proposed.





### 3.2.1. Dispersion of Carbon Nanocapsules in the Presence of Clays<sup>183</sup>

In this study, the GIF is applied for dispersed nanoparticle through the large geometric difference between spherical- and platelet-like nanomaterials (**Figure 13**).

The dispersion of nanoparticles can be greatly improved by pulverized the platelet-like clay with CNCs or CBs.

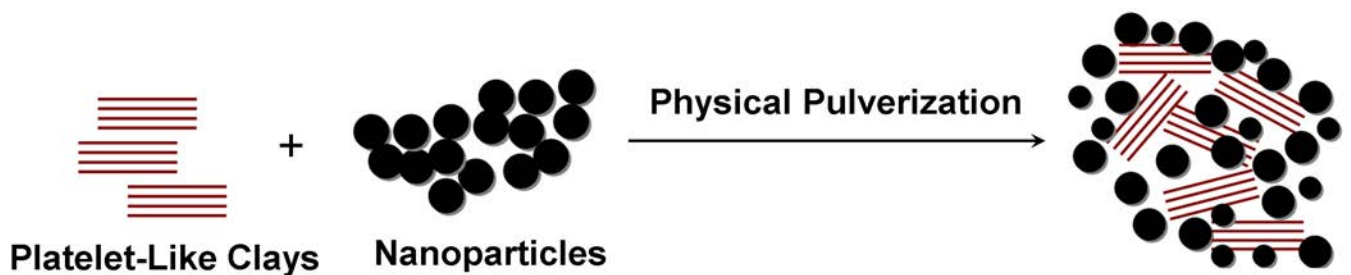


**Figure 13.** Conceptual Diagram of dispersion nanoparticles by geometric-shape inhomogeneity factor.

In the first case, four clays were used to realize the effectiveness of dispersing CNCs. According to the conclusion in **Section 3.1.**, the higher aspect ratio of platelet clay, the more effective dispersion can be achieved. The results of dispersing CNCs have a consisted with the previous results. As shown in **Figure 14**, the dispersion of CNCs was observed by compounding CNCs with the clays at varied weight ratios. The fine dispersion can be differentiated by naked eyes as a black suspension from solid precipitates in the bottom layer (**Figure 14a–d**). The controlled experiments showed that the pristine CNCs were not dispersible in water but forming severe aggregates (**Figure 14e**). These results indicate that the platelet size may be the dominating factor for the fine dispersion.

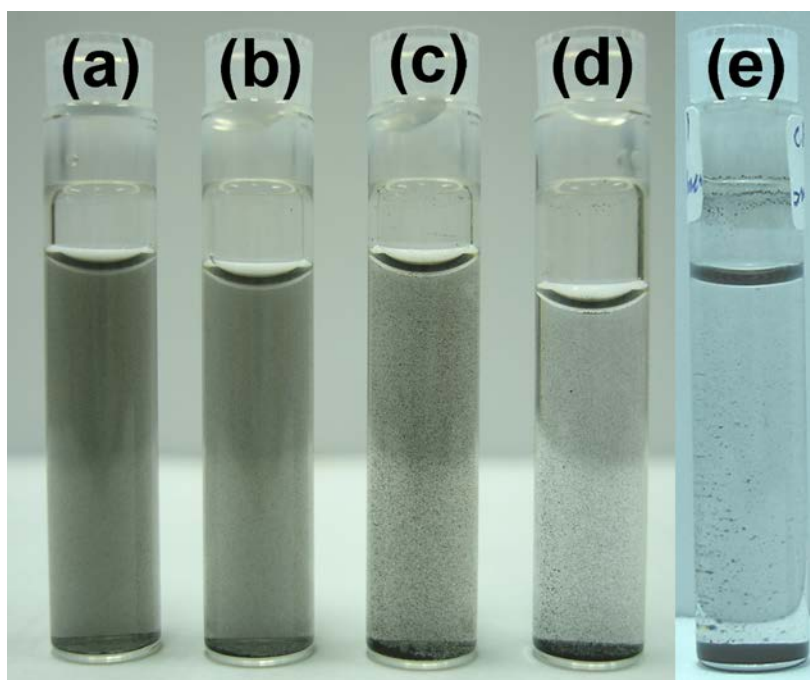


**Figure 14.** Visual observation of dispersing CNCs by different clays. (a) pristine CNCs (b) Mica (c) MMT (d) SWN (e) LDH (1 mg CNCs/5 g water; weight ratio of CNCs/clay = 1/1).

The dispersion was further measured by analyzing the suspension using a UV-visible spectrometer. As shown in **Figure 15**, the absorbance at 550 nm for the dispersion of CNCs has correlated to the dimension of clay. The larger dimension of clay has higher absorbance. For examples, UV-vis absorbance has a trend of CNC-Mica > CNC-MMT > CNC-SWN which is consisted with the dimension of Mica ( $300 \times 300 \times 1 \text{ nm}^3$ ) > MMT ( $80 \times 80 \times 1 \text{ nm}^3$ ) > SWN ( $50 \times 50 \times 1 \text{ nm}^3$ ). Consideration of the surface charge, the negative character of clay (i.e. Mica, NNT and SWN) is suitable for dispersing CNCs due to the result of LDH (positive surface charge) showed severe aggregation and precipitation. In summary, the Mica is the most suitable material for dispersion CNTs and CNCs.

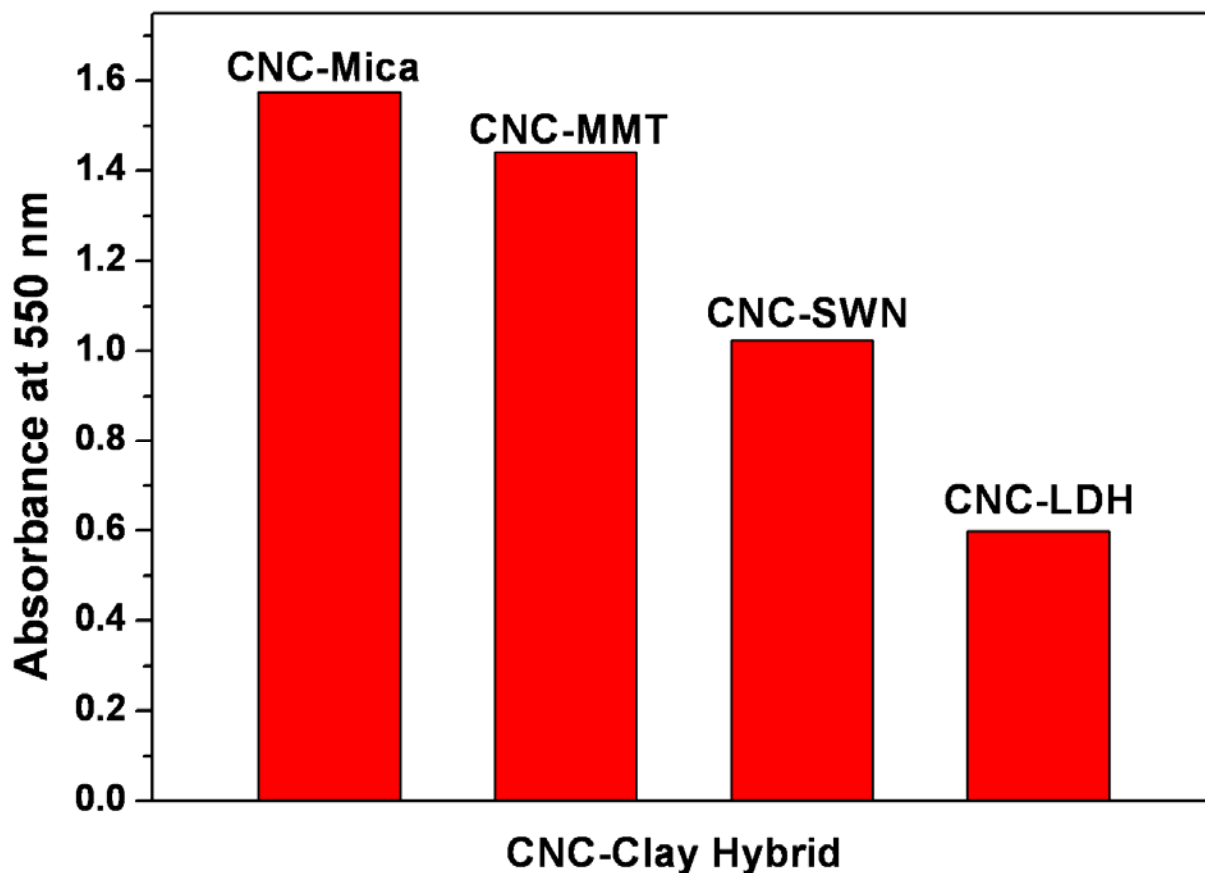


**Figure 15.** UV-vis absorbance of CNC-Clay hybrid in water.

Comparison to dispersion of CNTs, the CNCs showed the same trend and the dispersion efficiency can be controlled by the amount of Mica. Initially, it was found that the weight ratio of Mica/CNCs = 2/1, could render the mixtures easily dispersible in water to generate a deep-grey solution (**Figure 16d**). However, the dispersion of hybrid at weight ratio of Mica/CNCs = 0.5/1–1/1 showed light-grey color (**Figure 16a,b**). The difference of color indicated the degree of dispersion, for example, deep-grey color solution means homogeneous dispersion or light-grey color means poor dispersion.

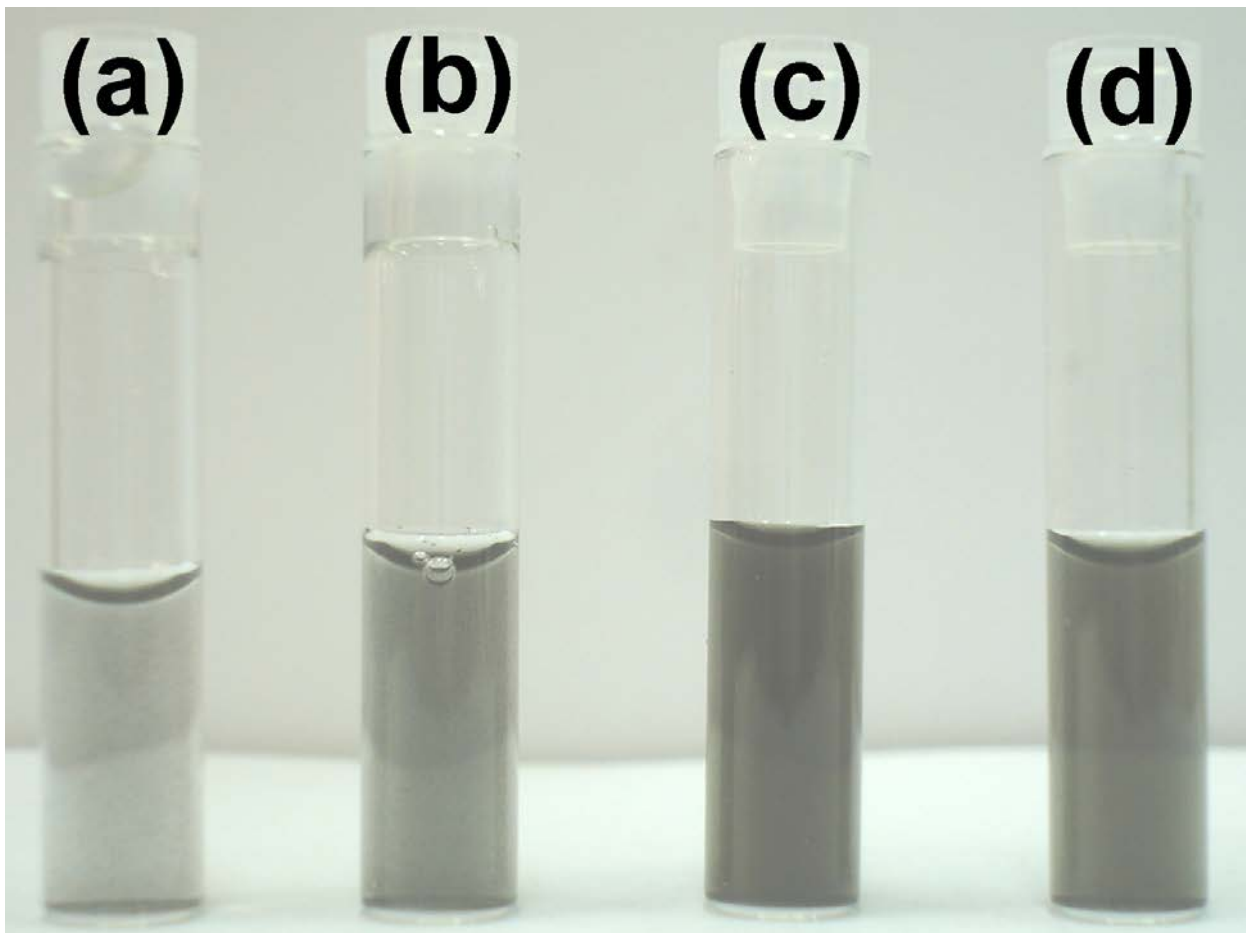


**Figure 16.** Visual observation of CNC-Mica hybrid in water at weight ratio of Mica/CNC = 0.5/1 (a), 1/1 (b), 2/1 (c) and 3/1 (d). (1 mg CNCs/5 g water)

By using UV-vis analysis, the result revealed enhancing absorbance with increasing Mica amount and an optimal weight ratio of Mica/CNCs was found at weight ratio of Mica/CNCs = 2/1 due to the strong van der Waal attractions of CNCs were decreased or redistributed by the presence of Platelet-Like Mica (**Figure 17**). Experimentally, the comparison of dispersing ability by the UV-vis absorbance is plausible since the absorbance actually correlates well to the hybrid concentration by following the Lambert-Beer's law. As shown in **Figure 17 insert**, the absorbance of CNC-Mica hybrid was well correlated with the content of hybrid.

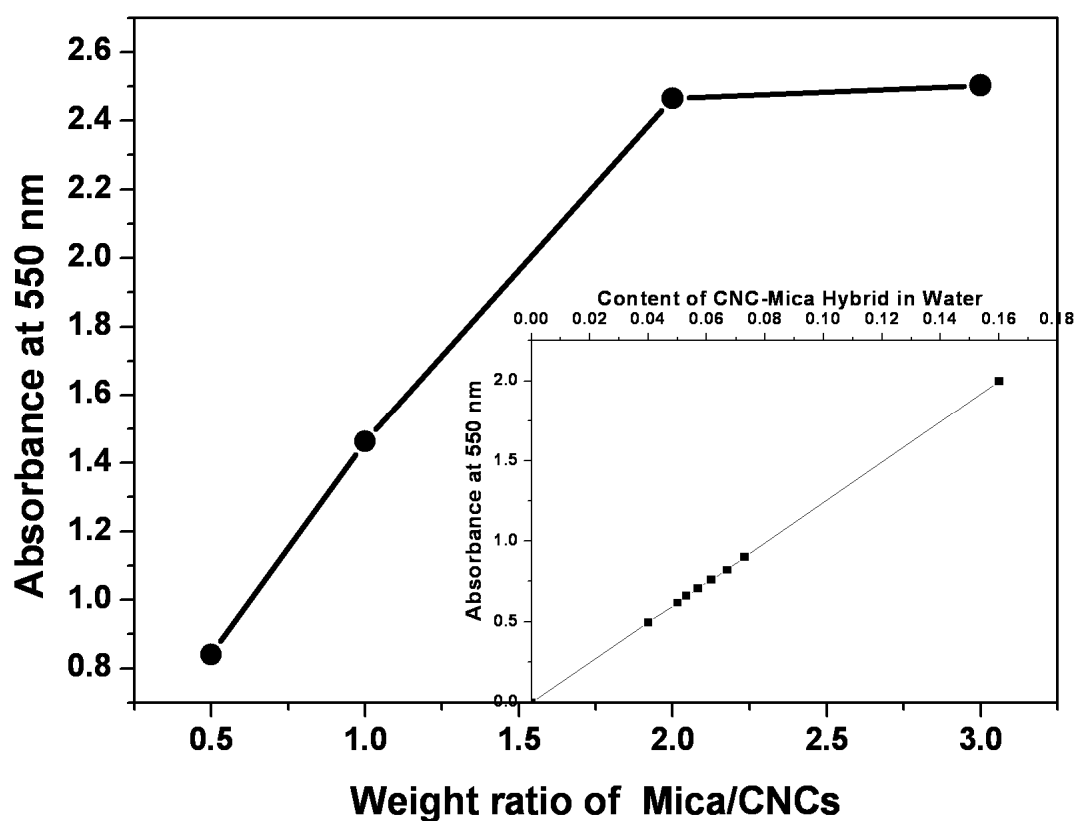


**Figure 17.** UV-vis absorbance of CNC-Mica hybrid in water and the standard curves of absorbance against concentration (insert).

The homogeneous hybrid powder and dispersion of CNC-Mica can be confirmed by SEM and TEM. After adequately pulverized the CNCs and Mica together, the SEM image showed homogeneous powder (**Figure 18a,b**). In the higher magnification of image (**Figure 18c,d**), the morphology rendered the platelet-like Mica surface were decorated by spherical CNCs. The dispersion of CNC-Mica hybrid was observed by TEM and the individual CNCs can be observed (**Figure 18e**). The higher resolution TEM showed the multi-layer structure of carbon nanocapsule (**Figure 18e insert**). On contrary, the pristine CNCs revealed severe aggregation and various carbon materials (amorphous carbon, CNTs) can be observed (**Figure 18f**).

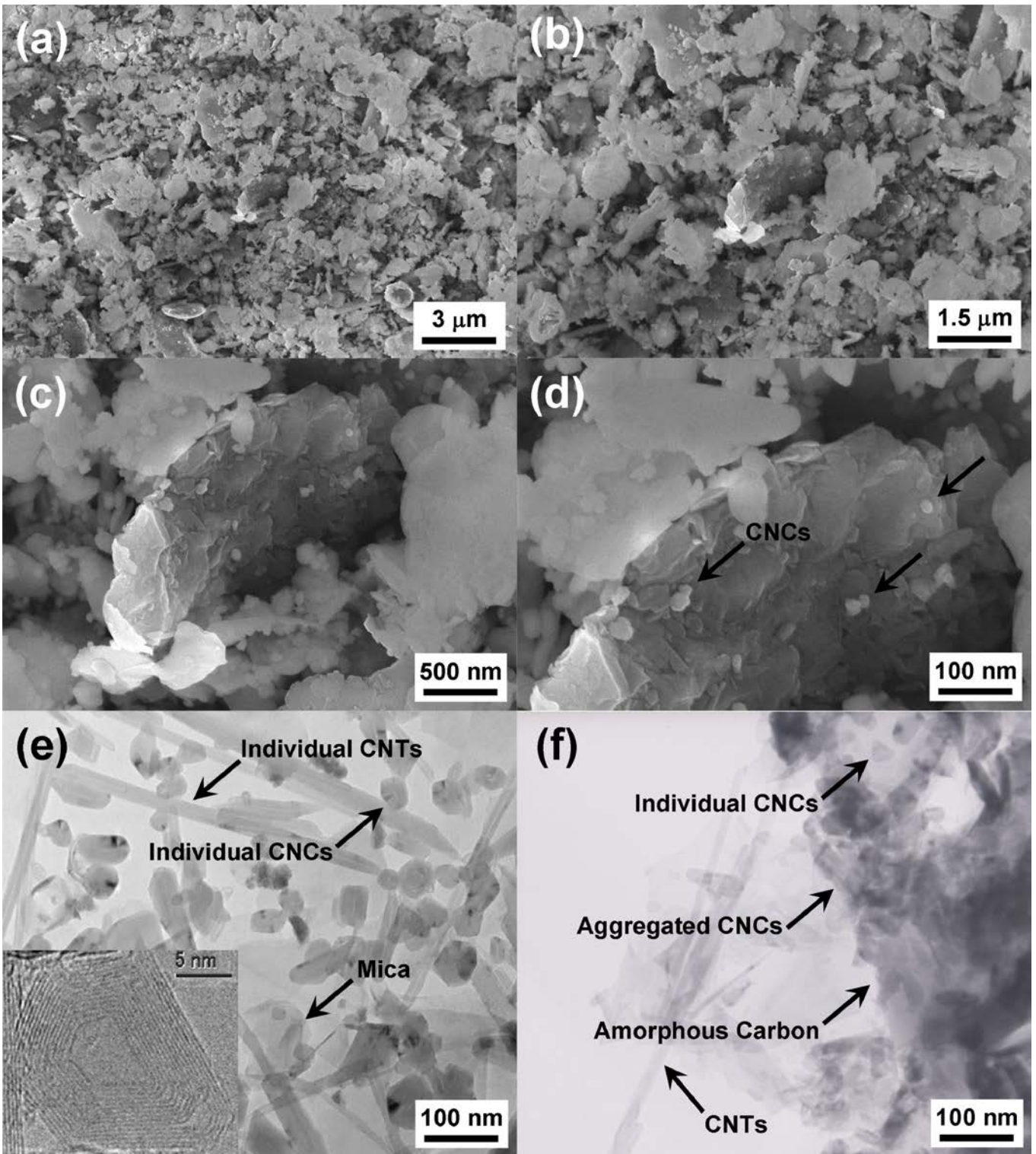


**Figure 18.** SEM image of CNC-Mica hybrid powder (a–d) and TEM morphology of dispersion of hybrid (e) and pristine CNCs (f).

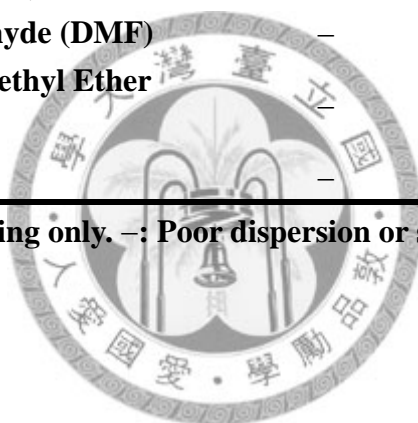


The solubility of hybrid powder is summarized in **Table 10**. Mica could generally affect the CNCs to dispersion in most organic mediums. For example, the pulverized hybrid at weight ratio of Mica/CNC = 2/1, after thoroughly grounding and ultrasonic agitation, became dispersible for most organic solvents.

**Table 10.** Dispersion of CNC and CNC-Mica Hybrid in Various Solvents.

Solvents	CNCs	CNC-Mica Hybrid
H <sub>2</sub> O	–	+
Isopropanol (IPA)	–	+
Methyl Ethyl Ketone (MEK)	–	+
N,N, Dimethyl Formaldehyde (DMF)	–	+
Propylene Glycol Monomethyl Ether Acetate (PGMEA)	–	+
Toluene	–	+

**+: Dispersed well by shaking only. –: Poor dispersion or sedimentation. (1 mg CNCs/5 g solvent)**



The result of solubility indicated the CNC-Mica powder is amphiphilic and the dispersion of hybrid has an irreversible manner (**Figure 19**). Compared to the CNTs, both carbon materials showed the same solvating behavior.

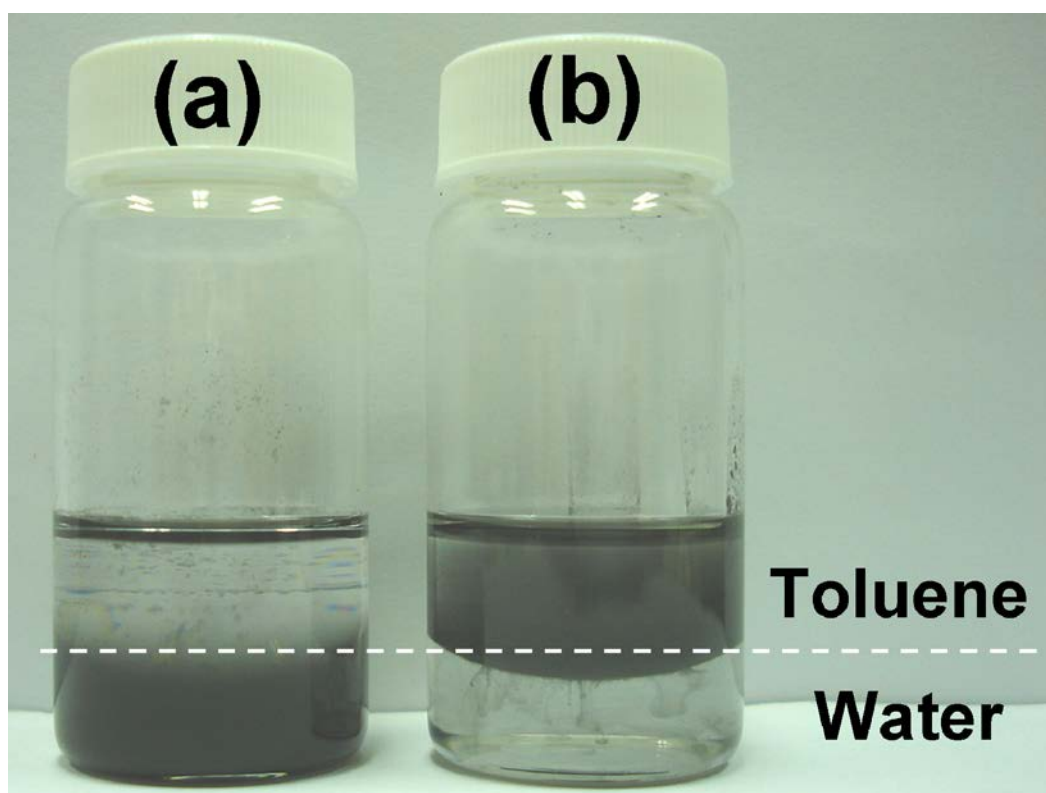


**Figure 19.** Amphiphilic dispersion of CNC-Mica hybrid in water (a) and toluene (b).



### 3.2.2. Dispersion of Carbon Black in the Presence of Clays<sup>5</sup>

The dispersion of CB has greatly improvement in the presence of platelet-like silicates. The CB-clay hybrid was first prepared at various weight ratios (i.e., CB/clay = 100/0, 85/15, and 67/33) and the degree of homogeneity was examined by using an SEM instrument. As shown in **Figure 20**, the control experiment with pristine CBs shows a serious aggregation effect with an average size of 100–300 nm in diameter. It appears that the CB powder can aggregate easily from the pristine structure of irregular spherical shape in average diameter of 40–60 nm. In general, it is the van der Waals force among nanoparticles to cause the aggregation of CB particles. The aggregation can thus occur during the preparation process since the CB powder cannot be completely dispersible in solvent. Actually the formed precipitates can easily be noticed even by naked eyes.

Interestingly, with the addition of clay, the CB-clay hybrid turns out to be dispersible in solvent by subjecting to an ultrasonic process. It is expected that the geometric structure of the pristine MMT clay with a well-defined structure of the primary units consisting of aluminosilicate platelets in stacks to improve the dispersion. The irregularly shaped unit platelets were estimated to be 100 nm×100 nm×1 nm for MMT. Due to the intensive ionic charge character, these clays are hydrophilic and swelling in solvents. As can be seen in **Figure 20**, the dispersion of CBs is very

effective in the presence of clay with an average particle size of *ca.* 40–60 nm.

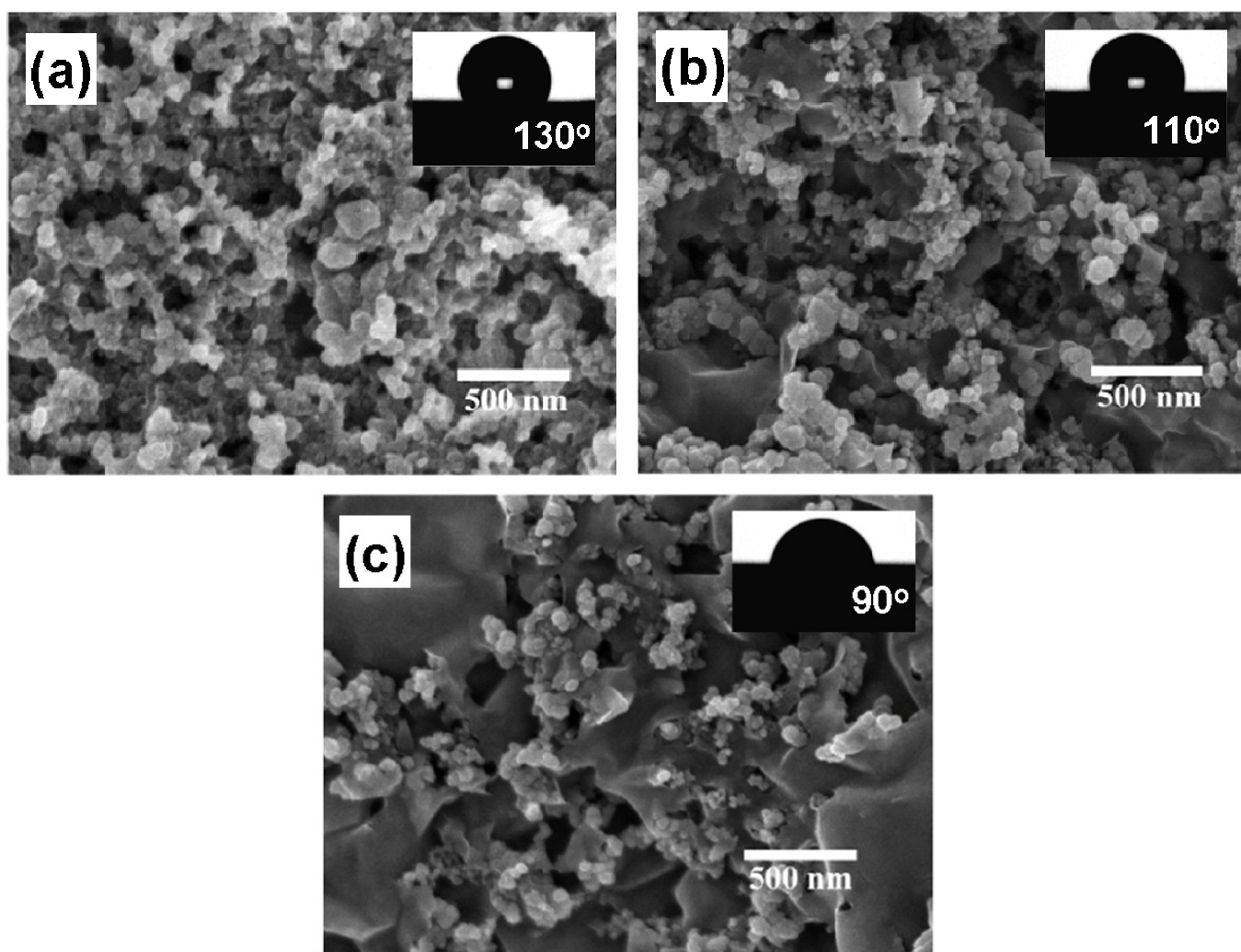


**Figure 20.** SEM morphology of CB-MMT hybrid at weight ratio of CB/MMT = 100/0 (a), 85/15 (b), 67/33 (c), and their hydrophilic property (insert).

The improvement in the hydrophilic property of the hybrid material was further studied. **Figure 20 insert** shows the results observed from the sessile-drop test. The water contact angles (WCA) for the CB-clay surface are 130°, 110° and 90° for the clay addition at 0, 15, and 33 wt%, respectively. Apparently, the wettability of the hybrid was effectively improved in the presence of the clay component.

### 3.2.3. Preparation and Dispersion of Silver Nanoparticles in the Presence of Clays<sup>4</sup>

The GIF also can manipulate the preparation of AgNPs and showed dramatically improvement of dispersion. In the presence of platelet-like silicate (**Figure 21a**), the particle size of AgNPs can be controlled from 20–70 nm due to the defects of silicate structures have strong interaction with  $\text{Ag}^+$  and promote the formation of  $\text{Ag}^0$  (i.e. AgNPs). The AgNPs with clay presence have good solubility in water. After heating at 110 °C, the AgNPs showed melting phenomenon and revealed the electrical conductivity behavior (**Figure 21b,c**).

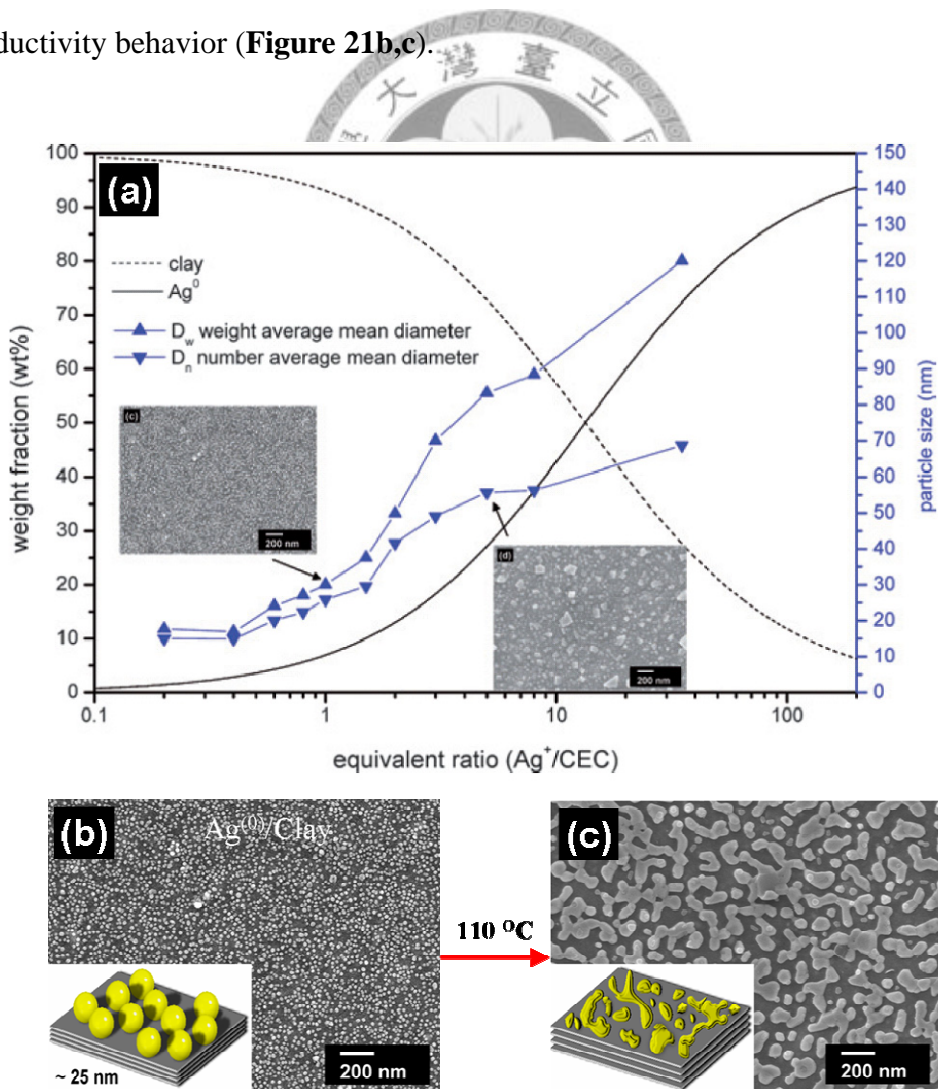


**Figure 21.** Preparation of AgNPs in the presence of clays and the melting behavior.

### 3.2.4. Preparation and Dispersion of Iron-Oxide Nanoparticles in the Presence of Clays<sup>184</sup>

Nanohybrids with embedded magnetic FeNPs were synthesized by in situ  $\text{Fe}^{2+}/\text{Fe}^{3+}$  co-precipitation in the presence of hydrophobic poly(oxypropylene)amine salts intercalated clay. With the combined hydrophobic and magnetic properties, the nanohybrid exhibited its ability to adsorbing hydrophobic organics and then be efficiently removed by using simple magnetic fields. It may be applied for environment-cleaning applications involving the spilt crude oil or possibly other pollutants.

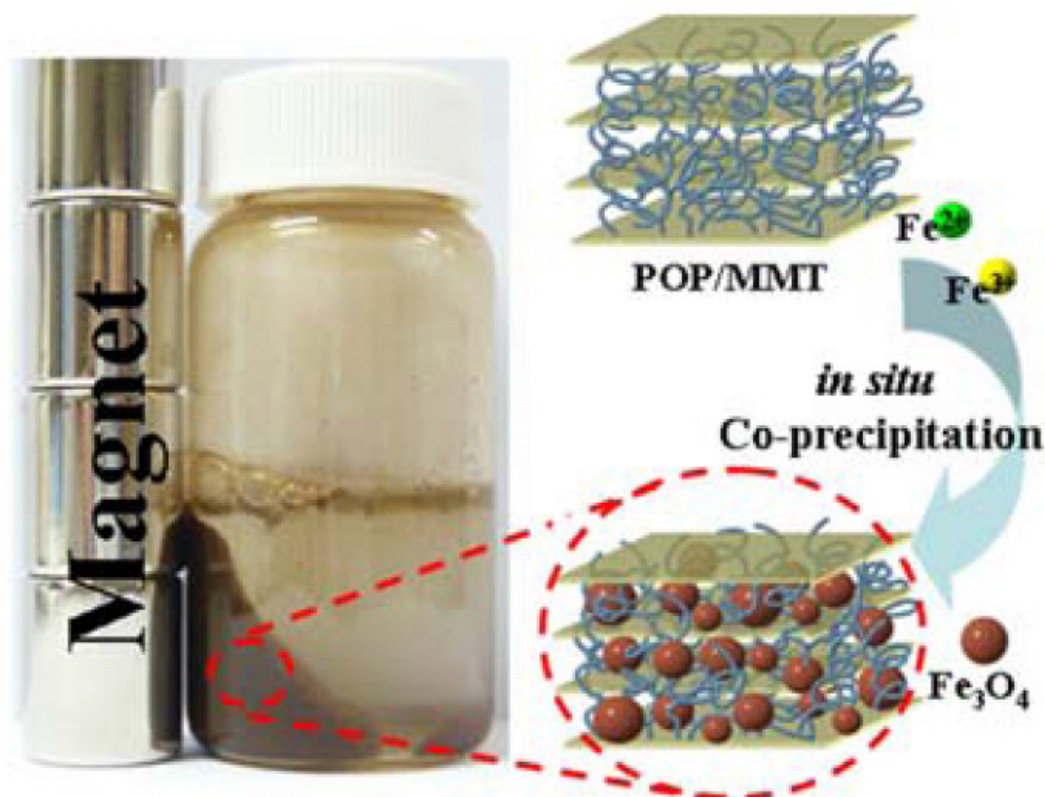
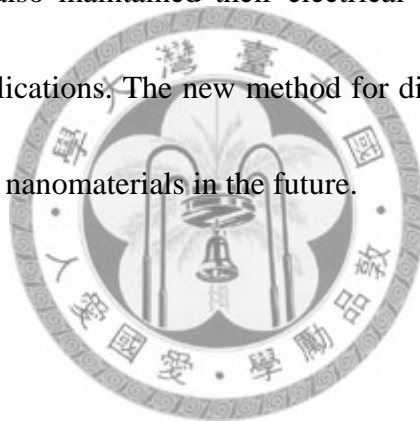


**Figure 22.** Preparation of FeNPs in the presence of organoclays and the magnetic behavior.

### 3.2.5. Conclusion

The dispersion of nanoparticles has successfully been improved by using mechanism of geometric-shape inhomogeneity. The dispersion of carbon nanocapsules, carbon black, silver nanoparticles and iron-oxide nanoparticles were effectively improved in the presence of platelet-like clay. Compared to tubular nanomaterials (e.g. carbon nanotubes), the dispersion of carbon nanoparticles also rendered amphiphilic behavior and irreversible manner in water/toluene co-solvent due to the exposure order. Both AgNPs and FeNPs also maintained their electrical conductivity and magnetic behavior for advanced applications. The new method for dispersion nanoparticles will broaden the applications of nanomaterials in the future.



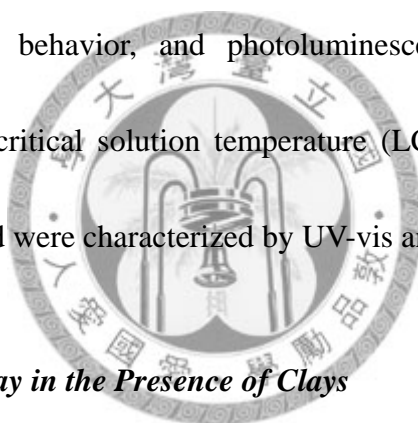
### 3.3. Dispersion of Hydrophobic Conjugated Polymers by Using Platelet-Like Clays and their Thermo-responsive Property<sup>169</sup>

In our previous researches, the dispersion of nanomaterials can be control or enhanced by a unique mechanism of geometric-shape inhomogeneity factor (GIF). The pulverization of two nanomaterials with large difference in geometric shaped will alternate their dispersed behavior by each other. The dispersion of Carbon black,<sup>5</sup> silver nanoparticle<sup>4</sup> and carbon nanotube<sup>7</sup> can be improved based on GIF. In this **Section 3.3.**, we reported the uses of colloidal clays to aqueous dispersion of hydrophobic CPs based on GIF. Three representative CPs, poly[2-methoxy-5-(2'-ethylhexyloxy)-1,4-phenylene vinylene] (MEH-PPV), sulfonated polyaniline (SPA) and triphenyl phosphine oxide cored polyaniline (TPOPA), were allowed to mix and grind with the ionic clays of plate-like geometric shape. Among the screened clays, the synthetic fluorinated mica (Mica) was the most effective for dispersing CPs in water. The clays with high aspect-ratio geometric shape and ionic charges could well interact with the hydrophobic polymers through non-covalent bonding forces. By varying the clay species, the geometric shape was found to be one of the important factors for influencing the CP dispersion. The clay affecting CP dispersion is generalized by using representative CPs of polyaniline structures with rigid shape and making into hybrid films. Their dispersion behavior and



photo-physical properties were characterized by ultraviolet-visible (UV-vis), photoluminescence (PL) spectrophotometer and transmission electron microscopy (TEM).

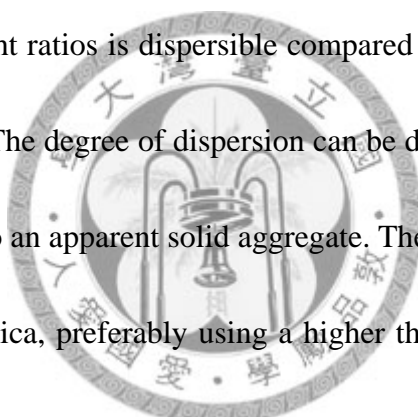
Furthermore, the platelet silicate clay were undergone exfoliation to form nano silicate platelet (NSP) and consequently tethered poly(*N*-isopropyl acrylamide) [PNiPAAm] by atom-transfer radical polymerization (ATRP). The new nanomaterial of NSP-PNiPAAm was advanced the dispersion of hydrophobic conjugated polymer to become thermoresponsive behavior, and photoluminescence (PL) responsiveness through GIF. Both lower critical solution temperature (LCST) and luminescence of NSP-PNiPAAm/CPs hybrid were characterized by UV-vis and PL spectrophotometer.



### ***3.3.1. Dispersion of CP/Clay in the Presence of Clays***

Conjugated polymers are generally water-insoluble and require a substantial side-chain modification to improve their solubility for processing. Moreover, the layered silicate clays are well established for their swelling and colloidal properties.<sup>9</sup> With pulverizing together, both materials in powder form of physical mixture altered their inherent aggregating behaviors and mutually affected their solvating abilities. To understand their dispersing behaviors, the representative MEH-PPV was selected for the initial tests. The clays including the fluorinated mica (Mica), sodium montmorillonite (MMT), synthetic clay (SWN) and a cationic type of layered double

hydroxide (LDH) were screened. Four clays represent different anionic and cationic species with a range of average geometric size: Mica ( $300 \times 300 \times 1 \text{ nm}^3$ ), MMT ( $100 \times 100 \times 1 \text{ nm}^3$ ), SWN ( $80 \times 80 \times 1 \text{ nm}^3$ ) and LDH ( $200 \times 200 \times 1 \text{ nm}^3$ ). Due to the presence of intensive ionic charges, these clays are capable of swelling and gelling in water. After physical pulverization, the MEH-PPV/Mica mixture showed an improvement in solvating ability in water, while the pristine MEH-PPV is only sluggishly dispersible. In **Figure 23a**, it is demonstrated that the MEH-PPV/Mica hybrid at 1/1 and 1/2 weight ratios is dispersible compared to a serious aggregation of MEH-PPV without Mica. The degree of dispersion can be differentiated by naked eyes from a red-color solution to an apparent solid aggregate. The dispersion was influenced by the amount of added Mica, preferably using a higher than 1/1 Mica in weight. By visualization, Mica has an ability of subsiding the MEH-PPV aggregation in water. Under an ultraviolet light (**Figure 23b**), a color was illuminated, implying the enhancement of MEH-PPV dispersion in the presence of Mica. For comparison, the pristine MEH-PPV is in aggregated form and the water solution showed none of light-emitting. In **Figure 23c**, it is demonstrated that the MEH-PPV dispersion by the assistance of different clays. Both MEH-PPV/Mica and MEH-PPV/MMT solutions demonstrated a deep-red appearance while MEH-PPV/SWN and MEH-PPV/LDH





revealed a light-red color, indicating the clay efficiency. Similar results were obtained for other CPs such as SPA and TPOPA, as indicated in **Figure 23d,e**.

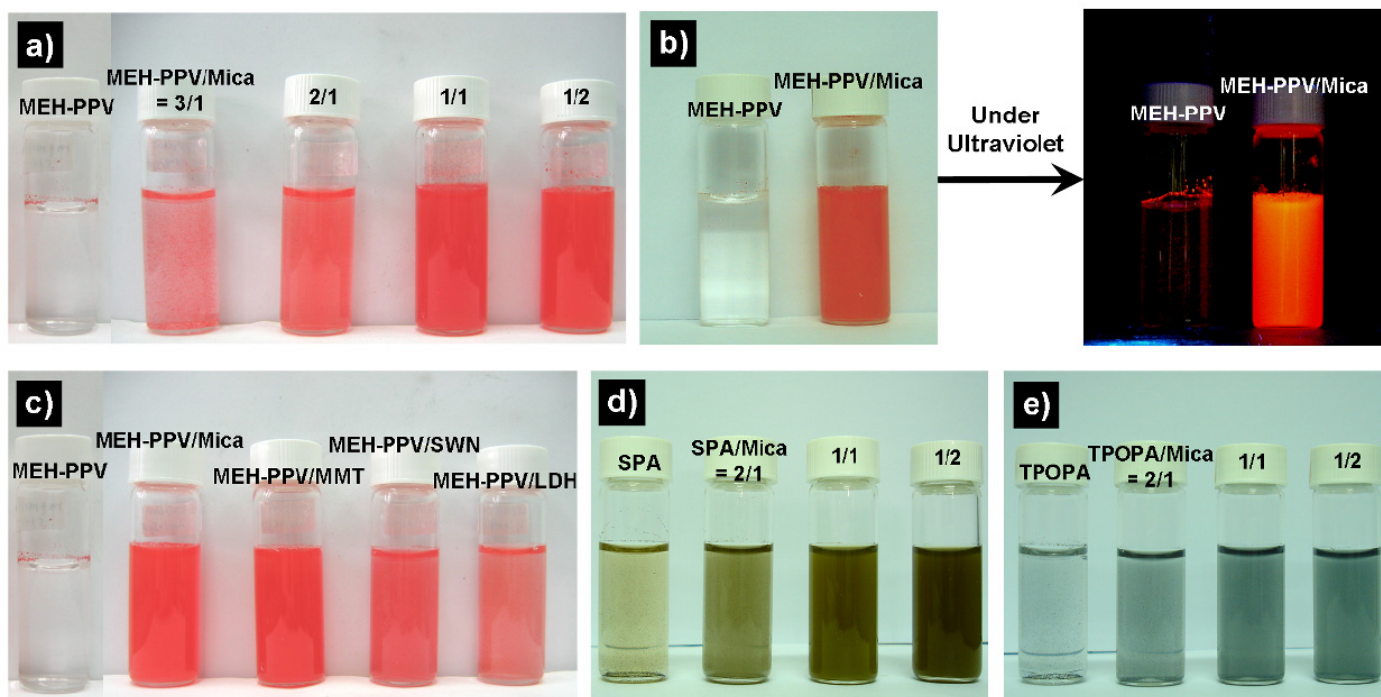


**Figure 23.** Dispersion of CP/Clay in water (1 mg CPs in 5 g water): (a) MEH-PPV/Mica at 3/1, 2/1, 1/1 and 1/2 weight ratios, (b) MEH-PPV/Mica (1/1) under UV light, (c) MEH-PPV/Clay (1/1), Clay=Mica, MMT, SWN and LDH, (d) SPA/Mica at 2/1, 1/1 and 1/2 ratios, and (e) TPOPA/Mica at 2/1, 1/1 and 1/2 ratios.

The dispersion is examined by UV-visible absorbance, shown in **Figure 24**. The Mica is most effective for enhancing the MEH-PPV dispersion in comparison with other clays. Based on the same weight ratio (MEH-PPV/clay=1/1), the intensity for MEH-PPV/Mica is higher than that of using other clays. In considering the ionic charges, LDH possesses cationic charges on the platelet surface and nitrate anionic species as the counter ions. The ionic charge interaction between MEH-PPV and clay through the clay surface anions ( $\equiv\text{SiO}^-$ ) in MMT and Mica structures or cations

( $[\text{Mg}_6\text{Al}_2(\text{OH})_{16}]^+$ ) in LDH may be another factor for affecting the MEH-PPV dispersion. According to the UV-vis absorbance in **Figure 25**, the MEH-PPV dispersion is closely correlated to the amount of Mica addition. The absorbance at 524 nm becomes more intensive with the increasing amount of Mica, implying the improvement of MEH-PPV dispersion. The control experiment for the pristine Mica indicates the increasing absorbance of UV-vis is fully contributed from MEH-PPV in water. For other CPs, the absorbance of SPA/Mica and TPOPA/Mica also increased by the Mica enhancement.

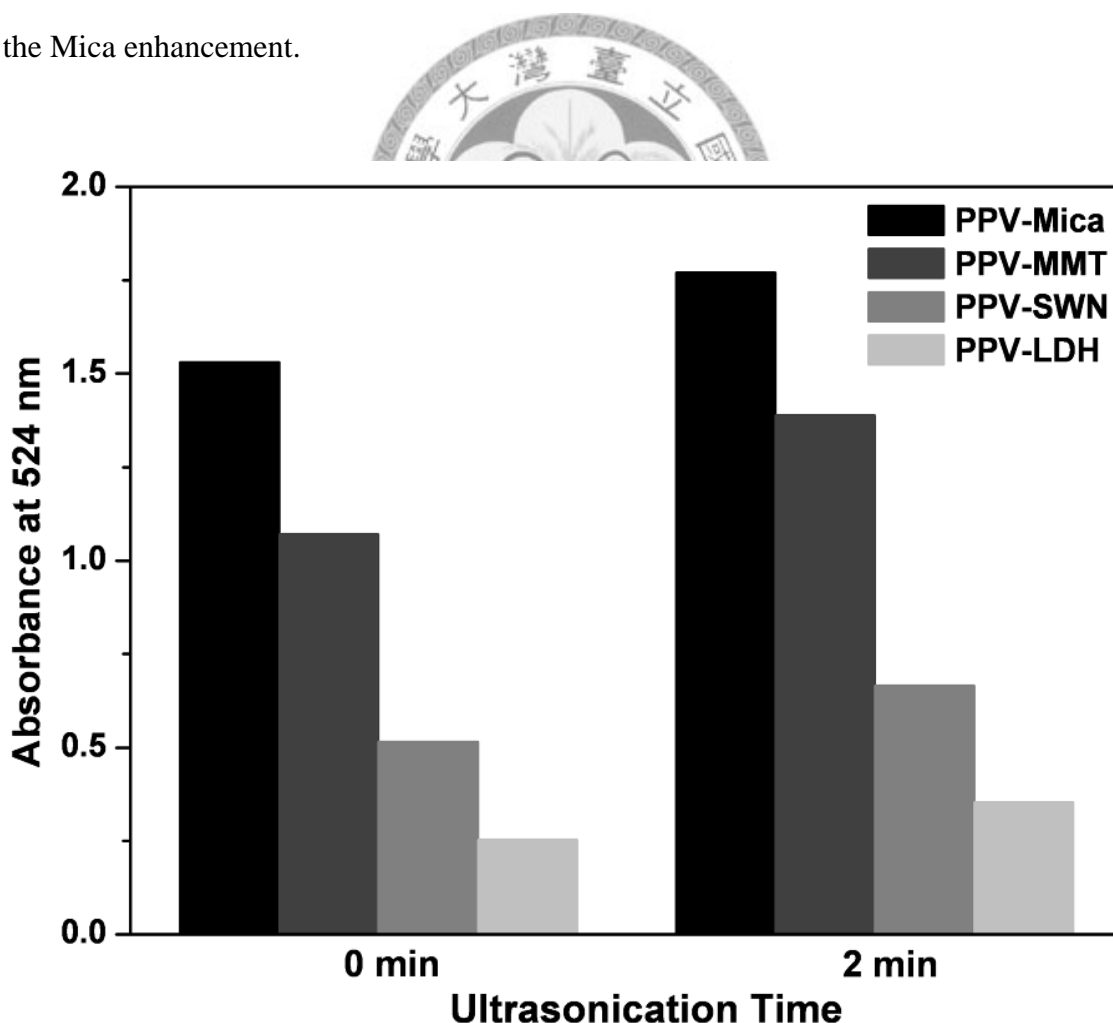


**Figure 24.** UV-vis absorbance of CP/clay in water: MEH-PPV dispersed by Mica, MMT, SWN or LDH, at weight ratio of 1/1.

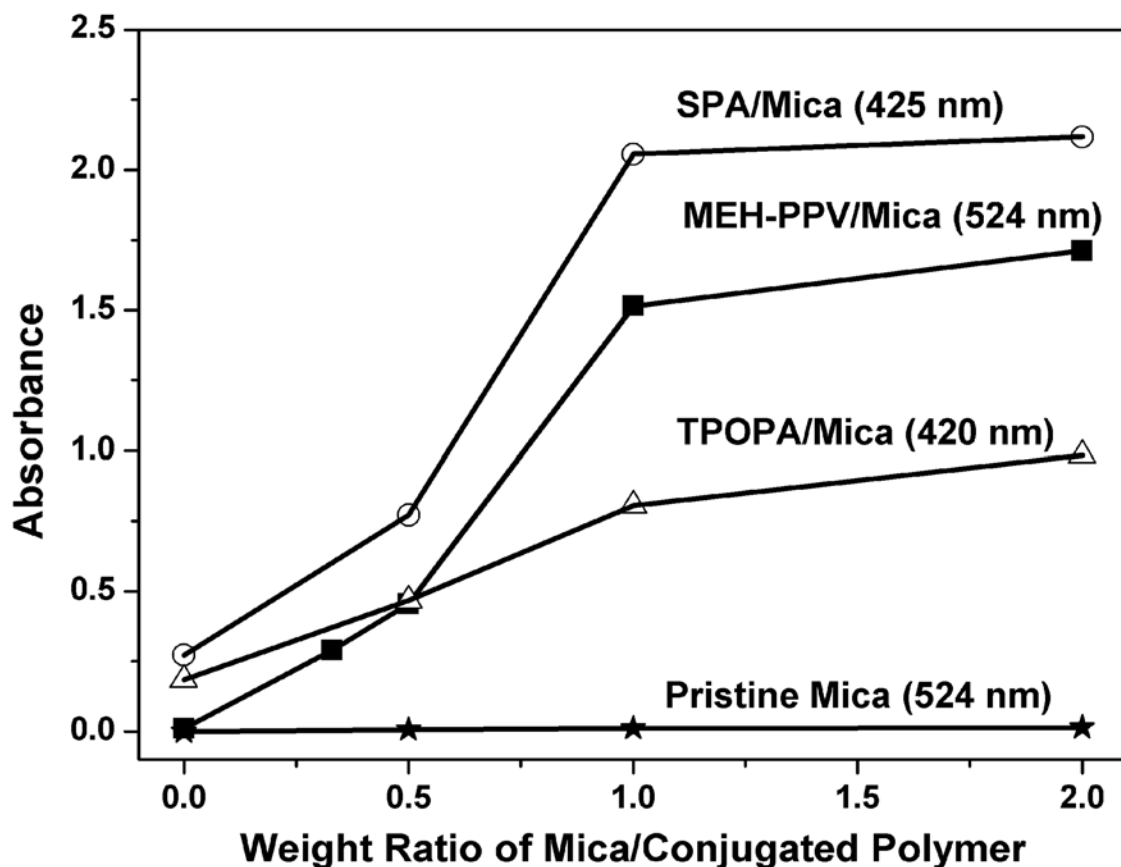


**Figure 25.** UV-vis absorbance of CP/clay in water: MEH-PPV, SPA and TPOPA polymers dispersed by Mica at different weight ratio.

The dispersion of CP/clay hybrid in water was further observed by TEM. In **Figure 26a,c,e**, the micrograms with a low magnification of MEH-PPV/Mica, SPA/Mica and TPOPA/Mica hybrids all revealed a homogeneous distribution. Under high magnification in **Figure 26b,d,f**, shown are the morphology of Mica in platelet-like shape with dimension in 300–1000 nm and the particle size of CPs at 1  $\mu\text{m}$  for MEH-PPV, 10–100 nm for SPA and 100 nm for TPOPA.



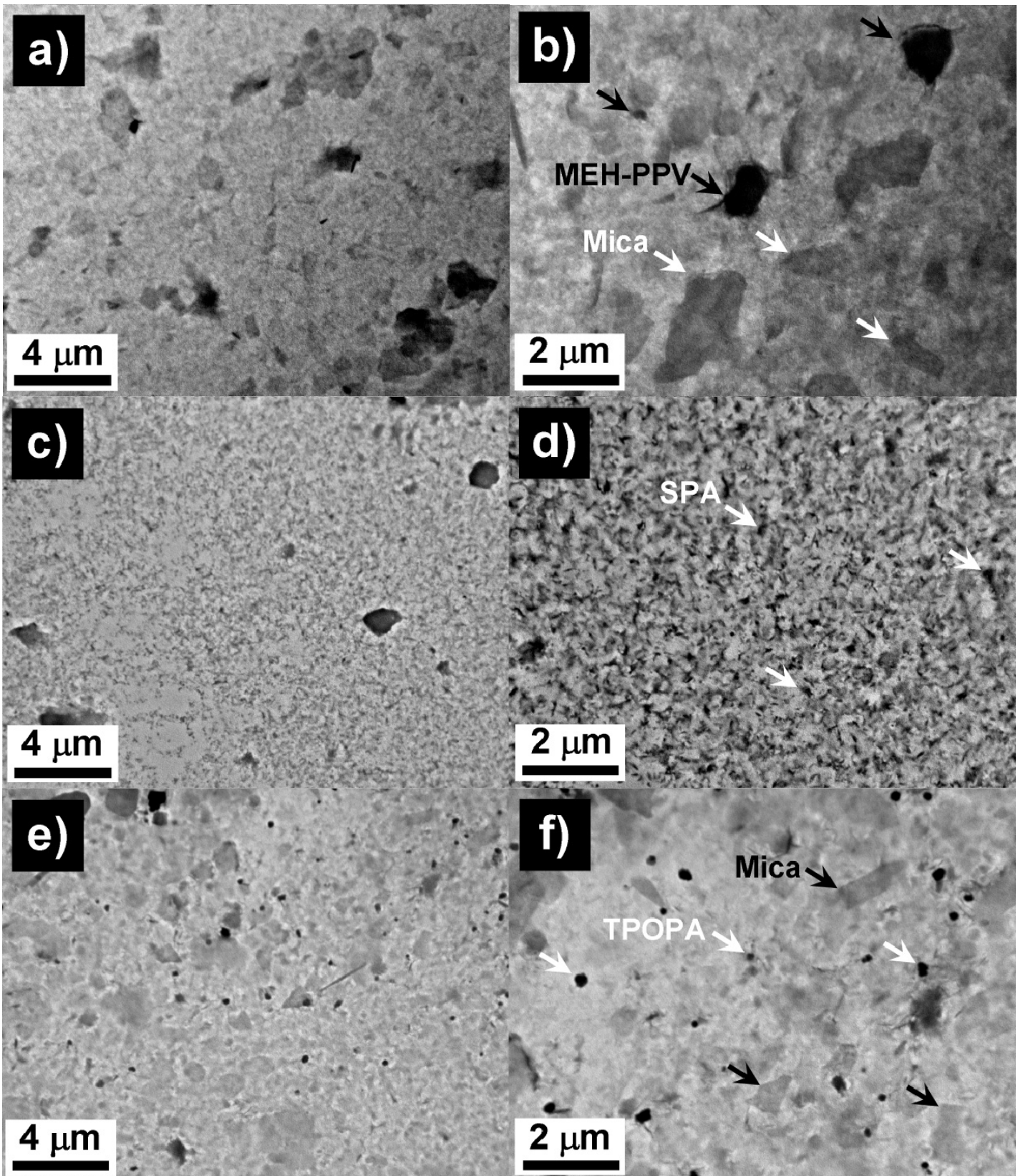


**Figure 26.** TEM images of CP/Mica dispersion (at 1/1 weight ratio) in water: MEH-PPV (a,b), SPA (c,d), and TPOPA (e,f).

These images were taken by dropping the dispersed solution on the copper-grid of the TEM sample holder. The observed images can only be extrapolated to the solution dispersion state. The MEH-PPV conjugated polymer appeared to have larger aggregated particles than that of SPA and TPOPA. The particle size measurements from TEM are well correlated to the zetasizer analysis (**Figure 27**).

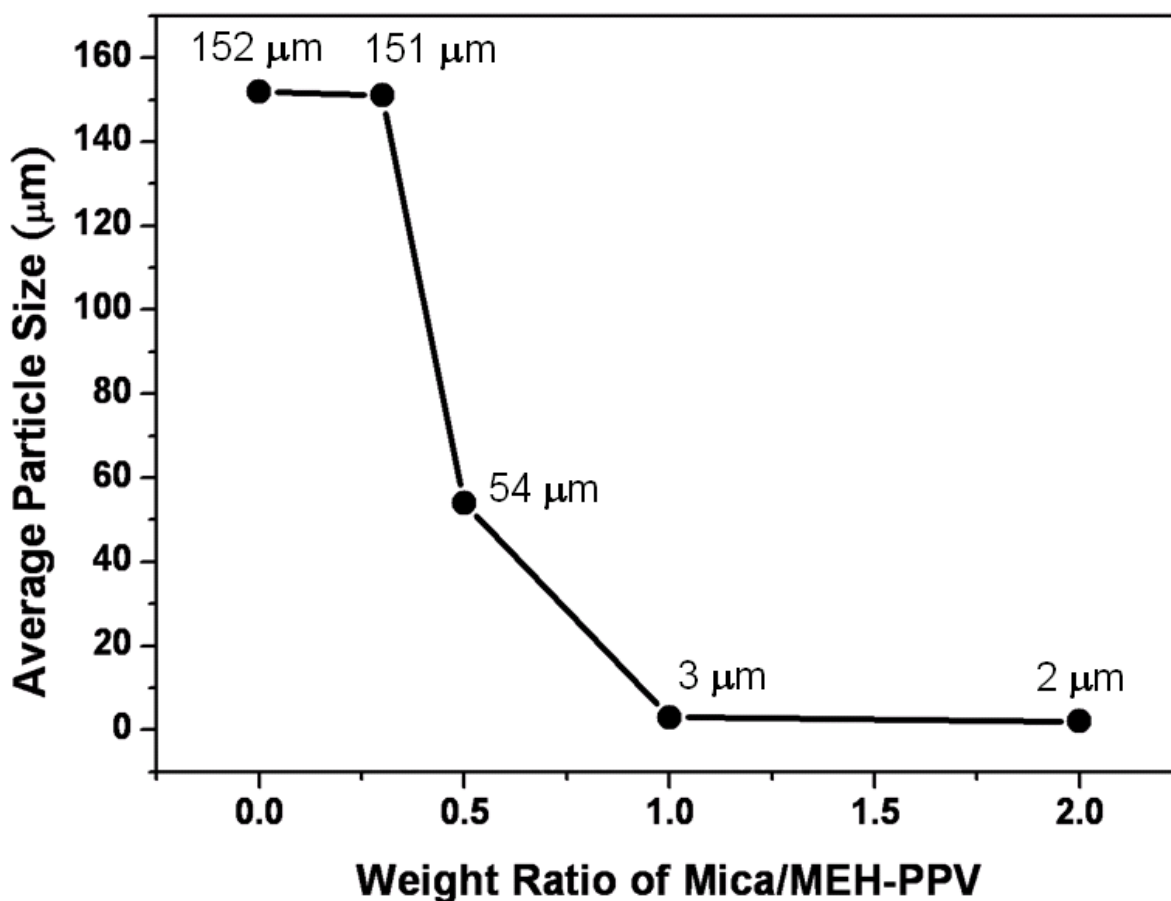


**Figure 27.** Particle Size of Mica/MEH-PPV hybrids.

Comparison to MEH-PPV, the pristine Mica has an average particle size (APS) of 152 µm, but decreased from 152 to 2 µm when hybridizing with MEH-PPV through the grinding procedure. It is noted that the size analysis is a relative correlation without

considering the deviation from the platelet shape of the clay particle. The zeta potentials (**Table 11**) for MEH-PPV in mixing with three clays were investigated. Negative zeta potentials remained when hybridizing with Mica or MMT, in contrast to the use of LDH. Due to the anionic LDH property, the MEH-PPV/LDH hybrid showed a zero zeta potential due to the opposite charge attraction and solution precipitation. It is interestingly noted that the zeta potential measurements could differentiate the MEH-PPV interaction with anionic LDH from cationic clays (Mica and MMT).

**Table 11.** Zeta Potential of Pristine Mica and MEH-PPV/Clay Hybrid.

No.	Mica <sup>a</sup>	MEH-PPV/Mica <sup>b</sup>	MMT <sup>a</sup>	MEH-PPV/MMT <sup>b</sup>	LDH <sup>a</sup>	MEH-PPV/LDH <sup>b</sup>
Run 1	-63	-78	-25	-39	+22	0
Run 2	-67	-79	-27	-36	+24	0
Run 3	-65	-78	-22	-37	+22	0
Run 4	-66	-80	-24	-39	+26	0
Run 5	-67	-82	-25	-38	+23	0
Average	-66	-80	-25	-38	+24	0

<sup>a</sup> 0.01 wt% clay in water at pH = 7. <sup>b</sup> 0.02 wt% MEH-PPV/clay hybrid in water at pH = 7, the weight ratio of MEH-PPV/clay = 1/1. Note: the unit of Zeta Potential is mV.

### 3.3.2. Optical Performance of CP/Mica Hybrids

The degree of dispersion influences the optical property of CPs. Photoluminescence spectrophotometer (PL) was performed at excited wavelength of 524 nm that was corresponded to the inherent MEH-PPV properties. The PL intensity is rated by the following trend: MEH-PPV/Mica>MEH-PPV/MMT>MEH-PPV/SWN

>MEH-PPV/LDH, as indicated by **Figure 28**. The trend of the PL emission reflected the degree of MEH-PPV dispersion in water and the PL trend is consistent to the UV-vis absorbance. The Mica clay appears to be performed better than other clays tested. The content of Mica has a slight influence on the PL spectrum of MEH-PPV/Mica due to the variation of dispersion (**Figure 29**). The PL spectrum of MEH-PPV/Mica has a slightly blue shift from 601 to 595 nm corresponding to the amount of Mica presence. The blue shift of MEH-PPV/Mica is due to the variation of CP conjugated length.<sup>185</sup>

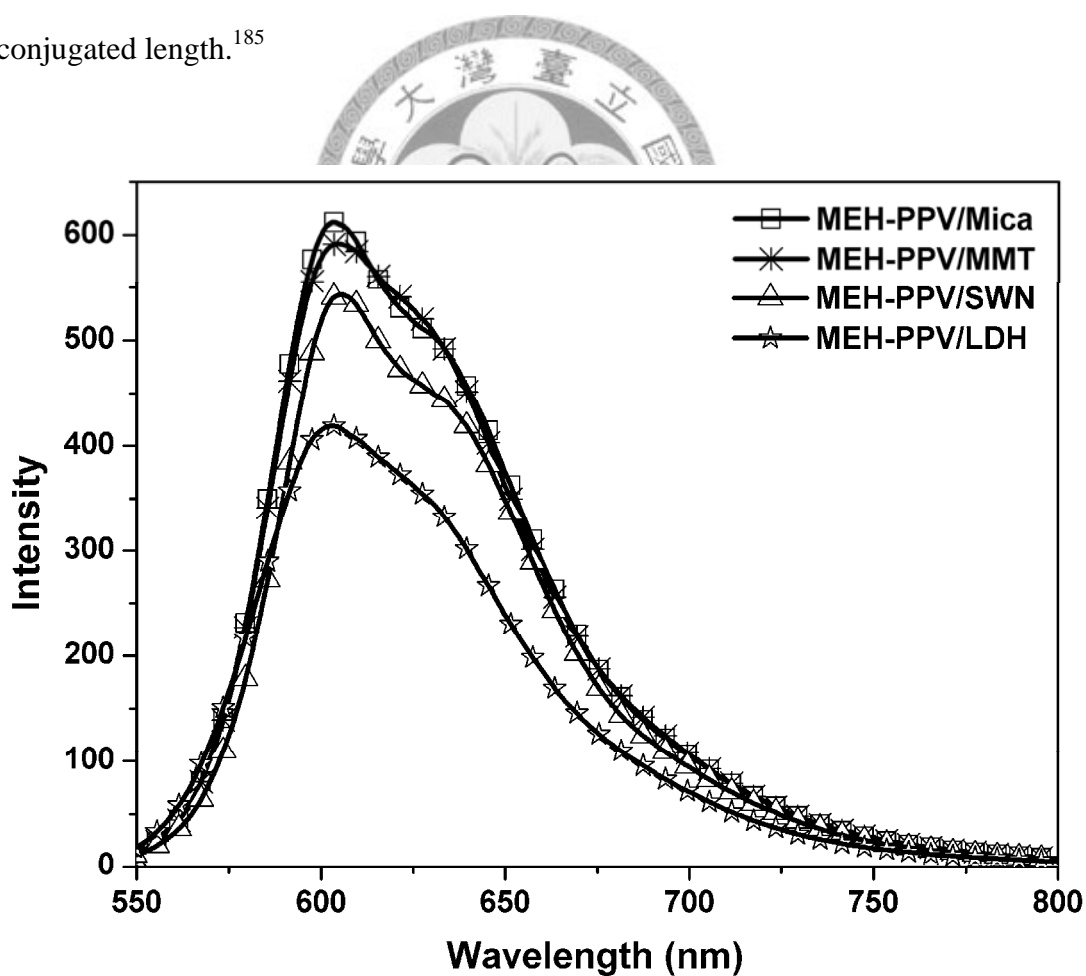


**Figure 28.** PL spectra of CP/clay solution with different clay.

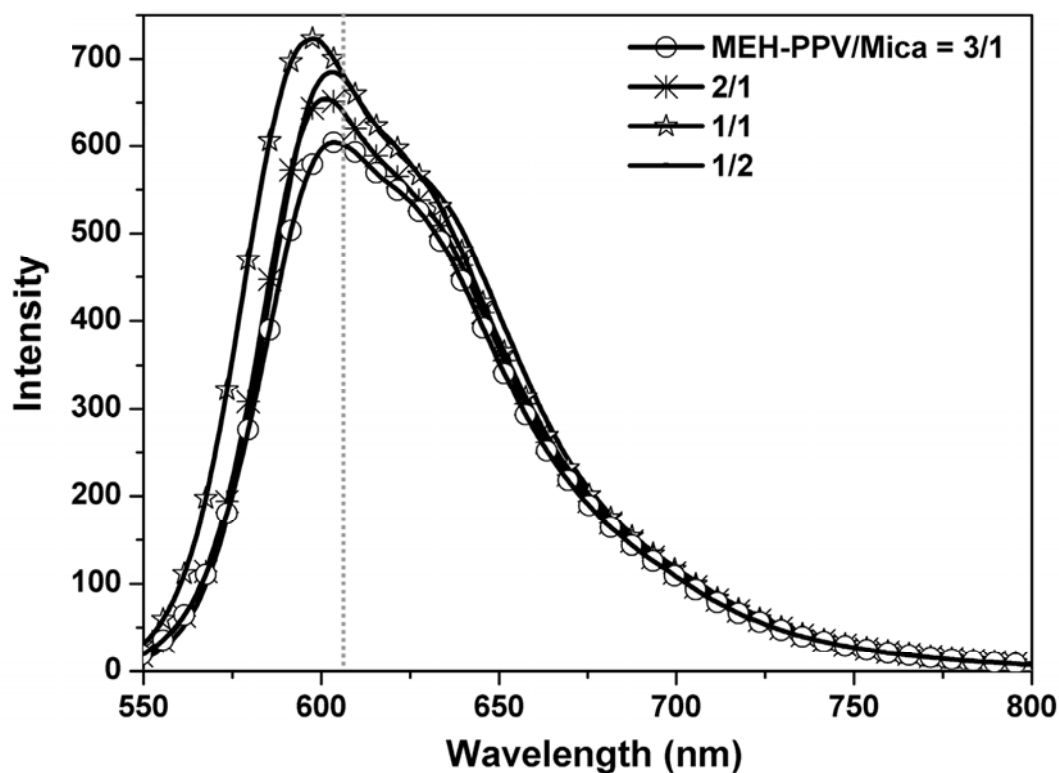


**Figure 29.** PL spectra of CP/clay solution with Mica but different weight ratio.

The MEH-PPV/Mica films prepared from the corresponding solution precursor were shown to have UV-vis and PL properties (**Figure 30–32**). For the MEH-PPV/Mica (weight ratio=1/1) film as shown in **Figure 30**, there are existed a maximal absorbance at  $\lambda_{\text{max.abs.}} = 580$  nm and a maximum emission at  $\lambda_{\text{max.em.}} = 605$  nm. In the inserted picture, the film exhibited a noticeable orange light-emitting when exposing to a UV lamp. The orange light is exactly correlated to the PL at 605 nm. In **Figure 31**, the SPA/Mica film has a spectrum at  $\lambda_{\text{max.abs.}} = 425$  nm and  $\lambda_{\text{max.em.}} = 560$  nm, with the corresponding olive light-emitting under UV lamp. For the TPOPA/Mica film, in **Figure 32**, the results of  $\lambda_{\text{max.abs.}} = 430$  nm and  $\lambda_{\text{max.em.}} = 530$  nm were obtained. Green light-emitting was corresponding to the PL of 530 nm.



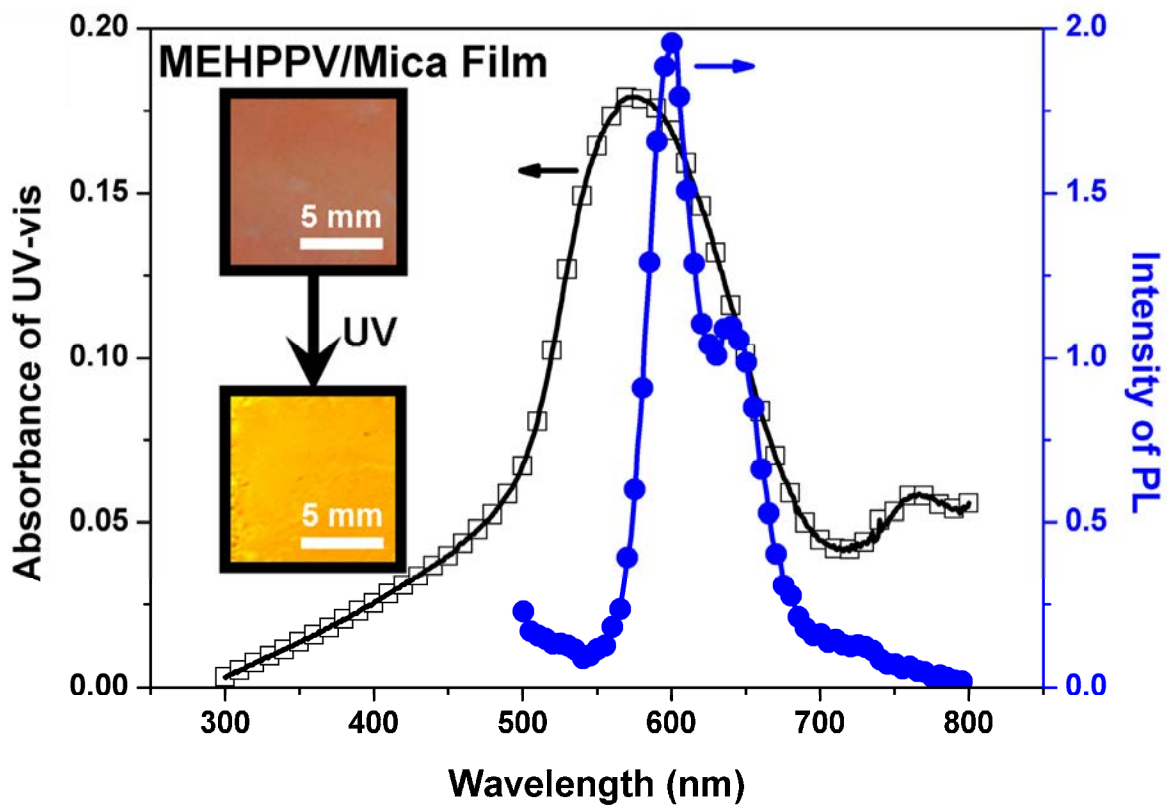


Figure 30. UV-vis and PL spectra of hybrid film of MEH-PPV/Mica (a).

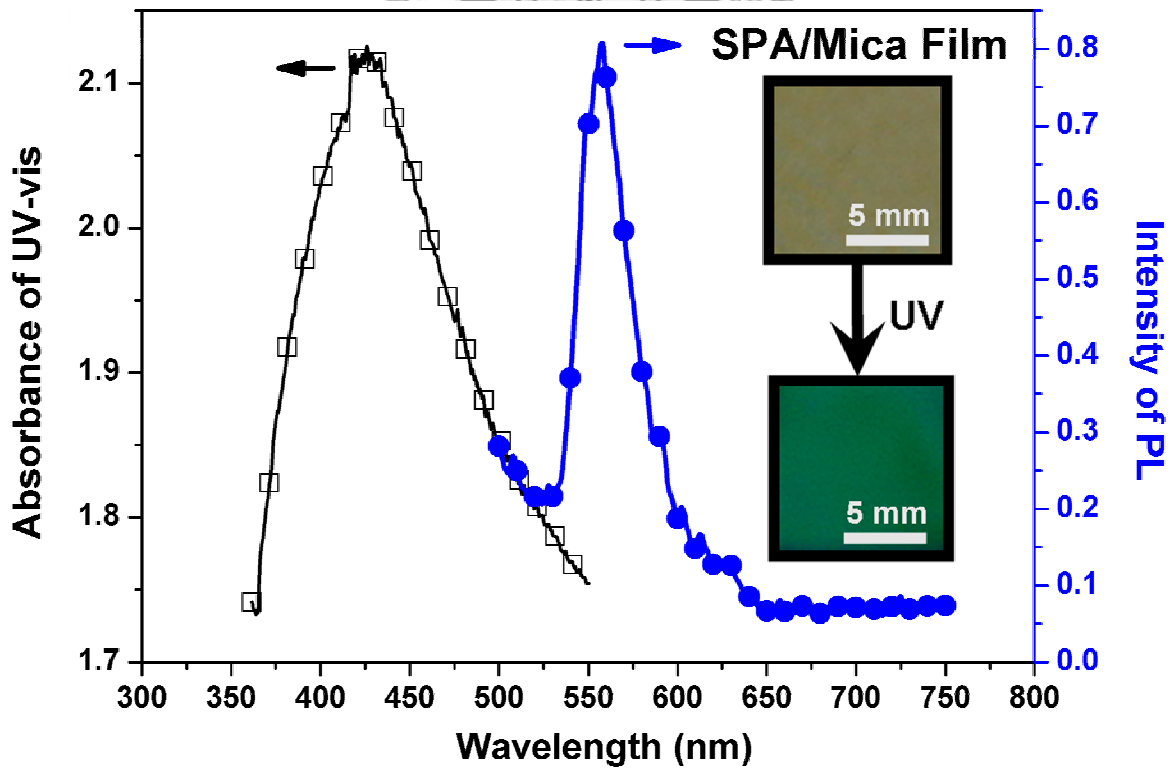
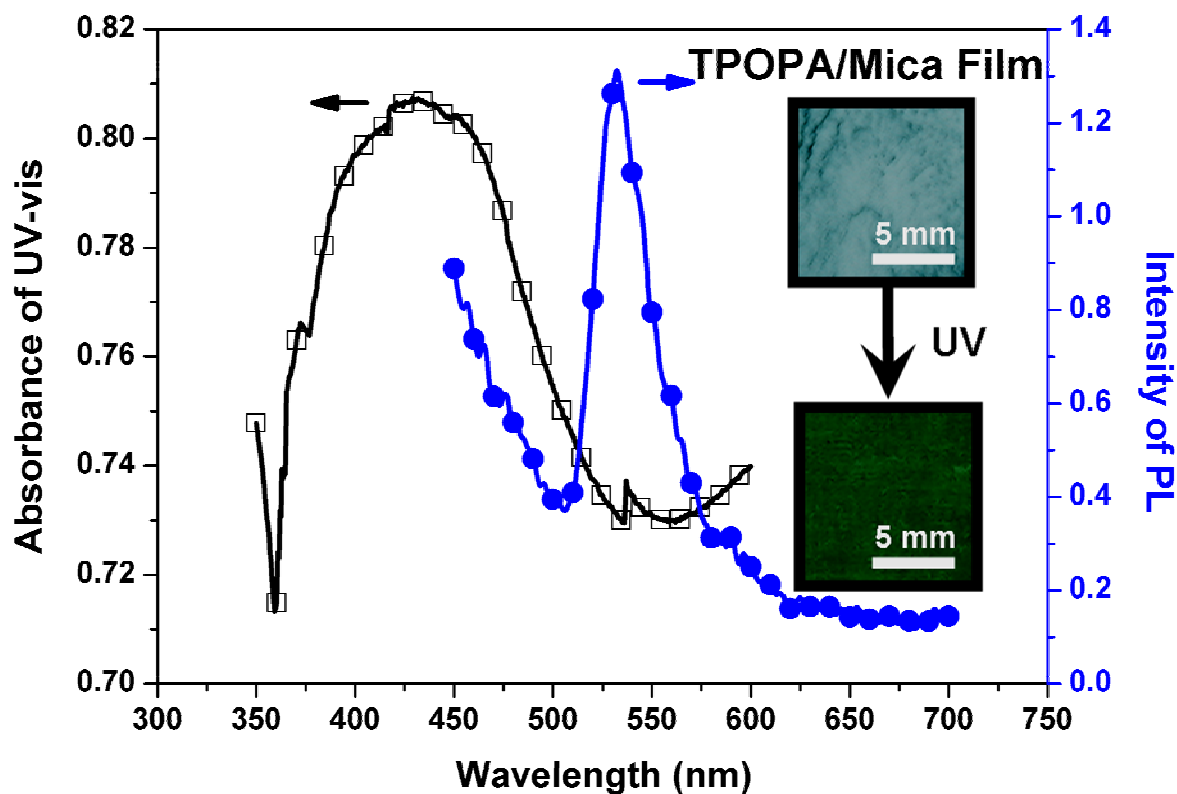


Figure 31. UV-vis and PL spectra of hybrid film of SPA/Mica (b).



**Figure 32.** UV-vis and PL spectra of hybrid film of TPOPA/Mica (c).

### 3.3.3. Explanation for the Dispersion Behavior of CP/Clay

The dispersion of CPs into water phase in the presence of the ionic clays is first rationalized by non-covalent bonding forces. The CPs are hydrophobic and only soluble in organic mediums. In water, the polymers are in aggregates or precipitates due to molecular-coil entanglement. Both UV-vis absorbance and TEM observation confirmed the fine distribution of the CP/Clay hybrids in aqueous dispersion. As illustrated GSI conception in **Figure 33**, the initial grinding of two distinctly different materials in nanometer scale may have homogenized two different materials in micrometer scale. When dispersing into water, the strong non-covalent bonding force between clay and water molecules could further exclude the CP molecular

self-aggregation. Both of the mutual interactions through non-covalent bonding forces such as ionic charges for clay surface, van der Waals force and  $\pi$ - $\pi$  stacking for CP entanglement attraction and the plate-like geometric shape blockage could all together influence the CP pristine aggregation. In other words, the CP polymer entanglement is mitigated and physically blocked by the neighboring Mica platelets. The presence of clay colloid in water effectively rendered the CP dispersion in water. The overall effect is to disperse CPs without going through a tedious chemical modification. It also implies the “green process” is possibly generalized for other hydrophobic polymers.

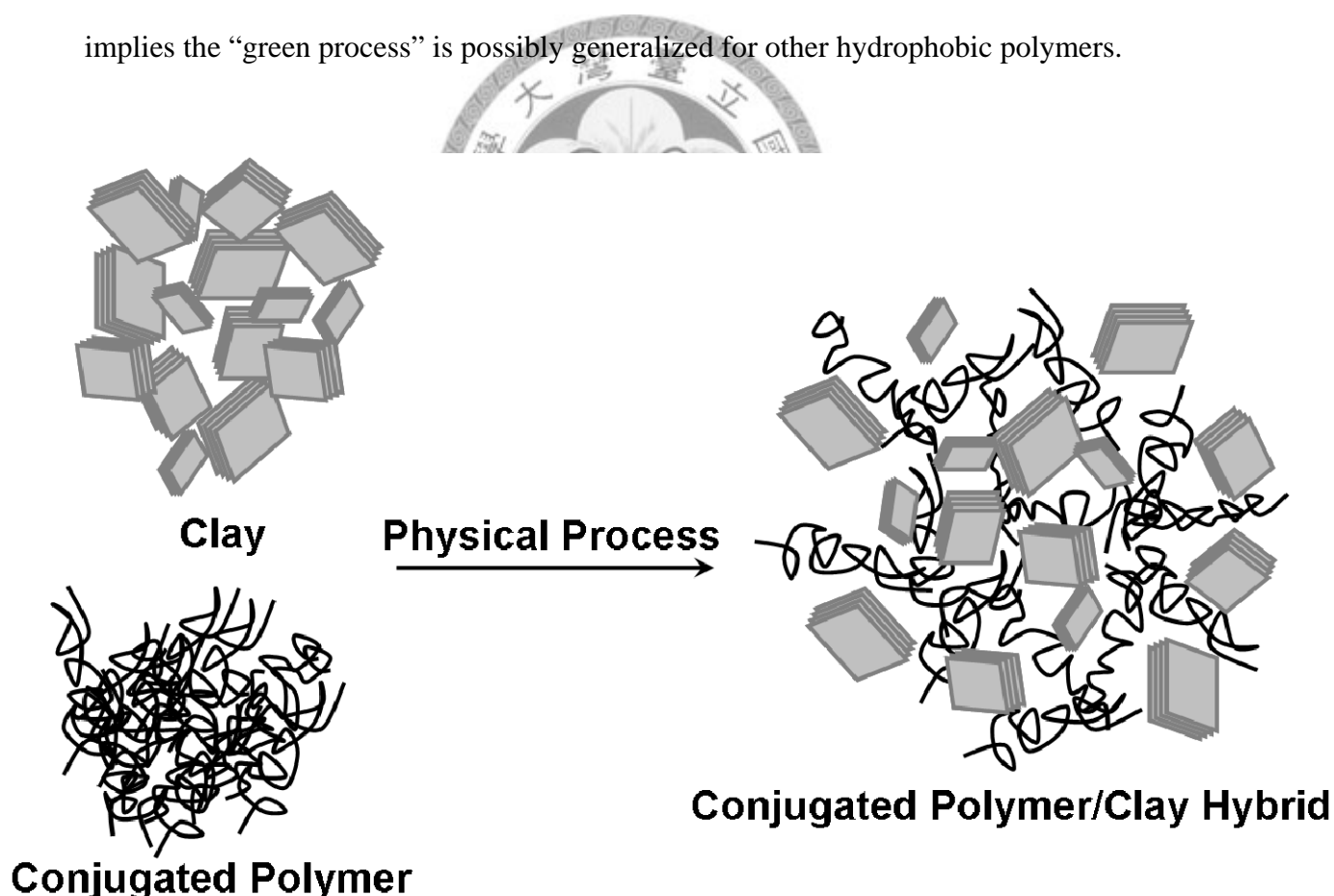
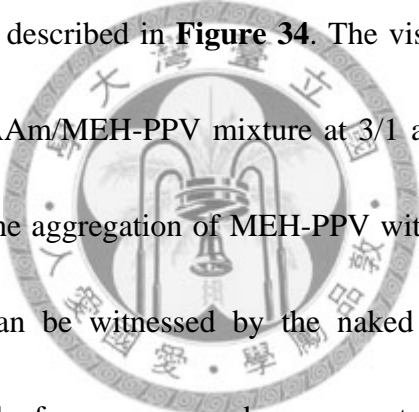


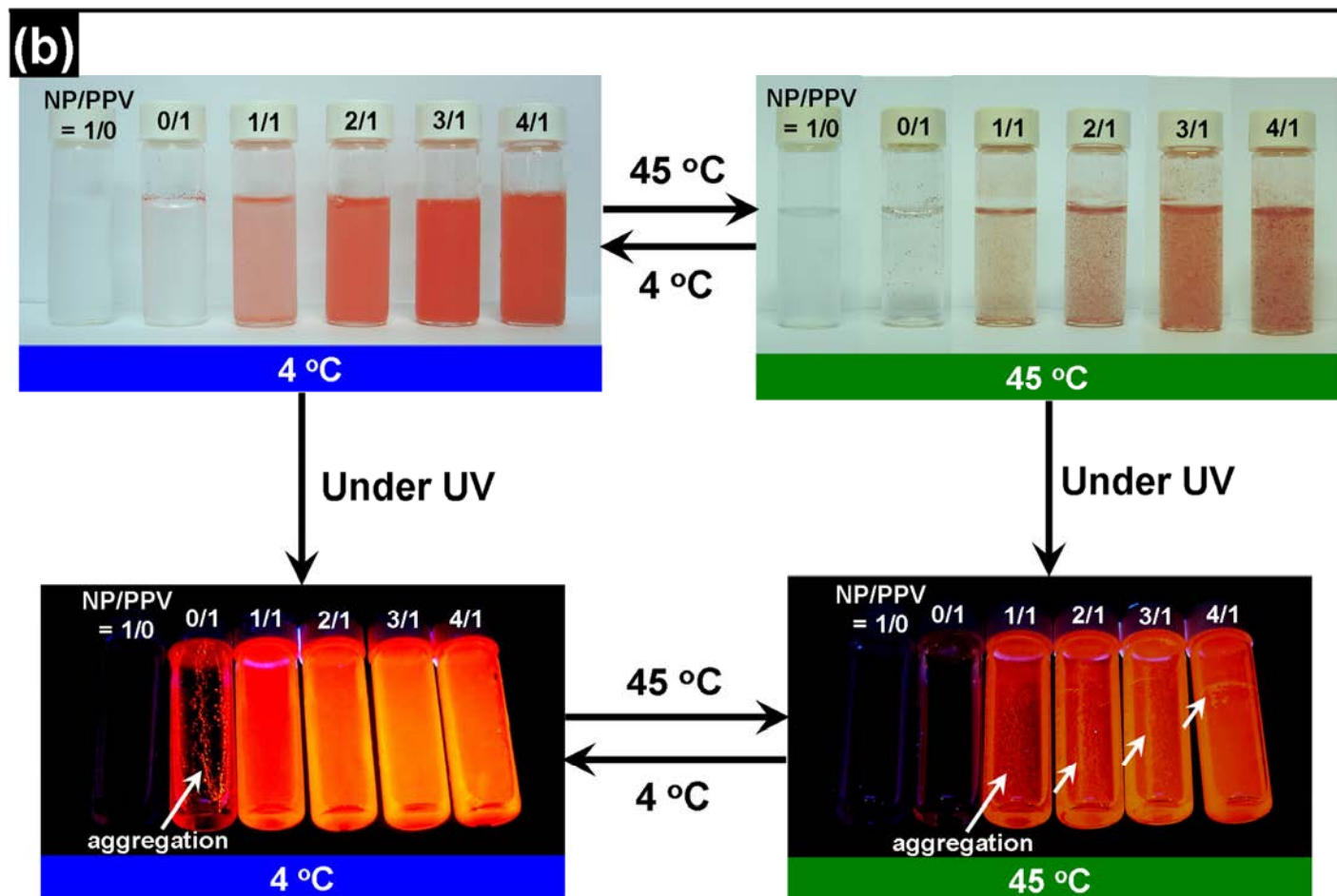
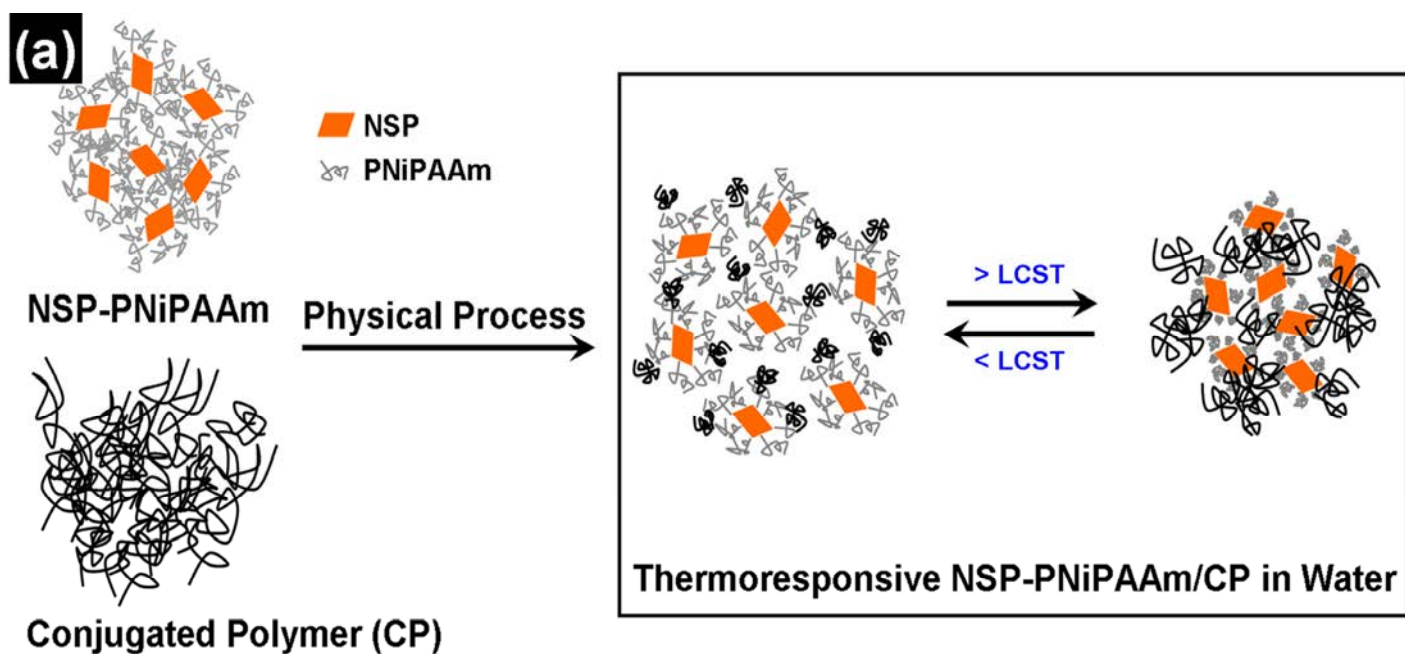
**Figure 33.** Conceptual illustration of homogeneous distribution between clay and CP through re-distribution of non-covalent bonding forces of the CP coils and rigid clay units.

### 3.3.4. Thermoresponsive behavior of conjugated polymer induced by NSP-PNiPAAm<sup>186</sup>

When pulverized together in a physical mixture, the two materials altered their inherent aggregating behaviors and mutually affected their solvation capacities (**Figure 34a**). The mixture of NSP-PNiPAAm and MEH-PPV showed a greatly improved solvation in water, whereas pristine MEH-PPV is non-dispersible. The fine dispersion of CP by the presence of NSP-PNiPAAm and demonstrated a thermoresponsive optical properties are conceptually described in **Figure 34**. The visual images in **Figure 34b** reveal that the NSP-PNiPAAm/MEH-PPV mixture at 3/1 and 4/1 weight ratios were dispersible as opposed to the aggregation of MEH-PPV without NSP-PNiPAAm. The difference in dispersion can be witnessed by the naked eyes, with a red-colored solution being obtained in the former cases and an apparent solid aggregate in the latter.

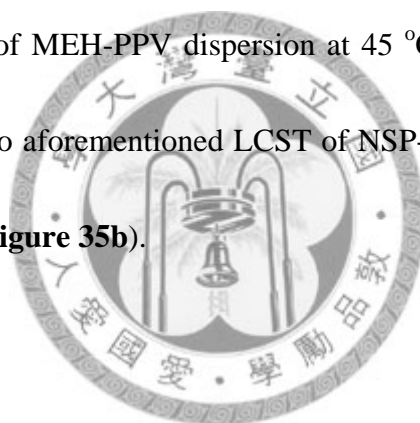


The same mixture also shows thermoresponsive behavior which stems from the attachment of PNiPAAm to the NSP surface. Under thermal cycling between 4 to 45°C, the aqueous dispersion of NSP-PNiPAAm/MEH-PPV showed reversible thermoresponsive aggregation due to the expulsion of water from the PNiPAAm hydrogen bonding interaction.



**Figure 34.** (a) Conceptual illustration of thermoresponsive NSP-PNiPAAm/MEH-PPV in water. (b) Thermoresponsive dispersion of NSP-PNiPAAm/MEH-PPV in water (1 mg MEH-PPV in 5 g water) at weight ratio of NSP-PNiPAAm/MEH-PPV = 1/0, 0/1, 1/1, 2/1, 3/1 and 4/1 weight ratios under temperature cycle and UV exposure.

Considering both the aqueous dispersion and thermoresponsive property, the NSP-PNiPAAm/MEH-PPV dispersions were examined by UV-visible spectrometer. As shown in **Figure 35a**, the MEH-PPV dispersion at 4 °C is greatly affected by the amounts of NSP-PNiPAAm added. The absorbance at 524 nm becomes more intense on increasing the amounts of NSP-PNiPAAm, implying improvement of the MEH-PPV dispersion. A control experiment (NSP-PNiPAAm/MEH-PPV = 1/0) indicated that the UV-vis absorbance stemmed fully from MEH-PPV in the water. For comparison, the same set of MEH-PPV dispersion at 45 °C exhibited a similar trend but weak absorbance due to aforementioned LCST of NSP-PNiPAAm that aggregates at elevated temperatures (**Figure 35b**).



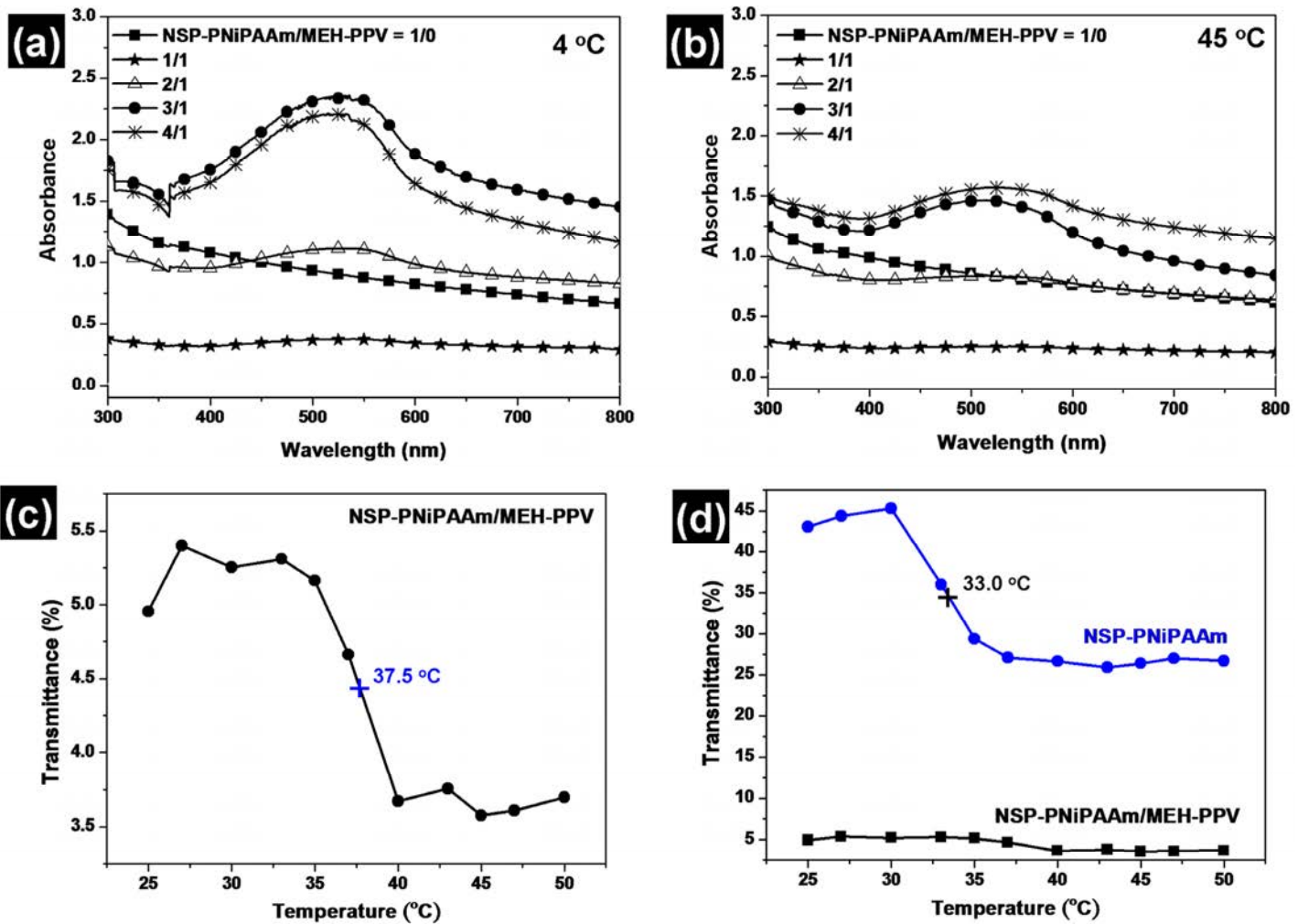


**Figure 35.** NSP-PNiPAAm/MEH-PPV dispersed in water at different weight ratio for UV-vis absorbance (a,b) and transmittance (c,d).

According to the definition of LCST, the thermoresponsive behavior can be precisely identified by temperature-dependence of UV-vis transmittance at 524 nm.

The NSP-PNiPAAm/MEH-PPV hybrid at 4/1 weight ratios was dispersed in water and has a solid content of 0.08 wt % NSP-PNiPAAm and 0.02 wt % MEH-PPV. The UV-vis transmittance of hybrid solution was monitored from 25 to 50 °C. As shown in

**Figure 35c**, the hybrid has a higher UV-vis transmittance at 25 to 30 °C, indicating the solution has a better dispersion in water than that after the transition temperature of

37.5 °C or LCST. At the elevated temperature, the solution transparency suddenly reduced due to the drop of particle aggregation through the expulsion of water from the PNiPAAm chains in the hybrids. Compared to the NSP-PNiPAAm (**Figure 35d**), the LCST of NSP-PNiPAAm/MEH-PPV (37.5 °C) is similar to that of NSP-PNiPAAm (33.0 °C). The LCST phenomenon of the dispersion can also be characterized by FE-SEM. Below the LCST (37.5 °C), the NSP-PNiPAAm/MEH-PPV dispersed very well in the water (**Figure 36a insert**) and spin-coated into film that exhibited a morphology with *ca.* 50 nm particle size (**Figure 36a,b**). In contrast, the dispersion at the temperature above LCST rendered the film with the observable larger particle size of *ca.* 100 nm (**Figure 36c,d**). The temperature difference altered the particle size of MEH-PPV due to the temperature-responded aggregation. For comparison, NSP-PNiPAAm itself revealed a smooth surface at both temperature of 25 °C (**Figure 36e,f**) and 80 °C (**Figure 36g,h**) in the absence of CPs. Without the association with MEH-PPV, the NSP-PNiPAAm film morphologies failed to demonstrate the surface differences perhaps due to the NSP predominance in controlling the aggregation.



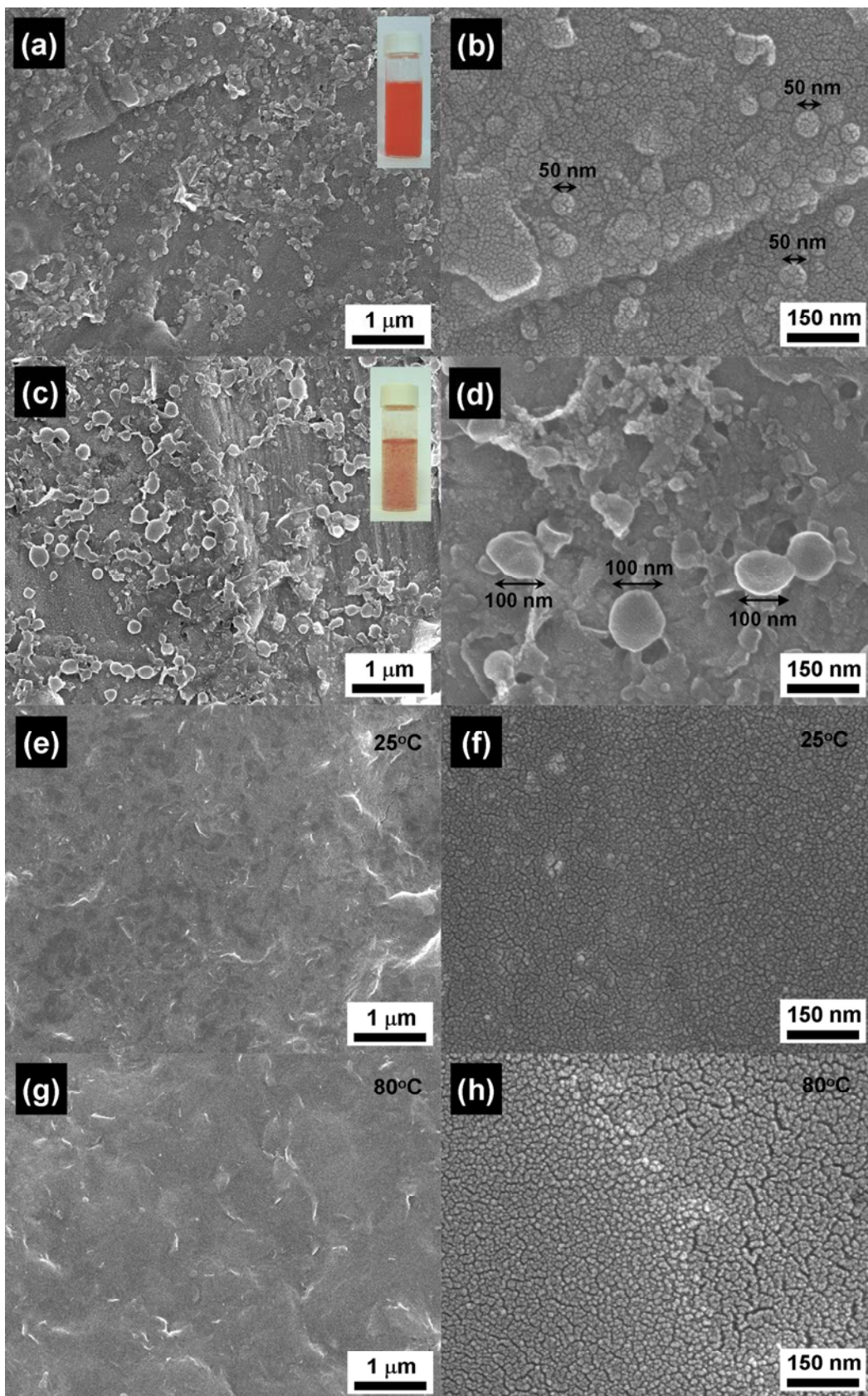


**Figure 36.** FE-SEM images of NSP-PNiPAAm/MEH-PPV dispersed in water and then dried at 25 °C (a,b) and 80 °C (c,d), and surface of NSP-PNiPAAm coating at 25 °C (e,f) and 80 °C (g,h).

The NSP-PNiPAAm/MEH-PPV dispersion showed a compounded property of thermoresponsive at the transition temperature of 37.5 °C from NSP-PNiPAAm and the photo-physical performance of MEH-PPV. At 4 °C under illumination from a UV lamp, the NSP-PNiPAAm/MEH-PPV dispersions showed good dispersion with orange light-emission, and the intensity of the emission was increased in the presence of NSP-PNiPAAm due to the enhanced degree of dispersion (**Figure 34b**). However, the NSP-PNiPAAm/MEH-PPV displayed aggregation with weak emission above the LCST or at 45 °C.

### ***3.3.5. Photoluminescence behavior of dispersion solution and solid film***

The photo-physical property of PNiPAAm/MEH-PPV was further examined by PL spectrometer. The PL was manifested at an excitation wavelength of 524 nm which corresponded to the inherent MEH-PPV properties. As shown in **Figure 37a**, the PL intensity of the NSP-PNiPAAm/MEH-PPV dispersion (at 4 °C) increased with the increasing amount of NSP-PNiPAAm, which is nicely consistent with the UV-vis results. When the same dispersion was heated to 45 °C, however, the intensity of PL from the MEH-PPV decreased due to the LCST behavior of the NSP-PNiPAAm (**Figure 37b**), which stemmed from expulsion of water from the PNiPAAm chains. The overall effect is that MEH-PPV mixed with NSP-PNiPAAm displays the compounded thermoresponsive-photoluminescence sensitivity.

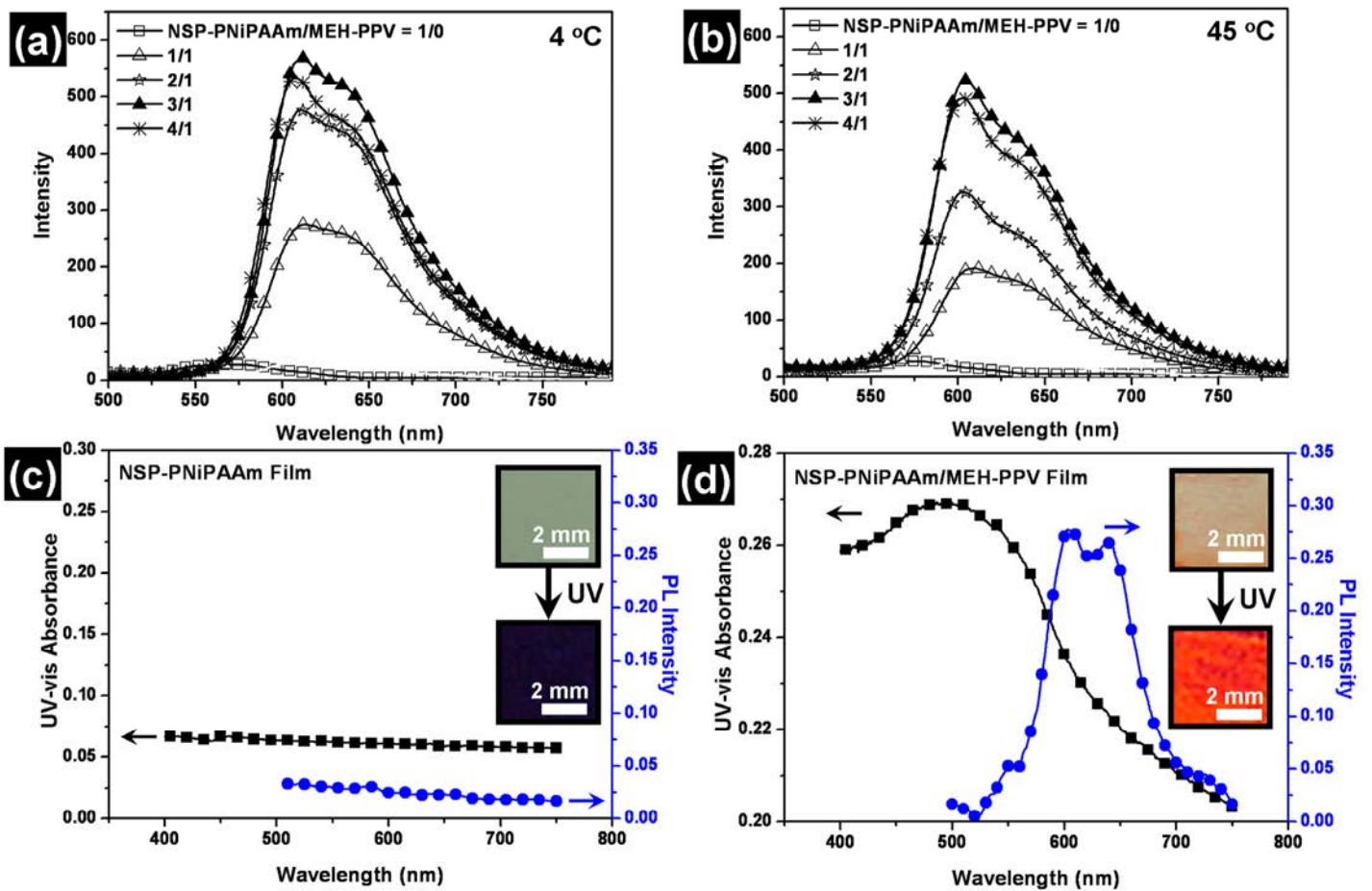


**Figure 37.** NSP-PNiPAAm/MEH-PPV dispersed in water at different weight ratio for PL emission (a,b), and their corresponding films at weight ratio of NSP-PNiPAAm/MEH-PPV = 3/1 and their optical properties (c,d).

For the practical application, NSP-PNiPAAm/MEH-PPV films were prepared from the corresponding solutions and shown to have UV-vis and PL properties. In a control experiment with NSP-PNiPAAm film (**Figure 37c**), no UV-vis or PL features were detected. This result was confirmed in that UV exposure and visual observation showed no emission (**inset in Figure 37c**). On the contrary, NSP-PNiPAAm/MEH-PPV film has a maximum absorption at  $\lambda_{\text{max.abs.}} = 485 \text{ nm}$  and a maximum emission at  $\lambda_{\text{max.em.}} = 605 \text{ nm}$  (**Figure 37d**). Comparing the UV-vis results

for the solution and film, the absorbance shows a blue shift from 524 nm (aqueous dispersion) to 482 nm (solid film) due to the influence of the conjugated length.<sup>187</sup> The inset in **Figure 337** shows that the film exhibited a noticeable orange light-emission when illuminated with a UV lamp. This orange emission is exactly correlated to the PL at 605 nm.

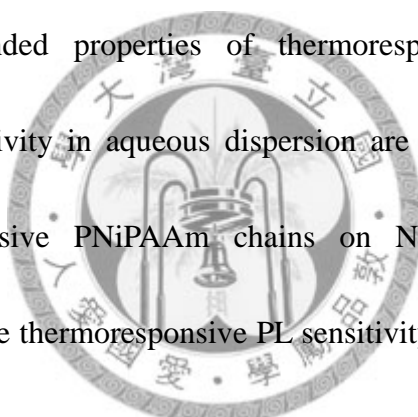
The thermoresponsive behavior seen for aqueous dispersion of CP in the presence of the NSP-PNiPAAm may be rationalized in terms of noncovalent bonding forces and the expulsion of water from the PNiPAAm chains. The CP is hydrophobic and only soluble in organic media. In water, the polymers are aggregated or precipitated due to molecular-coil entanglement. The aqueous dispersion, thermoresponsive behavior, and PL sensitivity of the hybrid must therefore stem from the NSP, PNiPAAm and MEH-PPV. Both visual observation and UV-vis absorbance confirmed the behavior of the NSP-PNiPAAm/MEH-PPV mixtures in aqueous dispersion. As illustrated conceptually in **Figure 34a**, the initial grinding of two distinctly different materials of nanometer dimensions may have homogenized these materials on the micrometer scale. Upon dispersal in water, the strong non-covalent bonding force between NSP-PNiPAAm and water molecules could further preclude the polymer self-aggregation. The mutual interactions through non-covalent bonding forces, such as ionic charges on the clay surface, van der Waals forces, and  $\pi$ - $\pi$  stacking for CP

entanglement attraction, as well as the plate-like geometric shape blockage, could all together influence the aggregation of the pristine CP. Below LCST, the NSP-PNiPAAm showed a good solubility in water because both PNiPAAm chains and NSP are hydrophilic. The well dispersion of NSP-PNiPAAm consequently assisted the dispersion of MEH-PPV in contacting with NSP. Above LCST, the PNiPAAm chains behave as hydrophobic moieties and aggregate together with MEH-PPV in water. Furthermore, the thermoresponsive behavior is induced by the PNiPAAm through a mechanism involving expulsion of water from the PNiPAAm chains, and the PL performance shows a strong correlation with the LCST behavior. The overall effect is that the CP becomes dispersible and thermoresponsive without the need for tedious chemical modification of the CP molecules. The results also imply the “green” process may be developed and generalized for other hydrophobic polymers.

### **3.3.6. Conclusion**

By simply pulverizing CPs with Mica, the powder mixture became conveniently dispersible in water. The fluorinated Mica is the best dispersing agent among the screened clays including MMT, SWN and LDH. The dispersion enhancement is measured by UV-vis absorbance in water. Three CPs (MEH-PPV, SPA and TPOPA) were used to generalize this colloidal process for dispersing CPs. The CP films were prepared and demonstrated for their photoluminescence properties. There are observed

maximum emission at 605 nm, 560 nm and 530 nm for three CPs and the corresponded color emitting, orange, olive and green under UV lamp. The dispersion mechanism is explained by non-covalent bonding redistribution in water medium and also a geometric shape exclusion effect derived from the high aspect-ratio plate structure. Furthermore, the NSP-PNiPAAm/MEH-PPV mixture displays thermoresponsive dispersion at the critical temperature of 37.5 °C and has photoluminescence at 605 nm. The corresponding films have been prepared and still maintain their UV-vis and PL properties. The compounded properties of thermoresponsive behavior and its correlation with PL sensitivity in aqueous dispersion are the results of fine mixing among the thermoresponsive PNiPAAm chains on NSP and MEH-PPV with light-emitting behavior. The thermoresponsive PL sensitivity of CPs in the presence of NSP-PNiPAAm provides a smart material, prepared by an organic solvent-free process, for biomedical and sensor applications.





### 3.4. Dispersion of Organic Pigments by Using Platelet-Like Clays

In our previous researches, a systematic approach for designing acrylic copolymers consisting of two monomers, butyl methacrylate (BMA) and glycidyl methacrylate (GMA), by using the synthetic method of atom transfer radical polymerization (ATRP) was reported. The synthetic method was previously reported for making polyacrylates of self-assembling properties.<sup>188</sup> For the purpose of interacting with pigment particles, the prepared BMA/GMA backbone was allowed to grafting with different polar pendants including hydroxyl, carboxylic acid and amine groups. The structure was varied with pendant polarities and evaluated for the performance of dispersing a representative Yellow pigment. The performance such as pigment particle size, viscosity, and stability was correlated with the copolymer structures. The mechanism for generating homogeneous dispersion was investigated and explained by a electrostatic charge interaction of 1,3-diamine on pigment acidic surface through the analysis of zeta potential.

In the **Section 3.4.**, an alternative approach of dispersion organic pigments was proposed. By using large difference of geometric shapes, the un-soluble organic pigments become dispersable. Various color pigments, including C.I. pigment red 177, green 36, blue 15, yellow 138 and violet 23, are simply pulverized with platelet-like clay and the mixtures are readily dispersing in organic mediums.

### 3.4.1. Dispersion of Organic Pigments in the Presence of Clays

Organic pigments are generally water-insoluble and require dispersants such as surfactants or copolymers to improve their solubility for processing.<sup>156–165</sup> In Section 3.1–3.3, a physical-geometric approach to control the degree of aggregation of nanomaterials such as CNTs, CBs, CNCs, AgNPs, FeNPs and CPs through geometric shaped exclusion were reported.<sup>166–170</sup> Compared to various clays, the synthetic fluorinated mica (Mica) is mostly suitable for improved the dispersion of nanomaterials. The mixture of organic pigment and platelet-like Mica showed a greatly improvement of salvation of pigment-Mica mixture in water, whereas pristine pigment is non-dispersible (**Figure 38**). As shown in **Figure 39**, the pristine pigment red 177 and green 36 were in-soluble in deionized water (**Figure 39a,b**). After vigorously grinding the pristine pigment, the fine pigment powder still rendered large aggregation and severely precipitation (**Figure 39c,d**). However, the fine dispersion of pigment can be achieved by the presence of platelet-like Mica and the resultant solution revealed homogeneous dispersion with colorful appearance of red or green (**Figure 39e,f**).

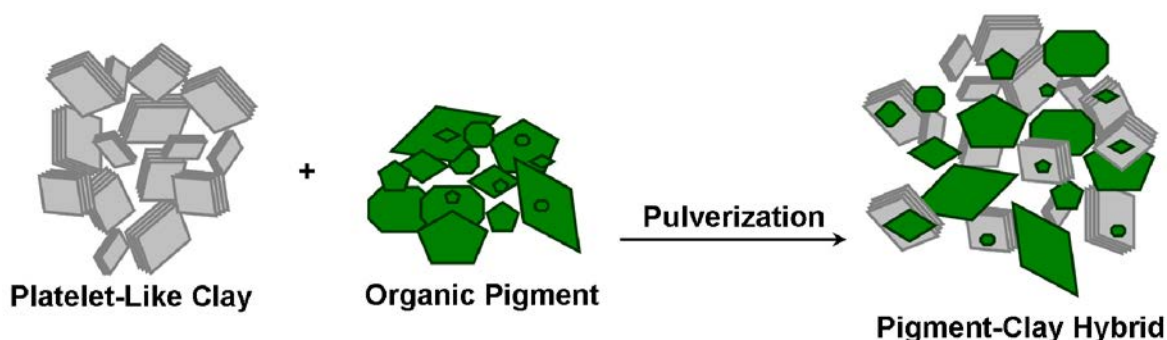


**Figure 38.** Conceptual diagram of dispersion organic pigment through GIF.



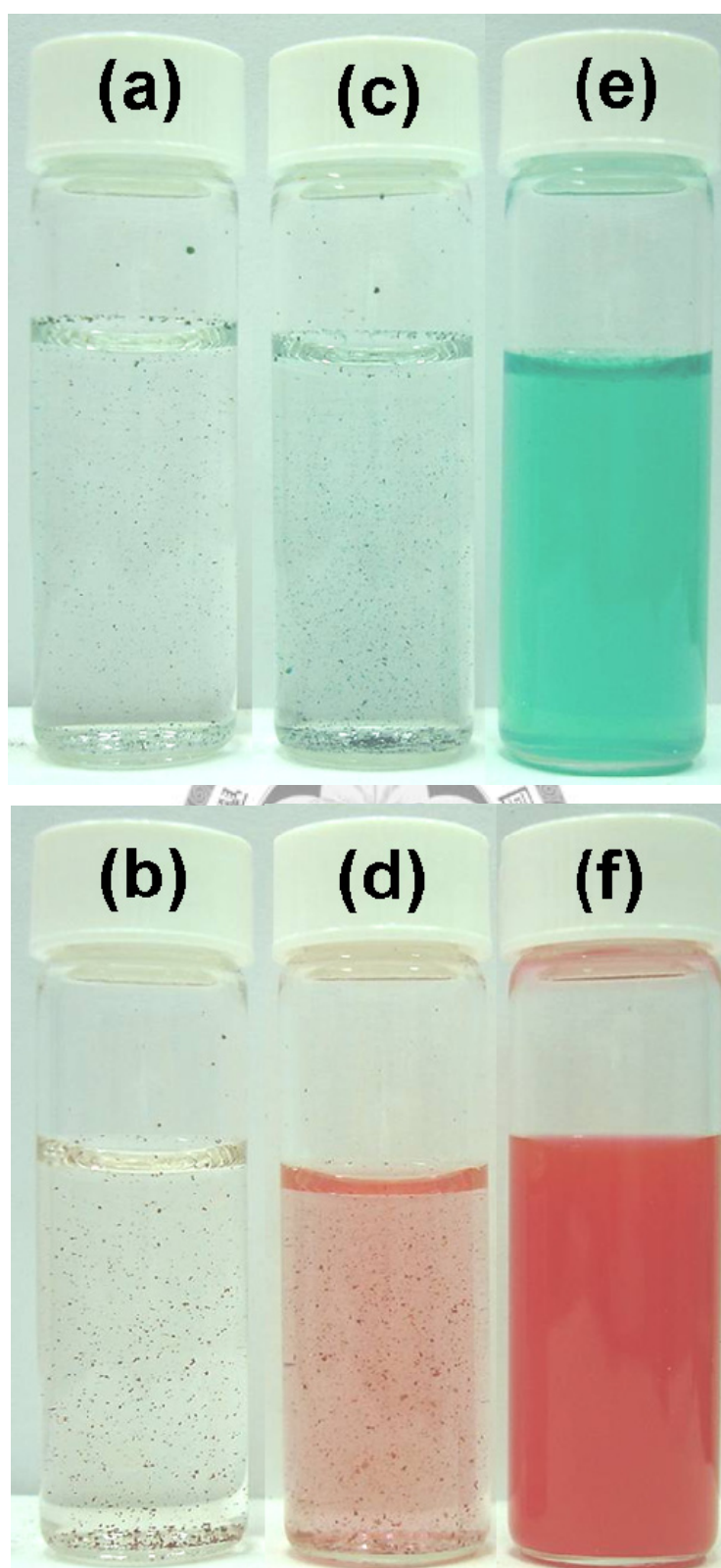


**Figure 39.** Visual pictures of dispersing pigments red 177 and green 36 and their control experiments. Pristine pigment directly added into water (a,b). Pristine pigment with grinding treatment and then added into water (c,d). The pigment grinding with Mica powder at weight ratio of 1/1 and the mixture powder is dispersible in water (e,f).

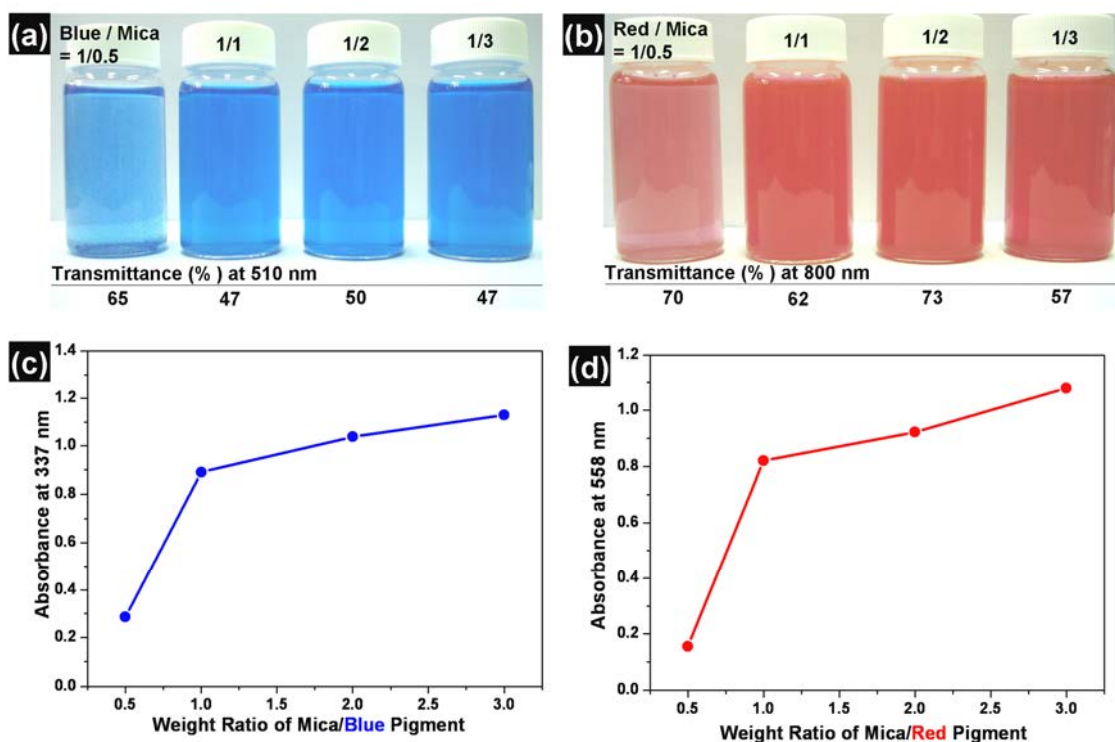


**Figure 40.** Visual observation of dispersing pigment blue 15 (a) and red 177 (b) at various amounts of Mica presence and their UV-vis absorbance at wavelength of 337 nm (c) and 558 nm (d).

To understand the effect of Mica clay on dispersing pigments, commercial product of blue 15 and red 177 was further chose for studied. The powder mixtures of pigment-Mica were prepared at weight ratio of Mica/pigment = 0.5/1, 1/1, 2/1, and 3/1, and then dispersed in the water. In the **Figure 40**, showed the visual observation of pigment dispersion in water and the solubility of pigment can be differentiated by naked eyes. For example, the Mica/blue mixture at 0.5/1 weight ratios was slightly dispersed in water and revealed light blue color, however, as increased the Mica amount at weight ration of Mica/blue = 1/1, 2/1 and 3/1, the blue pigment rendered homogeneous dispersion with deeply blue color (**Figure 40a**). The same trend of

dispersion pigment by using clay as inorganic dispersant was revealed in the red pigment (**Figure 40b**).

The dispersion solutions were further analyzed by UV-vis spectrometer. In the **Figure 40c,d**, the absorbance intensity was enhanced with increasing Mica amount which indicated the improvement of dispersing blue or red pigment.<sup>10</sup> Compared to the pigments, it was reported that the pristine Mica dispersing in water have no absorbance at wavelength of 400–800 nm.<sup>169</sup> The improvement of dispersion has a percolation at 1/1 for blue and red pigments. The percolation of UV-vis result indicated that the aggregation of pigment has been effectively reduced at the presence of Mica. In addition to the UV absorption, the performance of solution transmittance, 65%, 47%, 50% and 47% at the absorption of  $\lambda = 510$  nm were measured for blue pigment (**Figure 40a**) and 70%, 62%, 73% and 57% were measured for red pigment (**Figure 40b**), respectively. While a high transparency is required for the applications, the dispersible mixture powder at weight ratio of Mica/pigment = 2/1 may have potential of real practical devices.

The performance of platelet-like Mica for dispersing the representative blue and red pigments are examined by ZetaPlus zetameter and summarized in **Table 12**. After adding platelet-like Mica and adequately milling, the pigment was homogeneously dispersed in water. The result of particle size analyzer showed the average aggregated

size of pigment has been decreased from 7.2  $\mu\text{m}$  to 0.9  $\mu\text{m}$  for blue and 10  $\mu\text{m}$  to 0.5  $\mu\text{m}$  for red, respectively. The interaction between pigment and Mica can be probed by using zeta potential measurement and the result revealed that the zeta potential of pigment-Mica aqueous solutions decreased from  $-12$  to  $-24$  mV for blue and  $-13$  to  $-23$  mV for red.

**Table 12.** Particle Size and Zeta Potential of Pigment-Mica Dispersion in Water.

Weight Ratio of Mica/Pigment	C.I. Pigment Blue 15		C.I. Pigment Red 177	
	Average Particle Size ( $\mu\text{m}$ )	Zeta Potential (mV)	Average Particle Size ( $\mu\text{m}$ )	Zeta Potential (mV)
0.5/1	7.2	$-12$	10	$-13$
1/1	1.4	$-18$	1.0	$-18$
2/1	0.9	$-19$	0.5	$-24$
3/1	1.8	$-24$	0.7	$-23$

The measurements of average particle size and zeta potential were further combined and discussed in **Figure 41**. Both blue- and red-Mica hybrids have a percolation of particle size at weight ratio of Mica/pigment = 1/1. The result of size percolation is consisted with the trend of UV-vis analysis (**Figure 40c,d**). Consideration the surface charge, the zeta potential has been shifted and showed a positive change which indicated the strong surface-charge interaction between Mica and pigment particles through physical attraction.<sup>10,189</sup> For example in **Figure 41a**, at weigh ratio of Mica/pigment = 2/1, the blue-Mica hybrid can be well dispersed in the water and the particle size has minimized to 900 nm with zeta potential of  $-19$  mV.

Compared to the hybrid, the pristine Mica has the zeta potential of  $-39$  mV and consequently decreased to  $-19$  mV in the presence of blue pigment. For the dispersion of red pigment at Mica/red = 2/1, the red-Mica solution was obtained in particle size of 500 nm with zeta potential of  $-24$  mV (**Figure 41b**). In the control experiment, the pristine Mica has a zeta potential of  $-39$  mV and consequently decreased to  $-24$  mV in the presence of red pigment.



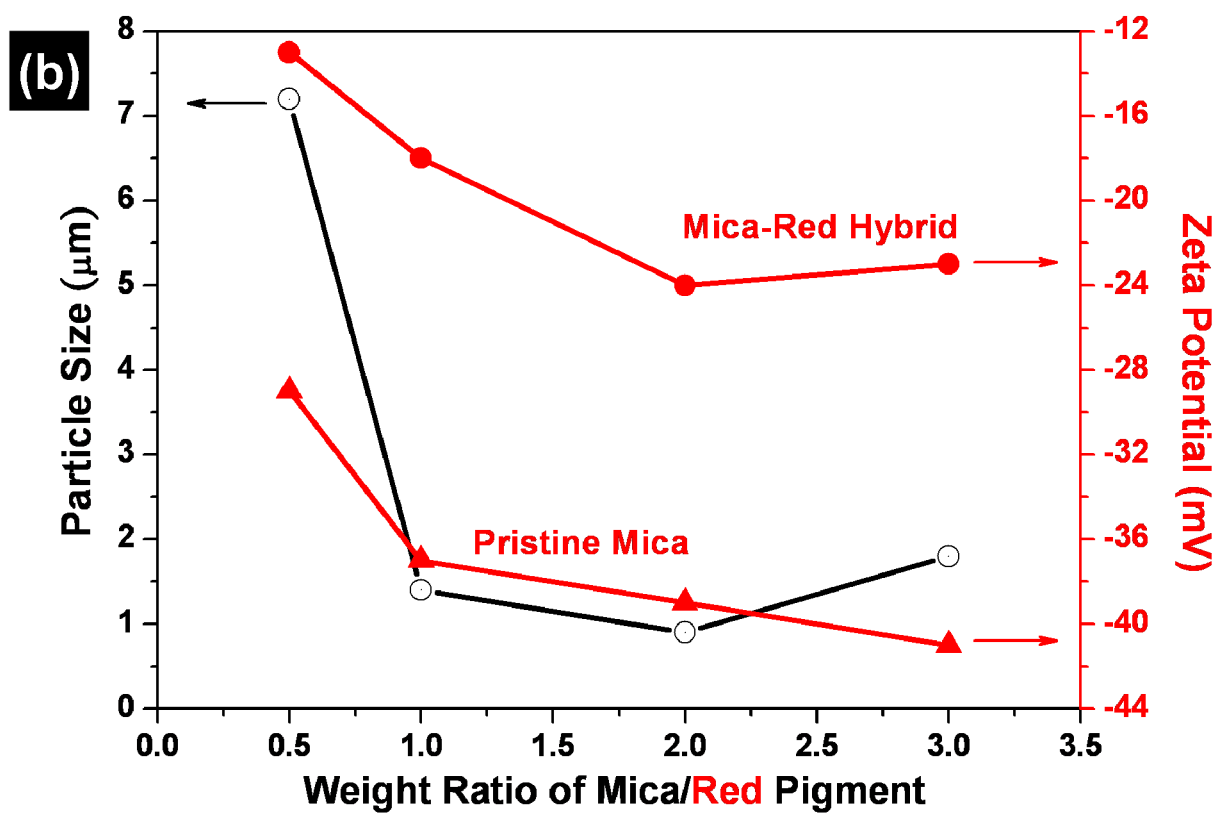
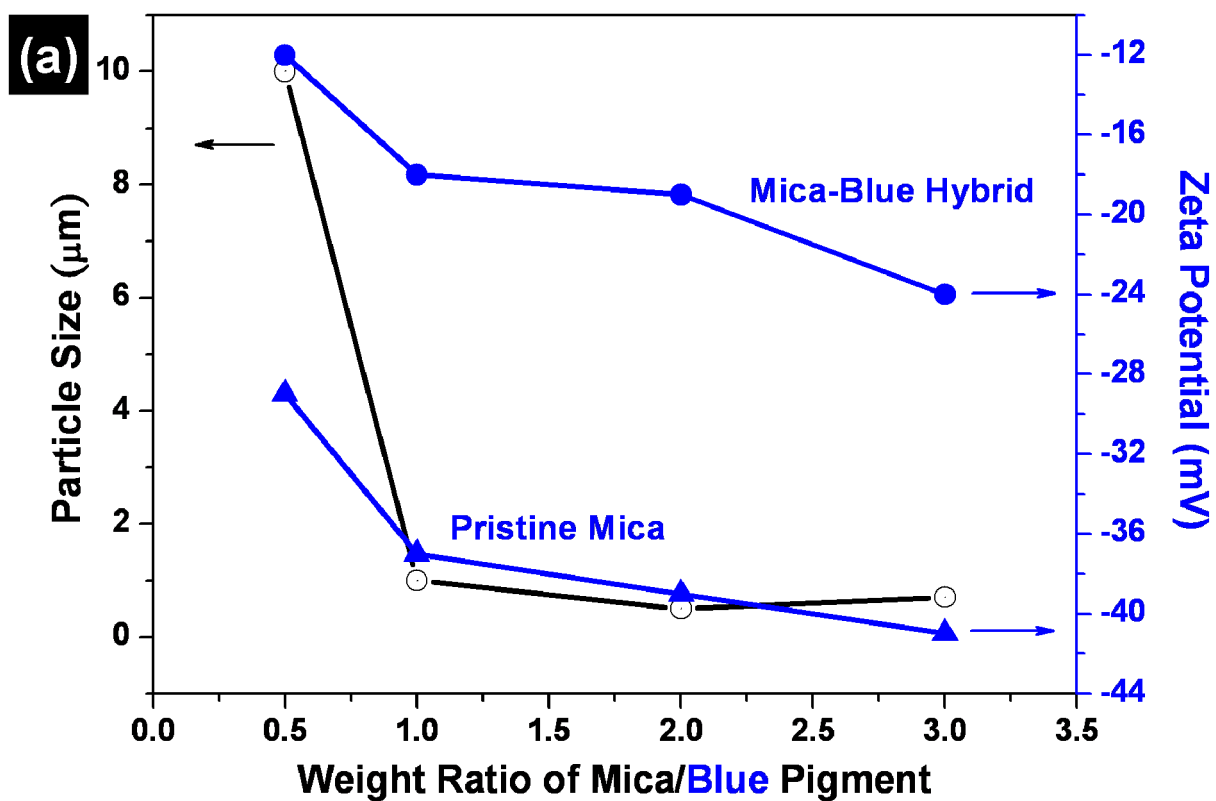


**Figure 41.** Particle size and zeta potential analysis of dispersing pigment blue 15 (a) and red 177 (b) in water.

The particle size and volume distribution could be characterized for the particular pigment dispersion in the medium. After adding different Mica amounts, the pigment was suspended in water to have a general distribution of particle sizes, for examples, the particle size distribution for blue pigment has decreased from 8377 nm/9152 nm to 735 nm or 474 nm at weight ratio of 1/1 or 2/1 (**Figure 42a**). However, in the case of Mica/blue = 3/1, the excess amount of Mica increased the distribution of 1058 nm/3554 nm due to the origin size of Mica is *ca.* 300–1000 nm.<sup>172</sup> The distribution of red pigment have the same trend and the dispersion result showed large size distribution of 10000 nm (**Figure 42b**) at Mica/red = 0.5/1 and then decreased to 439 nm or 474 nm at Mica/red = 1/1 or 2/1. The excess Mica in the water increased the size distribution from nano-scale (*ca.* 400 nm) to micro-scale (472 nm/ 2430 nm). The pigment size distribution is a good indication for the effectiveness of the inorganic dispersants, Mica, and the results revealed the relative effectiveness for the Mica interacting with pigment particles is optimized at weight ratio of Mica/pigment = 2/1.

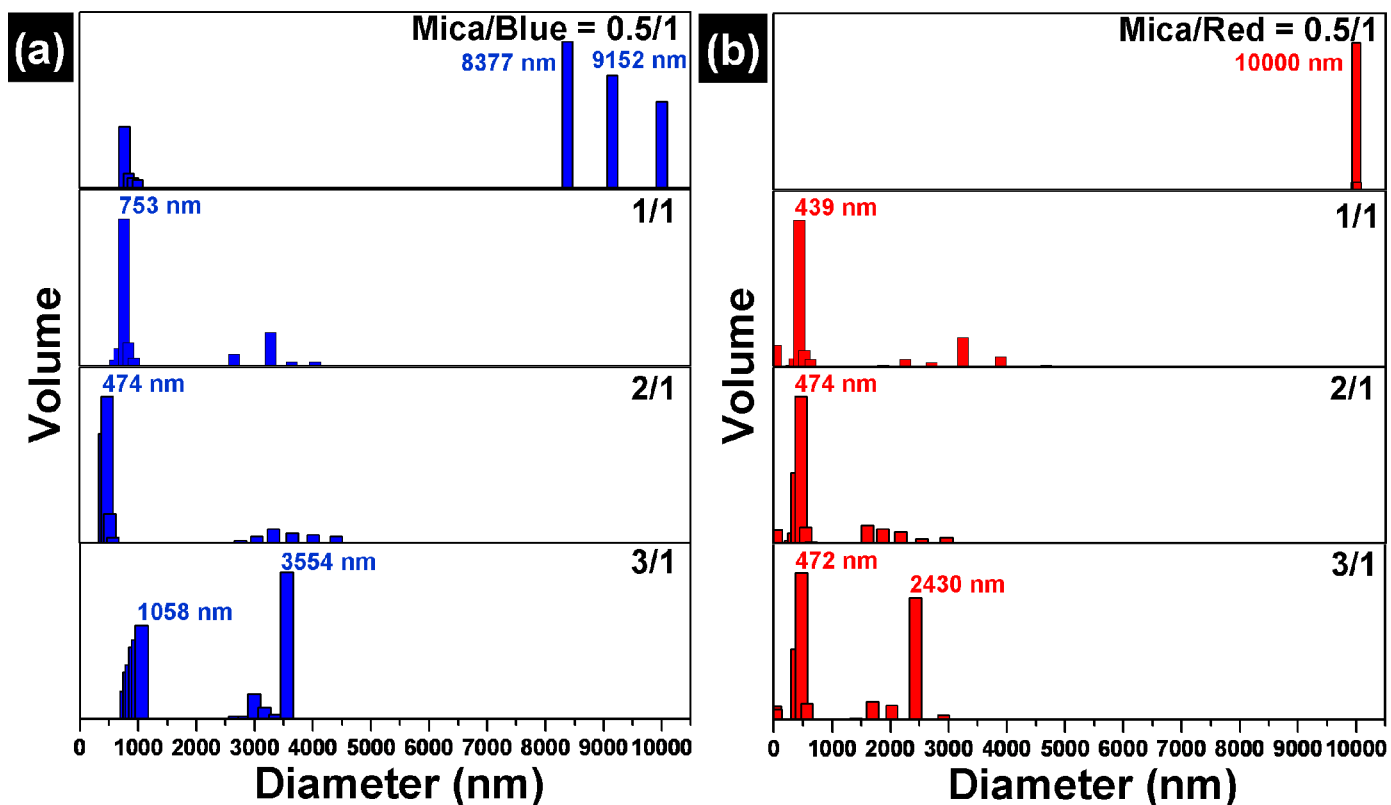


**Figure 42.** Size distribution of blue (a) and red (b) pigments dispersion in water.

Regarded platelet-like clay as an inorganic dispersant for pigments, various pigments were further dispersed in water by using Mica. The dispersion was observed by naked eyes and TEM. As showed in **Figure 43**, pigments in red, green, blue, yellow and violet color were homogeneously dispersed in water (**Figure 43 insert**). The TEM morphology revealed the particle sizes of pigments are *ca.* 300–700 nm for red, 0.4–2  $\mu\text{m}$  for green, 70–160 nm for blue, 70–240 nm for yellow and 70–570 nm for violet, respectively. Particularly, the geometric shape of dispersing the pigment violet 23 rendered rod-like assembly due to the rigid unit consisting from six and five member rings (**Figure 7**). Compared to the pigments, the pristine Mica is an irregular platelet with average dimension in *ca.* 300 nm.<sup>175</sup>



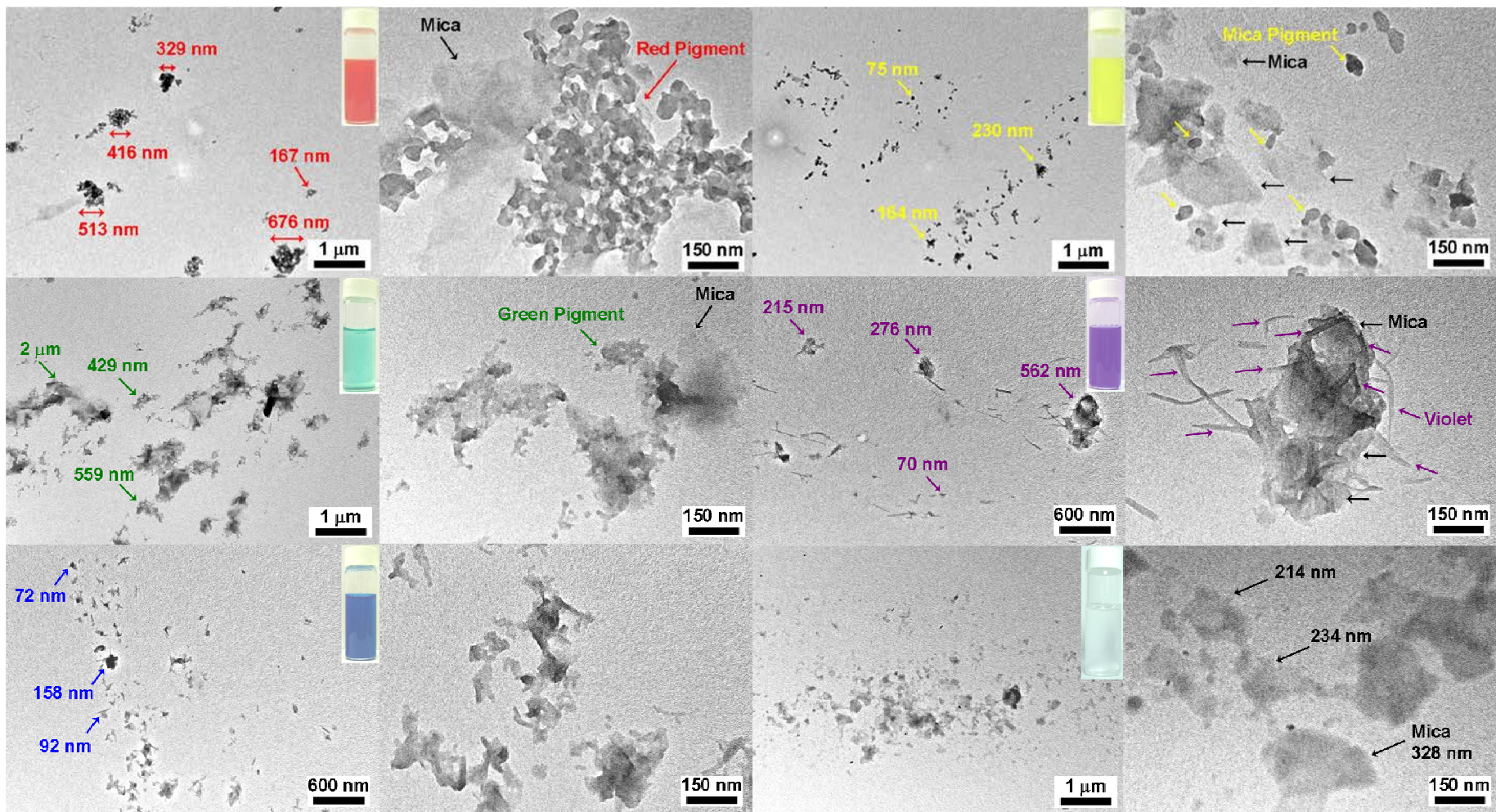


**Figure 43.** TEM morphology of dispersing pigment red 177, green 36, blue 15, yellow 138, violet 23 and pristine Mica in water (weight ratio of Mica/pigment = 1/1).

For practical applications in optoelectric devices, the pigment-clay solutions were used to prepared pigment-PVA composite film. The mixture solutions of pigment-PVA were showed in **Figure 44a,b**. The dispersion can be differentiated by naked eyes and the dispersion of pigment in PVA was improved due to the presence of platelet Mica. For example, the Mica/blue has large aggregation at weight ratio of 0.5/1, however, Mica/blue revealed homogeneous dispersion at 3/1. The dispersion of Mica/red has the same trend as Mica/blue. The mixture solutions of pigment-PVA were analyzed by UV-vis spectrophotometer. The blue-PVA solution has broad absorption at 625 nm. The absorbance intensity increased with increasing Mica amount indicated that the improvement of blue dispersion in PVA solution (**Figure 44c**). Red-PVA solutions have the same trend of dispersion behavior as blue-PVA solution (**Figure 44d**). The UV-vis result rendered strong broad absorption at 550 nm and the intensity increased with increasing Mica amount due to the improvement of pigment dispersion.

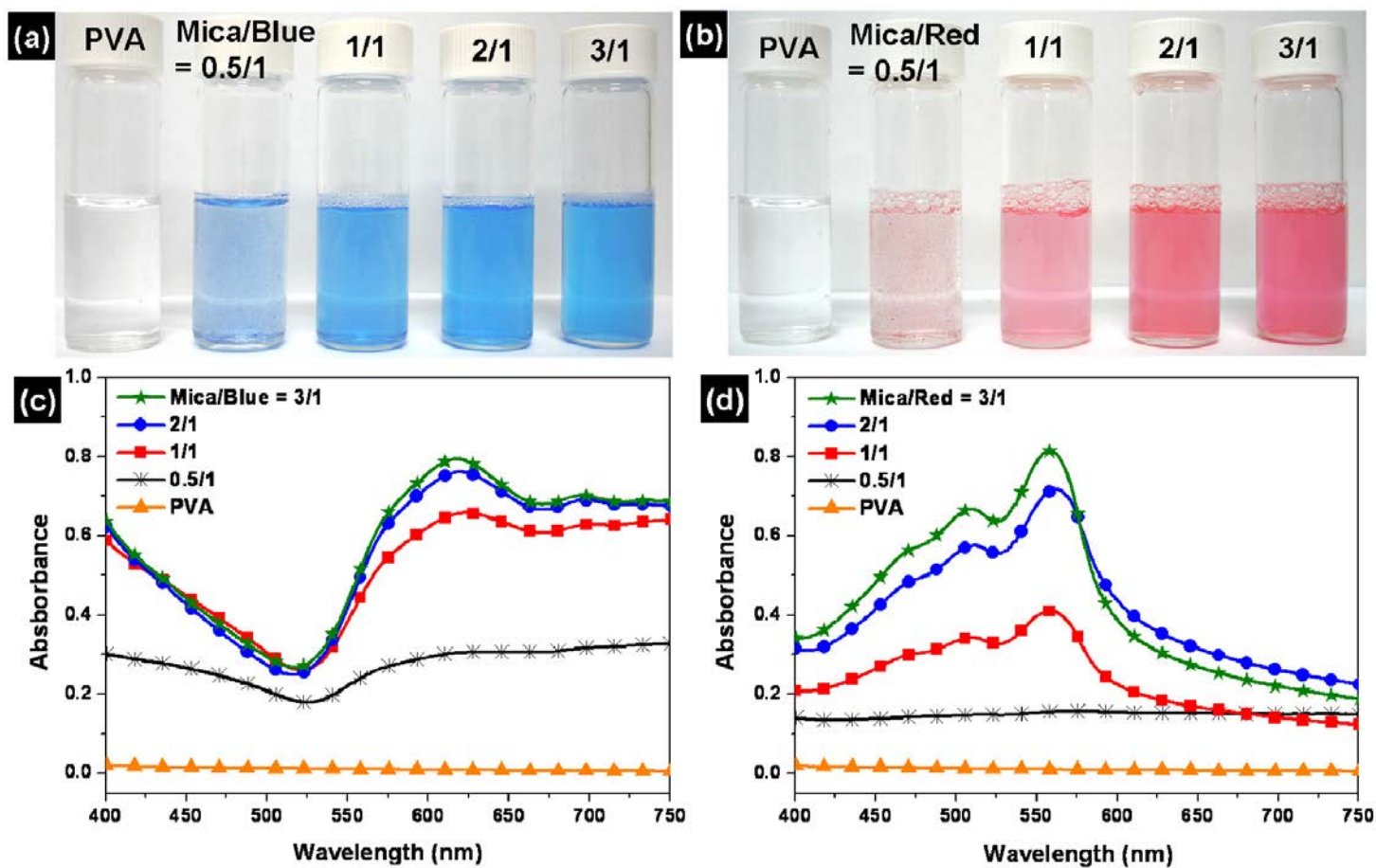


**Figure 44.** Visual observation of mixture solution of pigment-PVA: blue-PVA (a) and red-PVA (b) at various amounts of Mica presence and their UV-vis absorbance of blue (c) and red (d).

The pigment-PVA composite films with large aggregation rendered colorless appearance (**Figure 45a,b**), for example, blue-PVA film revealed blue at weight ratio of Mica/blue = 0.5/1. However, composite with homogeneous dispersion showed colorful appearance, for instance, red-PVA film revealed red at weight ratio of Mica/red = 3/1. The solid films were analyzed by using UV-vis spectrophotometer and the results were the same as in **Figure 44c,d**. The blue-PVA film has broad absorption at 625 nm. The absorbance intensity increased with increasing Mica amount indicated



that the improvement of blue dispersion in PVA matrix (**Figure 45c**). Red-PVA films have the same trend of dispersion behavior as blue-PVA (**Figure 45d**). The UV-vis result rendered strong broad absorption at 550 nm and the intensity increased with increasing Mica amount due to the improvement of pigment dispersion.

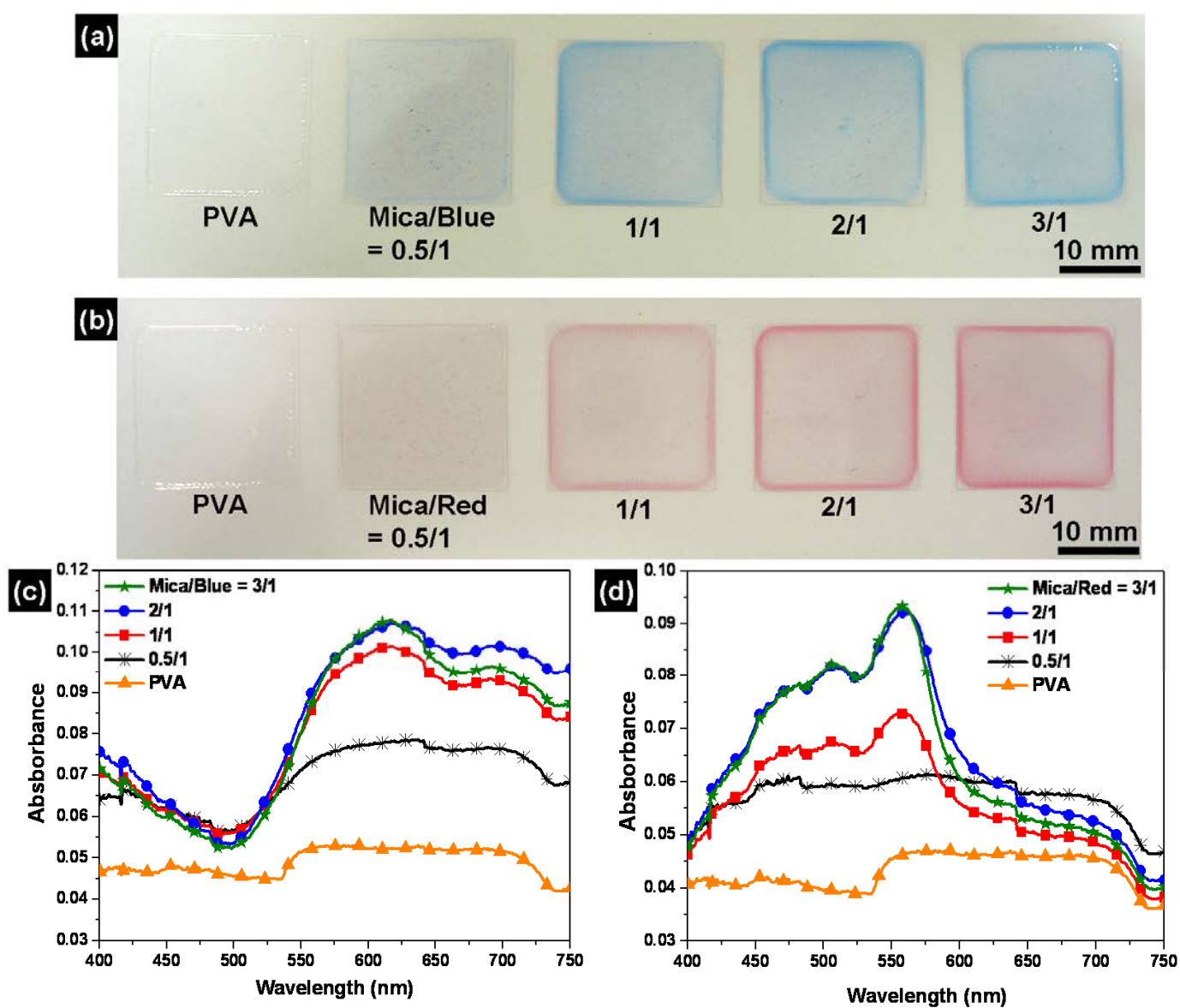
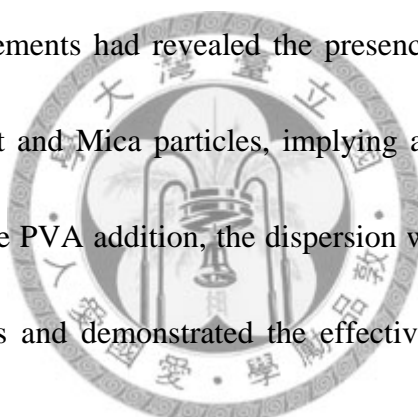


**Figure 45.** Visual observation of composite films of pigment-PVA: blue-PVA (a) and red-PVA (b) at various amounts of Mica presence and their UV-vis absorbance of blue (c) and red (d).

### 3.4.2. Conclusion

The use of inorganic Mica demonstrated the improvement of insoluble pigment dispersion in water mainly due to their difference in geometric shape. The dispersion method was generalized for C.I. pigments, red 177, green 36, blue 15, yellow 138 and violet 23, enabled by the Mica clay with geometric plate shape, high-aspect ratio and intensive-surface charge. By simple process of pulverization of pigment and Mica, the mixture became dispersible in water and controllable particle size at *ca.* 70 nm–2.0  $\mu\text{m}$ . The zeta potential measurements had revealed the presence of strong surface-charge attraction between pigment and Mica particles, implying another important factor of charge interaction. With the PVA addition, the dispersion was further coated into film in different pigment colors and demonstrated the effectiveness of Mica clay effect. Through the Mica interaction, the difficulty of dispersing pigment in water is overcome and the feasibility of utilizing pigments without organic solvent is evidenced.



## Chapter 4. Summary

The “Geometric-Shape Inhomogeneity Factor” has been generalized in various nanomaterials including carbon nanotubes, carbon nanocapsules, carbon blacks, silver nanoparticles, iron-oxide nanoparticles, conjugated polymers and organic pigments

(Figure 46).

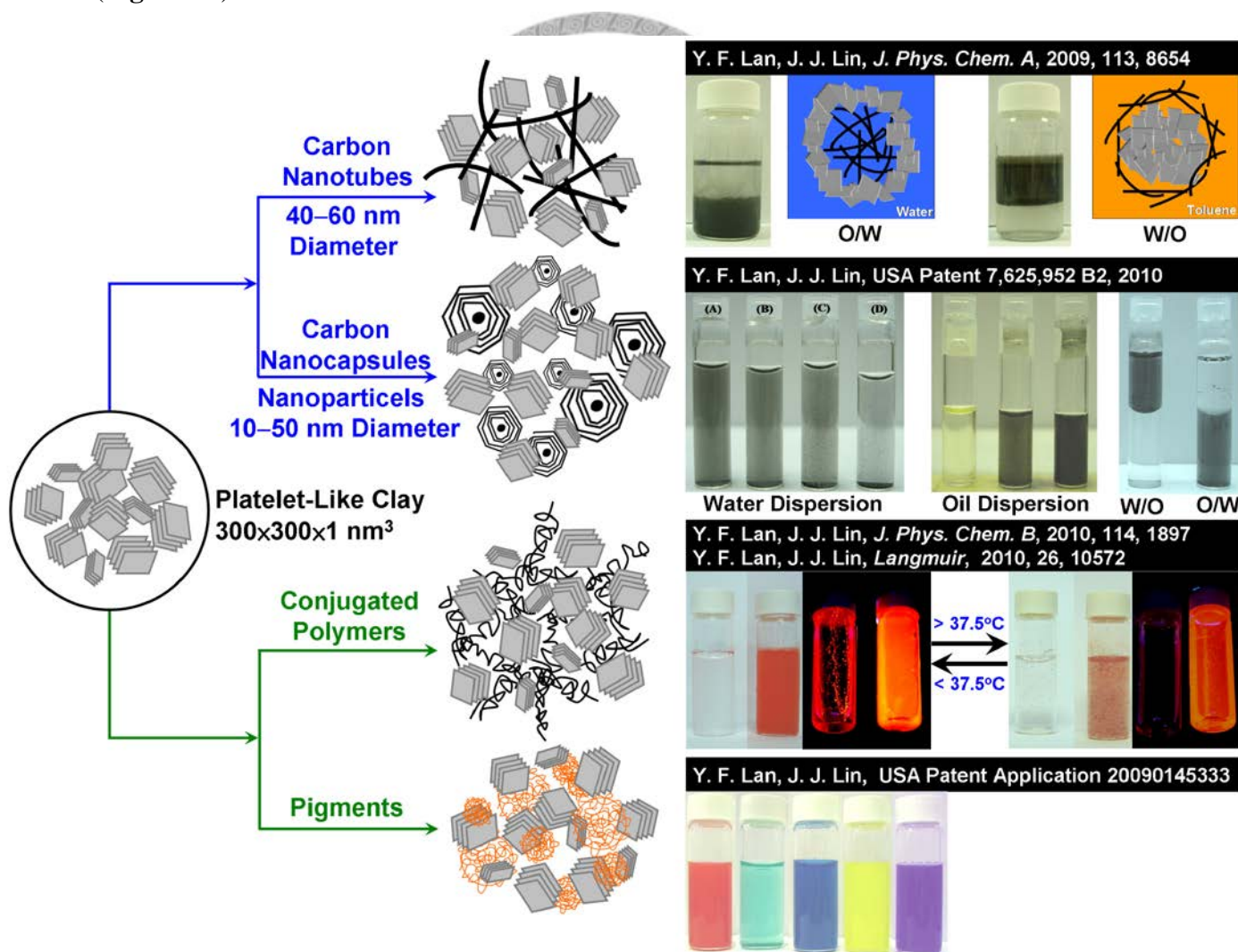
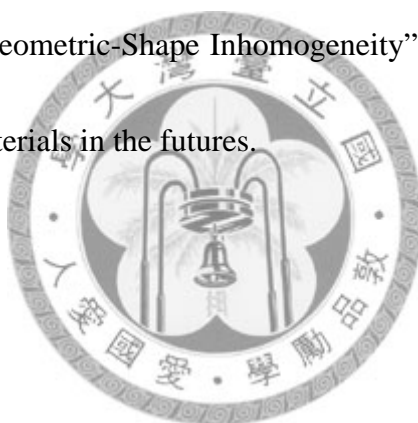


**Figure 46.** Generalization of Geometric-Shape Inhomogeneity Factor for dispersing Nanomaterials.

A new mechanism of “Geometric-Shape Inhomogeneity” was proposed and explained by the interaction between geometry and the non-covalent bonding such as van der Waal force, ionic attraction, surface charge and aspect ratio. Among these interaction forces, aspect ratio is the dominated factor for manipulated the dispersion ability of nanomaterials and the surface charge is the secondary factor to control the solubility. Compared to the organic pigments and hydrophobic polymers, the carbon materials showed amphiphilic solvation and irreversible dispersion. The new dispersion technique of “Geometric-Shape Inhomogeneity” will progress and advance the applications of nanomaterials in the futures.



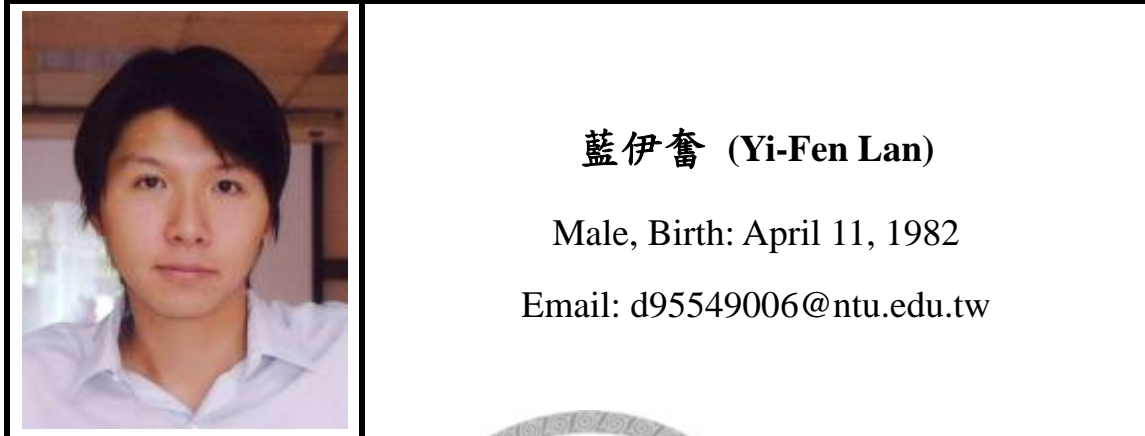
---

---

## Curriculum Vitae

---

---



### Educations

**Ph. D. (2006~2010)**

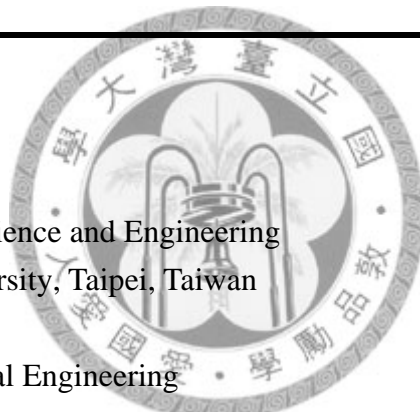
Institute of Polymer Science and Engineering  
National Taiwan University, Taipei, Taiwan

**M. S. (2004~2006)**

Department of Chemical Engineering  
National Chung-Hsing University, Taichung, Taiwan

**B. S. (2000~2004)**

Department of Chemical Engineering  
Feng-Chia University, Taichung, Taiwan





## List of Publications : 7 篇

### 2008~2009

1. Chia-Ming Chang, Jin-Chen Chiu, **Yi-Fen Lan**, Jhe-Wei Lin, Chao-Yung Yeh, Wern-Shiarng Jou, Jiang-Jen Lin and Wood-Hi Cheng, High Electromagnetic Shielding of a 2.5 Gbps Plastic Transceiver Module Using Dispersive Multiwall Carbon Nanotubes, *Journal of Lightwave Technology*, **2008**, 26, 1256–1262. [IF: **2.736** (2008), Journal Ranking: Engineering, Electrical & Electronic (Q1: **27/229**), Optics (Q1: **8/64**)]
2. **Yi-Fen Lan** and Jiang-Jen Lin, Observation of Carbon Nanotube and Clay Micelle-Like Microstructures with Dual Dispersion Property, *Journal of Physical Chemistry A*, **2009**, 113, 8654–8659. [IF: **2.899** (2009), Journal Ranking: Chemistry Physical (Q2: **39/121**), Physics, Atomic, Molecular & chemical (Q1: **8/33**)]

### 2010

1. **Yi-Fen Lan**, Rong-Ho Lee and Jiang-Jen Lin, Aqueous Dispersion of Conjugated Polymers by Colloidal Clays and Their Film Photoluminescence, *Journal of Physical Chemistry B*, **2010**, 114, 1897–1902. [IF: **3.471** (2009), Journal Ranking: Chemistry Physical (Q2: **32/121**)]
2. **Yi-Fen Lan**, Bi-Zen Hsieh, Hsiao-Chu Lin, Yu-An Su, Ying-Nan Chan and Jiang-Jen Lin, Poly(*N*-Isopropyl Acrylamide) Tethered Silicate Platelets for Colloidal Dispersion of Conducting Polymers with Thermoresponsive and Photoluminescence Properties, *Langmuir*, **2010**, 26, 10572–10577. [IF: **3.898** (2009), Journal Ranking: Chemistry, Multidisciplinary (Q1: **23/138**), Chemistry, Multidisciplinary (Q1: **26/121**), Material Science, Multidisciplinary (Q1: **25/212**)]
3. Jin-Chen Chiu, **Yi-Fen Lan**, Chia-Ming Chang, Xi-Zong Chen, Chao-Yung Yeh, Chao-Kuei Lee, Gong-Ru Lin, Jiang-Jen Lin, and Wood-Hi Cheng, Concentration Effect of Carbon Nanotube Based Saturable Absorber on Stabilizing and Shortening Mode-Locked Pulse, *Optics Express*, **2010**, 18, 3592–3600. [IF: **3.278** (2009), Journal Ranking: Optics (Q1: **3/70**)]
4. Yen-Chi Hsu, Yu-Min Chen, Wei-Li Lin, **Yi-Fen Lan**, Ying-Nan Chan and Jiang-Jen Lin, Hierarchical Synthesis of Silver Nanoparticles and Wires by Copolymer Templates and Visible-Light, *Journal of Colloid and Interface Science*, **2010**, 352, 81–86. [IF: **3.019** (2009), Journal Ranking: Chemistry Physical (Q2: **37/121**)]

5. Jiang-Jen Lin, Ying-Nan Chan and **Yi-Fen Lan**, Hydrophobic Modification of Layered Clays and Compatibility for Epoxy Nanocomposites, *Materials*, **2010**, 3, 2588–2605. [IF: Not Available]



## **International Conferences : 9 篇**

### **National Meetings & Expositions of the American Chemical Society (ACS) : 5 篇**

1. Jiang-Jen Lin, Ying-Nan Chan, Kuan-Liang Wei, and **Yi-Fen Lan**, "Layered-Clay-Skeleton Initiated Epoxy Polymerization and Formation of Unique Silicate/Polymer Hybrid Assemblies", 233<sup>th</sup> National Meetings & Expositions of the American Chemical Society, Chicago, IL. USA. March. 25–29, **2007**. (*Coauthor*)
2. Jiang-Jen Lin, **Yi-Fen Lan**, Kuan-Liang Wei and Ying-Nan Chan, "Effect of Geometric Shape on Nano-Dispersion of Carbon Nanotubes and Layered Platelets", 234<sup>th</sup> National Meetings & Expositions of the American Chemical Society, Boston, MA. USA. Aug. 19–23, **2007**. (*Oral Presentation*)
3. Yu-An Su, Hsiao-Chu Lin, Bi-Zen Hsieh, **Yi-Fen Lan** and Jiang-Jen Lin, "Clay-AgNP Nanohybrids Exhibiting New Temperature-Responsive and Antimicrobial Potency", 239<sup>th</sup> National Meetings & Expositions of the American Chemical Society, San Francisco, California, USA. March. 21–25, **2010**. (*Coauthor*)
4. Hsiao-Chu Lin, Bi-Zen Hsieh, Yu-An Su, Yu-Min Chen, **Yi-Fen Lan** and Jiang-Jen Lin, "Tailoring the Density of Poly(NiPAAm) on Silicate Platelet and Their Aggregating Behavior in Water", 239<sup>th</sup> National Meetings & Expositions of the American Chemical Society, San Francisco, California, USA. March. 21–25, **2010**. (*Coauthor*)
5. Bi-Zen Hsieh, Yu-An Su, Hsiao-Chu Lin, **Yi-Fen Lan**, Yu-Min Chen, Yu-Jane Sheng and Jiang-Jen Lin, "Reversible Phase Transition of Polymer Brushes Prepared from Dual-Head Initiator ATRP Grafting Poly(N-isopropylacrylamide) on Silicate Platelets", 240<sup>th</sup> National Meetings & Expositions of the American Chemical Society, Boston, MA. USA. Aug. 22–26, **2010**. (*Coauthor*)

### **Pacific Polymer Conference (PPC) : 1 篇**

1. **Yi-Fen Lan** and Jiang-Jen Lin, "Aqueous Colloidal Dispersion of Conducting Polymers Promoted by Platelet-Like Clays and their Film Photoluminescence Properties" 11<sup>th</sup> Pacific Polymer Conference, Cairns, Australia, Dec. 6–10, **2009**. (*Oral Presentation*)

**Electronic Components and Technology Conference (ECTC) : 3篇**

1. Chia-Ming Chang, Jin-Chen Chiu, Chao-Yung Yeh, Wern-Shiarng Jou, **Yi-Fen Lan**, Yen-Wer Fang, Jiang-Jen Lin and Wood-Hi Cheng, "Electromagnetic Shielding Performance for a 2.5 Gb/s Plastic Transceiver Module Using Dispersive Multiwall Carbon Nanotubes" 57<sup>th</sup> Electronic Components and Technology Conference, Reno, NV. USA. May 29–June 1, 2007. (*Coauthor*)
2. Jin-Chen Chiu, Chia-Ming Chang, Jhe-Wei Lin, Wood-Hi Cheng, **Yi-Fen Lan** and Jiang-Jen Lin, "High Electromagnetic Shielding of Multi-Wall Carbon Nanotube Composites Using Ionic Liquid Dispersant" 58<sup>th</sup> Electronic Components and Technology Conference, Lake Buena Vista, Florida, USA. May 27–30, 2008. (*Coauthor*)
3. Jin-Chen Chiu, **Yi-Fen Lan**, Jung-Jui Kang, Chia-Ming Chang, Zih-Shun Haung, Chao-Yung Yeh, Chao-Kuei Lee, Gong-Ru Lin, Jiang-Jen Lin, and Wood-Hi Cheng, "Passively Mode-locked Lasers Using Saturable Absorber Incorporating Dispersed Single Wall Carbon Nanotubes" 59<sup>th</sup> Electronic Components and Technology Conference, San Diego, California, USA. May 26–29, 2009. (*Coauthor*)



## 國內研討會：13 篇

### 中華民國高分子年會：7 篇

1. 藍伊奮、林江珍、李宗銘，“奈米碳管分散行為探討”，第二十九屆 中華民國高分子年會(29<sup>th</sup> ROC Polymer Symposium 2006)，Jan. 13–14, **2006**。(Oral Presentation/國立中山大學)。
2. 藍伊奮、林江珍，“Dispersing Conducting Polymers in Water by Geometric Inhomogeneity Factor”，第三十二屆 中華民國高分子年會(32<sup>th</sup> ROC Polymer Symposium 2009)，Jan. 9–10, **2009**。(Poster/大同大學)。
3. 藍伊奮、謝壁任、蘇佑安、林筱筑、林江珍，“Factor of Geometric Shaped In-homogeneity and Dispersion of Conjugated Polymers”，第三十三屆 中華民國高分子年會(33<sup>th</sup> ROC Polymer Symposium 2010)，Jan. 22–23, **2010**。(Oral Presentation /國立高雄大學)。
4. 謝壁任、蘇佑安、林筱筑、藍伊奮、陳育民、林江珍，“Synthesis of Double-Headed Initiators for ATRP Grafting of Poly(*N*-Isopropylacrylamide) from Silicate Platelets”，第三十三屆 中華民國高分子年會(33<sup>th</sup> ROC Polymer Symposium 2010)，Jan. 22–23, **2010**。(Coauthor /國立高雄大學)。
5. 林筱筑、謝壁任、蘇佑安、藍伊奮、陳育民、林江珍，“Water Surface Properties of Poly(*N*-Isopropylacrylamide)-Tethered Silicate Platelets”，第三十三屆 中華民國高分子年會(33<sup>th</sup> ROC Polymer Symposium 2010)，Jan. 22–23, **2010**。(Coauthor /國立高雄大學)。
6. 蘇佑安、林筱筑、謝壁任、藍伊奮、陳育民、林江珍，“Immobilization of Silver Nanoparticles on Poly(*N*-Isopropylacrylamide)-Tethered Silicate Platelets as Novel Antibacterial Agents”，第三十三屆 中華民國高分子年會(33<sup>th</sup> ROC Polymer Symposium 2010)，Jan. 22–23, **2010**。(Coauthor /國立高雄大學)。
7. 林偉立、藍伊奮、詹英楠、林江珍，“Poly(oxypropylene)-amine Derived Hydrophobic Copolymers for Dispersing Colloidal Silver Nanoparticles in Mixed Solvents”，第三十三屆 中華民國高分子年會(33<sup>th</sup> ROC Polymer Symposium 2010)，Jan. 22–23, **2010**。(Coauthor /國立高雄大學)。

### 工研院成果發表會：4 篇

1. 藍伊奮、林江珍、李宗銘，“奈米碳管於高分子半導體之分散及排列控制技術”，FY95期中成果發表會暨技術展望高峰會議大會，July 27–28, **2006**。(Coauthor/新竹工研院)。

2. **藍伊奮**、林江珍、李宗銘，“奈米碳管於高分子半導體之分散及排列控制技術”，FY95期末成果發表會暨技術展望高峰會議大會，Dec. 13-14, 2006。(Oral Presentation/新竹工研院)。
3. **藍伊奮**、詹英楠、林江珍、黃淑娟、李宗銘，“高導熱之奈米碳纖維/黏土環氧樹脂複合材料製備與應用”，FY96期中成果發表會暨技術展望高峰會議大會，June. 26-27, 2007。(Oral Presentation/新竹工研院)。
4. **藍伊奮**、詹英楠、林江珍、黃淑娟、李宗銘，“高導熱之奈米碳纖維/黏土環氧樹脂複合材料製備與應用”，FY96期末成果發表會暨技術展望高峰會議大會，Dec. 27-28, 2007。(Coauthor/新竹工研院)。

#### 台灣光電科技研討會：2 篇

1. 黃資順、邱金城、**藍伊奮**、張家銘、葉昭永、林江珍、李晁達、鄭木海，“Passive Mode-Locking Laser Using Dispersed Single Wall Carbon Nanotubes-Based Saturable Absorber”，台灣光電科技研討會，Dec. 4-6, 2008。(Coauthor/台北國際議會中心)。
2. 陳璽中、邱金城、**藍伊奮**、張家銘、葉昭永、李晁達、林恭如、林江珍、鄭木海，“奈米碳管飽和吸收體濃度對鎖模雷射脈衝波形的影響”，台灣光電科技研討會，Dec. 11-12, 2009。(Coauthor/國立台灣師範大學)。

#### 中華民國界面科學年會：2 篇

1. **藍伊奮**、謝壁任、林江珍，“Aqueous Colloidal Dispersion of Conjugated Polymers by Nanoscale Silicate Platelets”，中華民國界面科學年會，July 30, 2010。(Poster/國立成功大學化工系館)。
2. 謝壁任、**藍伊奮**、林江珍，“Phase Transformation of Double-Headed Initiators for ATRP Grafting of Poly(*N*-Isopropylacrylamide) from Silicate Platelets”，中華民國界面科學年會，July 30, 2010。(Coauthor/國立成功大學化工系館)。



## 中華民國專利：7 項

1. 黃贛麟、蔡世榮、林江珍、藍伊奮，“奈米碳球-層狀黏土混成物及其製備方法”。工研院材化所。公開號：200842107
2. 林江珍、藍伊奮、李宗銘，“利用幾何型態阻隔效應分散碳簇與黏土奈米無機材料之新方法”，無法申請(已過法定申請時效)。工研院材化所。
3. 林江珍、藍伊奮、陳文章、李宗銘、邱國展，“共軛高分子-層狀黏土混成物及防止共軛高分子聚集的方法”。工研院材化所。公開號：200840837
4. 林江珍、藍伊奮、許彥琦，“分散顏料於溶劑中之方法”。台灣大學。公開號：200925216
5. 林江珍、藍伊奮、黃淑娟，“利用幾何型態阻隔效應以分散奈米碳纖維之新方法”，申請中(Aug., 2007)，無法申請(已過法定申請時效)。工研院材化所。
6. 林江珍、藍伊奮、鄭木海、張家銘、邱金成、林哲葳，“高電磁波屏蔽之聚亞醯胺樹脂/奈米碳管複合材料”，專利事務所(June, 2009)。台灣大學、中山大學共有。
7. 林江珍、邱智偉、藍伊奮、董瑞軒，“雲母奈米矽片/奈米銀粒子之製備及其低溫熔融方法”，智財局(Jan. 11, 2010)。台灣大學。

## 美國專利：3 項

1. Gan-Lin Hwang, Shih-Jung Tsai, Jiang-Jen Lin and Yi-Fen Lan “New Method of Dispersing Carbon Nanocapsule by Geometric Shape Inhomogeneity Factor”, 2009. Patent No.: US 7,625,952 B2
2. Jiang-Jen Lin and Yi-Fen Lan and Yen-Chi Hsu “New Method of Dispersing Pigments by Layered Clays”, 2009. Application No.: USPTO 20090145333
3. Jiang-Jen Lin, Wood-Hi Cheng, Jin-Chen Chiu, Yi-Fen Lan, Jhe-Wei Lin, Chia-Ming Chang “Polyimide/Carbon Nanotube Complexed Films for Electric Conductive and Electromagnetic Shielding”. (Jane, 2009, submitted)

## 中國專利：1 項

1. 林江珍、藍伊奮、陳文章、李宗銘、邱國展，“共軛高分子-層狀黏土雜化物”，申請專利號: 200710101997，公開號: 101293988，公開日: 2008-10-29。

## 技術移轉：1 項

1. 林江珍，“利用層狀黏土幾何差異以分散奈米碳管之技術”，2007，國立台灣大學技術移轉，新揚科技股份有限公司。(權利金: 100 萬元。)

## Awards/Scholarships

### 研究所(2004~2010)

1. 警友會 九十五學年度 品學兼優獎
2. 警友會 九十六學年度 品學兼優獎

### 國科會-出席國際會議獎助金

1. 第 234 屆美國化學年會，美國—波士頓 (2007)
2. 第11屆太平洋高分子會議，澳洲—凱恩斯 (2009)

### 高分子年會(2010)

1. 佳作。謝壁任、蘇佑安、林筱筑、藍伊奮、陳育民、林江珍，“Synthesis of Double-Headed Initiators for ATRP Grafting of Poly(*N*-Isopropylacrylamide) from Silicate Platelets”，第三十三屆 中華民國高分子年會(33<sup>th</sup> ROC Polymer Symposium 2010)，Jan. 22–23, 2010。(Coauthor /國立高雄大學)。
2. 入圍。蘇佑安、林筱筑、謝壁任、藍伊奮、陳育民、林江珍，“Immobilization of Silver Nanoparticles on Poly(*N*-Isopropylacrylamide)-Tethered Silicate Platelets as Novel Antibacterial Agents”，第三十三屆 中華民國高分子年會(33<sup>th</sup> ROC Polymer Symposium 2010)，Jan. 22–23, 2010。(Coauthor /國立高雄大學)。





## References

- <sup>1</sup> M. Ardenne, *Zeitschrift für technische Physik*, **1938**, 19, 407.
- <sup>2</sup> D. H. Kruger, P. Schneck, H. R. Gelderblom, *Lancet*, **2000**, 355, 1713.
- <sup>3</sup> F. J. Giessibl, *Rev. Mod. Phys.*, **2003**, 75, 949.
- <sup>4</sup> R. X. Dong, C. C. Chou, J. J. Lin, *J. Mater. Chem.*, **2009**, 19, 2184.
- <sup>5</sup> Y. H. Pai, J. H. Ke, C. C. Chou, J. J. Lin, J. M. Zen, F. S. Shieu, *J. Power Sources*, **2006**, 163, 398.
- <sup>6</sup> D. Jain, A. Winkel, R. Wilhelm, *Small*, **2006**, 2, 752.
- <sup>7</sup> Y. F. Lan, J. J. Lin, *J. Phys. Chem. A*, **2009**, 113, 8654.
- <sup>8</sup> Y. Si, E. T. Samulski, *Nano Lett.*, **2008**, 8, 1679.
- <sup>9</sup> J. J. Lin, Y. M. Chen, *Langmuir*, **2004**, 20, 4261.
- <sup>10</sup> Y. M. Chen, R. S. Hsu, H. C. Lin, S. J. Chang, S. C. Chen, J. J. Lin, *J. Coll. Inter. Sci.*, **2009**, 334, 42.
- <sup>11</sup> J. J. Lin, Y. C. Hsu, *J. Coll. Inter. Sci.*, **2009**, 336, 82.
- <sup>12</sup> E. N. Salgado, R. A. Lewis, S. Mossin, A. L. Rheingold, F. A. Tezcan, *Inorg. Chem.*, **2009**, 48, 2726.
- <sup>13</sup> Z. Xu, X. Yang, Z. Yang, *Langmuir*, **2007**, 23, 9201.
- <sup>14</sup> H. L. Su, C. C. Chou, D. J. Hung, S. H. Lin, I. C. Pao, J. H. Lin, F. L. Huang, R. X. Dong, J. J. Lin, *Biomaterials*, **2009**, 30, 5979.
- <sup>15</sup> J. J. Lin, C. C. Chu, M. L. Chiang, W. C. Tsai, *Adv. Mater.*, **2006**, 18, 3248.
- <sup>16</sup> C. M. Chang, J. C. Chiu, Y. F. Lan, J. W. Lin, C. Y. Yeh, W. S. Jou, J. J. Lin, W. H. Cheng, *J. Lightwave Tech.*, **2008**, 26, 1256.
- <sup>17</sup> J. C. Chiu, Y. F. Lan, C. M. Chang, X. Z. Chen, C. Y. Yeh, C. K. Lee, G. R. Lin, J. J. Lin, W. H. Cheng, *Optics Express*, **2010**, 18, 3592.
- <sup>18</sup> R. J. Jeng, S. M. Shau, J. J. Lin, W. C. Su, Y. S. Chiu, *Euro. Polym. J.*, **2002**, 38, 683.
- <sup>19</sup> I. N. Jan, T. M. Lee, K. C. Chiou, J. J. Lin, *Indus. Eng. Chem. Res.*, **2005**, 44, 2086.
- <sup>20</sup> J. J. Lin, J. C. Wei, W. C. Tsai, *J. Phys. Chem. B*, **2007**, 111, 10275.
- <sup>21</sup> (a) S. K. Pang, J. D. Saxby, S. P. Chatfield, *J. Phys. Chem.*, **1993**, 97, 6941. (b) J. P. Lu, *Phys. Rev. Lett.*, **1995**, 74, 1123. (c) H. Dai, E. W. Wong, C. M. Lieber, *Science*, **1996**, 272, 523. (d) A. M. Rao, P. C. Eklund, S. Bandow, A. Thess, R. E. Smalley, *Nature*, **1997**, 388, 257.
- <sup>22</sup> (a) J. Liu, S. Tian, W. Knoll, *Langmuir*, **2005**, 21, 5596. (b) K. Kim, S. H. Lee, W. Yi, J. Kim, J. W. Choi, Y. Park, J. I. Jin, *Adv. Mater.*, **2003**, 15, 1618. (c) H. M. So, K. Won, Y. H. Kim, B. K. Kim, B. H. Ryu, P. S. Na, H. Kim, J. O. Lee, *J. Am. Chem. Soc.* **2005**, 127, 11906. (d) Z. Q. Tian, S. P. Jiang, Y. M. Liang, P. K. Shen, *J. Phys. Chem. B*, **2006**, 110, 5343.
- <sup>23</sup> J. Liu, A. G. Rinzler, H. Dai, J. H. Hafner, R. K. Bradley, P. J. Boul, A. Lu, T. Iverson, K. Shelimov, C. B. Huffman, F. Rodriguez-Macias, Y. S. Shon, T. R. Lee, D. T. Colbert, R. E. Smalley, *Science*, **1998**, 280, 1253.
- <sup>24</sup> K. S. Coleman, *J. Am. Chem. Soc.*, **2003**, 125, 8722.
- <sup>25</sup> A. Adronov, *J. Am. Chem. Soc.*, **2003**, 125, 16015.
- <sup>26</sup> (a) C. C. Tsiang, *Macromolecules*, **2004**, 37, 283. (b) Q. Liangwei, *Macromolecules*, **2005**, 38, 10328.
- <sup>27</sup> (a) K. A. Williams, *Nature*, **2002**, 420, 761. (b) K. Jiang, *J. Mater. Chem.*, **2004**, 14, 37. (c) M. Guo, *Bioelectrochemistry*, **2004**, 62, 29.
- <sup>28</sup> (a) J. Chen, *Sciencetec*, **1998**, 282, 95. (b) Y. Qin, L. Liu, J. Shi, W. Wu, J. Zhang, Z. X. Guo, Y. Li, D. Zhu, *Chem. Mater.*, **2003**, 15, 3256. (c) H. Kong, *Macromolecules*, **2004**, 37, 4022. (d) U. D. Weglikowska, *J. Am. Chem. Soc.*, **2005**, 127, 5125.
- <sup>29</sup> (a) W. T. Ford, *J. Am. Chem. Soc.*, **2004**, 126, 170. (b) W. T. Ford, *Macromolecules*, **2004**, 37, 752. (c) G. Gao, *J. Am. Chem. Soc.*, **2004**, 126, 412. (d) G. Gao, *Macromolecules*, **2005**, 38, 8634. (e) G. Gao, *Polymer*, **2005**, 46, 2472.
- <sup>30</sup> (a) R. Jerome, *Polymer*, **2004**, 45, 6097. (b) A. Adronov, *Macromolecules*, **2005**, 38, 1172.

- <sup>31</sup> A. Hirsch, *Angew. Chem. Int. Ed.*, **2002**, 41, 1853.
- <sup>32</sup> (a) H. T. Ham, Y. S. Choi, I. J. Chung, *J. Colloid Interf. Sci.*, **2005**, 286, 216. (b) D. Chattopadhyay, I. Galeska, F. Papadimitrakopoulos, *J. Am. Chem. Soc.*, **2003**, 125, 3370. (c) E. Camponeschi, B. Florkowski, R. Vance, G. Garrett, H. Garmestani, R. Tannenbaum, *Langmuir*, **2006**, 22, 1858. (d) Y. Tan, D. E. Resasco, *J. Phys. Chem. B*, **2005**, 109, 14454. (e) O. Matarredona, H. Rhoads, Z. Li, J. H. Harwell, L. Balzano, D. Resasco, *J. Phys. Chem. B*, **2003**, 107, 13357.
- <sup>33</sup> (a) G. S. Duesberg, M. Burghard, J. Muster, G. Philipp, S. Roth, *Chem. Commun.*, **1998**, 435. (b) L. Jiang, L. Gao, J. Sun, *J. Colloid Interf. Sci.*, **2003**, 260, 89. (c) K. Shen, S. Curran, H. Xu, S. Rogelj, Y. Jiang, *J. Phys. Chem. B*, **2005**, 109, 4455. (d) M. F. Islam, E. Rojas, D. M. Bergey, A. T. Johnson, A. G. Yodh, *Nano Lett.*, **2003**, 3, 269. (e) T. Hertel, A. Hagen, V. Talalaev, K. Arnold, F. Hennrich, M. Kappes, *Nano Lett.*, **2005**, 5, 511. (f) P. Poulin, B. Vigolo, P. Launois, *Carbon*, **2002**, 40, 1741. (g) B. Vigolo, A. Pénicaud, C. Coulon, C. Sauder, R. Paillet, C. Journet, P. Bernier, P. Poulin, *Science*, **2000**, 290, 1331. (h) M. J. O'Connell, S. M. Bachilo, C. B. Huffman, V. C. Moore, M. S. Strano, E. H. Haroz, K. L. Rialon, P. J. Boul, W. H. Noon, C. Kittrell, J. Ma, R. H. Hauge, R. B. Weisman, R. E. Smalley, J. Dewald, T. Pietrass, *Science*, **2002**, 297, 593.
- <sup>34</sup> (a) V. Krstic, G. S. Duesberg, J. Muster, M. Burghard, S. Roth, *Chem. Mater.*, **1998**, 10, 2338. (b) T. Chatterjee, K. Yurekli, V. G. Hadjiev, R. Krishnamoorti, *Adv. Funct. Mater.*, **2005**, 15, 1832.
- <sup>35</sup> (a) V. C. Moore, M. S. Strano, E. H. Haroz, R. H. Hauge, R. E. Smalley, *Nano Lett.*, **2003**, 3, 1379. (b) L. Vaisman, G. Marom, H. D. Wagner, *Adv. Funct. Mater.*, **2006**, 16, 357. (c) M. J. O'Connell, P. Boul, L. M. Ericson, C. Huffman, Y. Wang, E. Haroz, *Chem. Phys. Lett.*, **2001**, 342, 265.
- <sup>36</sup> E. V. Basiuk, V. A. Basiuk, J. G. Bañuelos, J. M. Saniger-Blesa, V. A. Pokrovskiy, T. Y. Gromovoy, A. V. Mischanchuk, B. G. Mischanchuk, *J. Phys. Chem. B*, **2002**, 106, 1588.
- <sup>37</sup> (a) J. Kong, H. Dai, *J. Phys. Chem. B*, **2001**, 105, 2890. (b) N. Choi, M. Kimura, H. Kataura, S. Suzuki, Y. Achiba, *Jpn. J. Appl. Phys.*, **2002**, 41, 6264.
- <sup>38</sup> Y. Maeda, S. I. Kimura, Y. Hirashima, M. Kanda, Y. Lian, T. Wakahara, T. Akasaka, T. Hasegawa, H. Tokumoto, *J. Phys. Chem. B*, **2004**, 108, 18395.
- <sup>39</sup> S. Bandow, A. M. Rao, R. E. Smalley, P. C. Eklund, *J. Phys. Chem. B*, **1997**, 101, 8839.
- <sup>40</sup> X. Gong, J. Liu, S. Baskaran, R. D. Voise, J. S. Young, *Chem. Mater.*, **2000**, 12, 1049.
- <sup>41</sup> H. Wang, W. Zhou, D. L. Ho, J. E. Fischer, C. J. Glinka, E. K. Hobbie, *Nano Lett.*, **2004**, 4, 1789.
- <sup>42</sup> S. Cui, R. Canet, A. Derre, M. Couzi, P. Delhaes, *Carbon*, **2003**, 41, 797.
- <sup>43</sup> E. Gregan, S. M. Keogh, A. Maguire, T. G. Hedderman, L. O. Neill, G. Chambers, H. J. Byrne, *Carbon*, **2004**, 42, 1031.
- <sup>44</sup> C. Y. Li, L. Li, W. Cai, S. L. Kodjie, K. K. Tenneti, *Adv. Mater.*, **2005**, 17, 1198.
- <sup>45</sup> A. Star, J. F. Stoddart, D. Steuerman, M. Diehl, A. Boukai, E. W. Wong, X. Yang, S. W. Chung, H. Choi, J. R. Heath, *Angew. Chem.*, **2001**, 113, 1771.
- <sup>46</sup> M. Yudasaka, M. Zhang, C. Jabs, S. Iijima, *Appl. Phys. A*, **2000**, 71, 449.
- <sup>47</sup> J. Chen, H. Liu, W. A. Weimer, M. D. Halls, D. H. Waldeck, G. C. Walker, *J. Am. Chem. Soc.*, **2002**, 124, 9034.
- <sup>48</sup> A. Carrillo, J. A. Swartz, J. M. Gamba, R. S. Kane, *Nano Lett.*, **2003**, 3, 1437.
- <sup>49</sup> Y. Kang, T. A. Taton, *J. Am. Chem. Soc.*, **2003**, 125, 5650.
- <sup>50</sup> X. Lou, R. Daussin, S. Cuenot, A. S. Duwez, C. Pagnouille, C. Detrembleur, C. Bailly, R. Jérôme, *Chem. Mater.*, **2004**, 16, 4005.
- <sup>51</sup> K. El-Hami, K. Matsushige, *Chem. Phys. Lett.*, **2003**, 368, 168.
- <sup>52</sup> V. A. Sinani, M. K. Gheith, A. A. Yaroslavov, A. A. Rakhnyanskaya, K. Sun, A. A. Mamedov, J. P. Wicksted, N. A. Kotov, *J. Am. Chem. Soc.*, **2005**, 127, 3463.
- <sup>53</sup> H. Kitano, K. Tachimoto, T. Nakaji-Hirabayashi, H. Shinohara, *Macromol. Chem.*

*Phys.*, **2004**, 205, 2064.

<sup>54</sup> (a) F. Balavoine, P. Schultz, C. Richard, V. Mallouh, T. W. Ebbesen, C. Mioskowski, *Angew. Chem. Int. Ed.*, **1999**, 38, 1912. (b) K. Bradley, M. Briman, A. Star, G. Grulner, *Nano Lett.*, **2004**, 2, 253.

<sup>55</sup> (a) S. C. Tsang, Z. Guo, Y. K. Chen, M. L. H. Green, H. A. Hill, T. W. Hambley, P. J. Sadler, *Angew. Chem. Int. Ed. Engl.*, **1997**, 36, 2198. (b) Z. Guo., P. J. Sadler, S. C. Tsang, *Adv. Mater.*, **1998**, 10, 701. (c) M. Zheng, A. Jagota, M. S. Strano, A. P. Santos, P. Barone, S. G. Chou, B. A. Diner, M. S. Dresselhaus, R. S. Mclean, G. B. Onoa, G. G. Samsonidze, E. D. Semke, M. Usrey, D. J. Walls, *Science*, **2003**, 302, 1545.

<sup>56</sup> G. R. Dieckmann, A. B. Dalton, P. A. Johnson, J. Razal, J. Chen, G. M. Giordano, E. Muñoz, I. H. Musselman, *J. Am. Chem. Soc.*, **2003**, 125, 1770.

<sup>57</sup> A. Ortiz-Acevedo, H. Xie, V. Zorbas, W. M. Sampson, A. B. Dalton, R. H. Baughman, R. K. Draper, I. H. Musselman, G. R. Dieckmann, *J. Am. Chem. Soc.*, **2005**, 127, 9512.

<sup>58</sup> Y. Wu, J. S. Hudson, Q. Lu, J. M. Moore, A. S. Mount, A. M. Rao, E. Alexov, P. C. Ke, *J. Phys. Chem. B*, **2006**, 110, 2475.

<sup>59</sup> S. S. Karajanagi, H Yang, P. Asuri, E. Sellitto, J. S. Dordick, R. S. Kane, *Langmuir*, **2006**, 22, 1392.

<sup>60</sup> A. Ikeda, T. Hamano, K. Hayashi, J. Kikuchi, *Org. Lett.*, **2006**, 8, 1153.

<sup>61</sup> T. Fukushima, A. Kosaka, Y. Ishimura, T. Yamamoto, T. Takigawa, N. Ishii, T. Aida, *Science*, **2003**, 300, 2072.

<sup>62</sup> H. B. Kim, J. S. Chio, S. T. Lim, H. J. Lim, H. S. Kim, *Syn. Met.*, **2005**, 154, 189.

<sup>63</sup> Y. Zhang, Y. Shen, J. Li, L. Niu, S. Dong, A. Ivaska, *Langmuir*, **2005**, 21, 4797.

<sup>64</sup> B. K. Price, J. L. Hudson, J. M. Tour, *J. Am. Chem. Soc.*, **2005**, 127, 14867.

<sup>65</sup> A. Star, D. W. Steuerman, J. R. Heath, J. F. Stoddart, *Angew. Chem.*, **2002**, 41, 2508.

<sup>66</sup> Q. Li, I. A. Kinloch, A. H. Windle, *Chem. Commun.*, **2005**, 3283.

<sup>67</sup> (a) R. Bandyopadhyaya, E. Nativ-Roth, O. Regev, R. Yerushalmi-Rozen, *Nano Lett.*, **2002**, 2, 25. (b) Y. Dror, W. Pyckhout-Hintzen, Y. Cohen, *Macromolecules*, **2005**, 38, 7828.

<sup>68</sup> O. K. Kim, J. Je, J. W. Baldwin, S. Kooi, P. E. Pehrsson, L. J. Buckley, *J. Am. Chem. Soc.*, **2003**, 125, 4426.

<sup>69</sup> R. J. Chen, Y. Zhang, D. Wang, H. Dai, *J. Am. Chem. Soc.*, **2001**, 123, 3838.

<sup>70</sup> J. Chen, M. J. Dyer, M. F. Yu, *J. Am. Chem. Soc.*, **2001**, 123, 6201.

<sup>71</sup> D. Uy, A. E. O'Neill, S. J. Simko, A. K. Gangopadhyay, *Lubrication Science*, **2010**, 22, 19.

<sup>72</sup> J. S. Im, J. G. Kim, Y. S. Lee, *Carbon*, **2009**, 47, 2640.

<sup>73</sup> Y. W. Chen-Yang, T. F. Hung, J. Huang, F. L. Yang, *J. Power Sources*, **2007**, 173, 183.

<sup>74</sup> C. K. Leong, D. D. L. Chung, *Carbon*, **2003**, 41, 2459.

<sup>75</sup> (a) L. Jong, *Composites: Part A*, **2007**, 38, 252. (b) G. Sui, W. H. Zhong, X. P. Yang, Y. H. Yu, S. H. Zhao, *Polym. Adv. Technol.*, **2008**, 19, 1543.

<sup>76</sup> (a) P. C. Ma, M. Y. Liu, H. Zang, S. Q. Wang, R. Wang, K. Wang, Y. K. Wong, B. Z. Tang, S. H. Hong, K. W. Paik, J. K. Kim, *ACS Appl. Mater. Interfaces*, **2009**, 1, 1090. (b) X. Y. Ji, H. Li, D. Hui, K. T. Hsiao, J. P. Ou, A. K.T. Lau, *Composites: Part B*, **2010**, 41, 25.

<sup>77</sup> N. Wang, X. X. Zang, X. F. Ma, J. M. Fang, *Polym. Degrad. Stab.*, **2008**, 93, 1044.

<sup>78</sup> S. Xu, M. Wen, J. Li, S. Guo, M. Wang, Q. Du, J. Shen, Y. Zhang, S. Jiang, *Polymer*, **2008**, 49, 4861.

<sup>79</sup> T. Noguchi, T. Nagai, J. Seto, *J. Appl. Polym. Sci.*, **1986**, 31, 1913.

<sup>80</sup> Q. Li, G. Wu, Y. Ma, C. Wu, *Carbon*, **2007**, 45, 2411.

<sup>81</sup> Y. S. Kim, *Curr. Appl. Phys.*, **2010**, 10, 10.

<sup>82</sup> (a) W. J. Thomas, *Carbon*, **1966**, 3, 435. (b) J. Rappeneau, J. L. Taupin, J. Grehier, *Carbon*, **1966**, 4, 135. (c) K. Kamegawa, K. Nishikubo, H. Yoshidak, *Carbon*, **1998**, 36, 433. (d) 1998 Kamegaw, K. Nishikubo, M. Kodama, Y. Adachi, H. Yoshida, *Carbon*, **2002**, 40, 1447.

<sup>83</sup> N. Tsubokawa, K. Fujiki, T. Sasaki, Y. Sone, *Kobunshi Ronbunshu*, **1987**, 44, 605.

- <sup>84</sup> (a) S. Hayashi, T. Iida, N. Tsubokawa, *J. Macromol. Sci., Pure Appl. Chem.*, **1997**, A34, 1381. (b) N. Tsubokawa, K. Fujiki, Y. Sone, *Polym. J.*, **1988**, 20, 213. (c) K. Fujiki, N. Tsubokawa, Y. Sone, *Polym. J.*, **1990**, 22, 661. (d) N. Tsubokawa, K. Seno, *J. Macromol. Sci. Pure Appl. Chem.*, **1994**, A31, 1135.
- <sup>85</sup> (a) S. Hayashi, Dr. Thesis, Niigata University, **1997**, 90. (b) T. Yamamoto, K. Aoshima, H. Ohmura, Y. Moriya, N. Suzuki, Y. Oshibe, *Polymer*, **1991**, 32, 19. (c) K. Ohkita, N. Tsubokawa, E. Saitoh, M. Noda, N. Takashima, *Carbon*, **1975**, 13, 443. (d) K. Ohkita, N. Tsubokawa, E. Saitoh, *Carbon*, **1978**, 16, 41.
- <sup>86</sup> (a) Y. Shirai, N. Tsubokawa, *Reactive Functional Polym.*, **1997**, 32, 153. (b) Y. Shirai, K. Shirai, N. Tsubokawa, *J. Polym. Sci., Part A: Polym. Chem.*, **2001**, 39, 2157.
- <sup>87</sup> (a) N. Tsubokawa, N. Takeda, T. Iwasa, *Polym. J.*, **1981**, 13, 1093. (b) N. Tsubokawa, N. Takeda, K. Kudoh, *Nippon Kagaku Kaishi*, **1980**, 1264. (c) N. Tsubokawa, N. Takeda, A. Kanamaru, *J. Polym. Sci., Polym. Lett. Ed.*, **1980**, 18, 625. (d) N. Tsubokawa, *Carbon*, **1993**, 31, 1257. (e) S. Yoshikawa, R. Nishizaka, K. Oyanagi, N. Tsubokawa, *J. Polym. Sci., Part A: Polym. Chem.*, **1995**, 33, 2251. (f) N. Tsubokawa, K. Oyanagi, S. Yoshikawa, *J. Macromol. Sci., Pure Appl. Chem.*, **2000**, A37, 529. (g) K. Fujiki, J. Chen, W. Gang, S. Saitoh, N. Tsubokawa, *Polymer Preprints, Jpn.*, **2001**, 50, 2696.
- <sup>88</sup> (a) S. Hayashi, S. Handa, N. Tsubokawa, *J. Polym. Sci., Part A: Polym. Chem.*, **1996**, 34, 1589. (b) S. Yoshikawa, S. Machida, N. Tsubokawa, *J. Polym. Sci., Part A: Polym. Chem.*, **1998**, 36, 3165.
- <sup>89</sup> (a) N. Tsubokawa, K. Yanadori, *Kobunshi Ronbunshu*, **1992**, 49, 865. (b) N. Tsubokawa, S. Handa, *J. Jpn. Soc. Color Mater.*, **1993**, 66, 468. (c) S. Hayashi, N. Tsubokawa, *J. Macromol. Sci., Pure Appl. Chem.*, **1998**, A35, 1781.
- <sup>90</sup> J. Chen, Y. Maekawa, M. Yoshida, N. Tsubokawa, *Polym. J.*, **2002**, 34, 30.
- <sup>91</sup> J. Lin, H. Chen, K. Tung, F. Liaw, *J. Mater. Chem.*, **1998**, 8, 2169.
- <sup>92</sup> (a) E. Papirer, N. Tao, J. B. Donner, *J. Polym. Sci., Polym. Lett. Ed.*, **1971**, 9, 195. (b) E. Papirer, N. Tao, J. B. Donnet, *Angew. Makromol. Chem.*, **1971**, 19, 65. (c) S. Yoshikawa, N. Tsubokawa, *Polym. J.*, **1996**, 28, 317.
- <sup>93</sup> N. Tsubokawa, N. Abe, Y. Seida, K. Fujiki, *Chem. Lett.*, **2000**, 900.
- <sup>94</sup> N. Tsubokawa, T. Saitoh, M. Murota, S. Sato, H. Simizu, *Polym. Adv. Technol.*, **2001**, 12, 596.
- <sup>95</sup> K. Fujiki, T. Ogasawara, N. Tsubokawa, *J. Mater. Sci.*, **1998**, 33, 1871.
- <sup>96</sup> (a) N. Tsubokawa, T. Ogasawara, J. Inaba, K. Fujiki, *J. Polym. Sci.: Part A: Polym. Chem.*, **1999**, 37, 3591. (b) N. Tsubokawa, J. Inaba, K. Arai, K. Fujiki, *Polym. Bull.*, **2000**, 44, 317.
- <sup>97</sup> T. Liu, S. Jia, T. Kowalewski, K. Matyjaszewski, *Langmuir*, **2003**, 19, 6342.
- <sup>98</sup> A. Basch, R. Horn, J. O. Besenhard, *Coll. Sur. A: Physicochem. Eng. Aspects*, **2005**, 253, 155.
- <sup>99</sup> L. Bossoleiti; R. Ricceri; G. Giabrielli, *J. Disper. Sci. Tech.*, **1995**, 16, 205.
- <sup>100</sup> H. Ridaoui, A. Jada, L. Vidal, J. B. Donnet, *Coll. Sur. A: Physicochem. Eng. Aspects*, **2006**, 278, 149.
- <sup>101</sup> Y. Lin, T. W. Smith, P. Alexandridis, *J. Coll. Inter. Sci.*, **2002**, 255, 1.
- <sup>102</sup> D. Kozaka, D. Moretonb, B. Vincenta, *Coll. Sur. A: Physicochem. Eng. Aspects*, **2009**, 347, 245.
- <sup>103</sup> H. Y. Li, H. Z. Chen, J. Z. Sun, J. Cao, Z. L. Yang, M. Wang, *Macromol. Rapid Commun.*, **2003**, 24, 715.
- <sup>104</sup> K. Nagai, Y. Igarashi, T. Taniguchi, *Coll. Sur. A: Physicochem. Eng. Aspects*, **1999**, 153, 161.
- <sup>105</sup> F. Nsib, N. Ayed, Y. Chevalier, *Progress in Organic Coatings*, **2006**, 55, 303.
- <sup>106</sup> (a) C. S. Hutchins, A. C. Shor, US Patent 4 656 226, **1987**. (b) J. A. Simms, H. J. Spinelli, *J. Coat. Technol.* **1987**, 59, 125.
- <sup>107</sup> W. Hertler, S. Ma, US Patent 5 519 085, **1996**.

- <sup>108</sup> I. C. Chu, M. Fryd, L. E. Lynch, US Patent 5 231 131, **1993**.
- <sup>109</sup> H. J. Spinelli, US Patents 4 659 782 and 4 659 783, 1987. H. J. Spinelli, in Proc. 13<sup>th</sup> Int. Conf. in Organic Coatings Science and Technology (Ed: A. Patsis), SUNY New Platz, New York **1987**, Vol. 13, p. 417.
- <sup>110</sup> (a) C. Johans, J. Clohessy, S. Fantini, K. Kontturi, V. J. Cunnane, *Electrochemistry Commu.*, **2002**, 227. (b) Y. Zhang, F. Chen, J. Zhuang, Y. Tang, D. Wang, Y. Wang, A. Dong, N. Ren, *Chem. Commu.*, **2002**, 24, 2814. (c) H. Ma, B. Yin, S. Wang, Y. Jiao, W. Pan, S. Huang, S. Chen, F. Meng, *ChemPhysChem*, **2004**, 24, 68–75.
- <sup>111</sup> (a) Y. Zhou, S. H. Yu, C. Y. Wang, X. G. Li, Y. R. Zhu, Z. Y. Chen, *Adv. Mater.*, **1999**, 850. (b) Y. Socol, O. Abramson, A. Gedanken, Y. Meshorer, L. Berenstein, A. Zaban, *Langmuir*, **2002**, 18, 4736.
- <sup>112</sup> (a) D. G. Shchukin, I. L. Radtchenko, G. B. Sukhorukov, *ChemPhysChem*, **2003**, 4, 1101. (b) R. Jin, Y. C. Cao, E. Hao, G. S. Metraux, G. C. Schatz, C. A. Mirkin, *Nature*, **2003**, 425, 487.
- <sup>113</sup> (a) F. K. Liu, P. W. Huang, Y. C. Chang, F. H. Ko, T. C. Chu, *J. Mater. Res.*, **2004**, 19, 469. (b) S. Komarneni, D. Li, B. Newalkar, H. Katsuki, A. S. Bhalla, *Langmuir*, **2002**, 18, 5959. (c) H. Yin, T. Yamamoto, Y. Wada, S. Yanagida, *Mater. Chem. Phys.*, **2004**, 83, 66.
- <sup>114</sup> (a) V. Hornebecq, M. Antonietti, T. Cardinal, M. Treguer-Delapierre, *Chem. Mater.*, **2003**, 15, 1993. (b) S. H. Choi, S. H. Lee, Y. M. Hwang, K. P. Lee, H. D. Kang, *Radi. Phys. Chem.*, **2003**, 67, 517. (c) T. Tsuji, T. Kakita, M. Tsuji, *Appl. Surf. Sci.*, **2003**, 206, 314.
- <sup>115</sup> (a) X. Zheng, L. Zhu, X. Wang, A. Yan, Y. Xie, *J. Crystal Growth*, **2004**, 260, 255. (b) J. Zhang, B. Han, M. Liu, D. Liu, Z. Dong, J. Liu, D. Li, J. Wang, B. Dong, H. Zhao, L. Rong, *J. Phys. Chem. B*, **2003**, 107, 3679. (c) M. C. McLeod, R. S. McHenry, E. J. Beckman, C. B. Roberts, *J. Phys. Chem. B*, **2003**, 107, 2693.
- <sup>116</sup> (a) R. R. Naik, S. J. Stringer, G. Agarwal, S. E. Jones, M. O. Stone, *Nature*, **2002**, 1, 169. (b) M. Kowshik, S. Ashtaputre, S. Kharrazi, W. Vogel, J. Urban, S. K. Kulkarni, K. M. Paknikar, *Nanotechnology*, **2003**, 95. (c) S. S. Shankar, A. Rai, A. Ahmad, M. Sastry, *J. Colloid Interf. Sci.*, **2004**, 275, 496.
- <sup>117</sup> (a) K. K. Caswell, C. M. Bender, C. J. Murphy, *Nano Lett.*, **2003**, 3, 667. (b) Z. S. Pillai, P. V. Kamat, *J. Phys. Chem. B*, **2004**, 108, 945. (c) K. S. Chou, C. Y. Ren, *Mater. Chem. Phys.*, **2000**, 64, 241. (d) Y. Sun, B. Mayers, T. Herricks, Y. Xia, *Nano Lett.*, **2003**, 3, 955. (e) Y. Sun, Y. Xia, *Science*, **2002**, 298, 2176.
- <sup>118</sup> (a) D. H. Chen, Y. W. Huang, *J. Colloid Interf. Sci.*, **2002**, 255, 299. (b) X. Wang, H. Itoh, K. Naka, Y. Chujo, *Langmuir*, **2003**, 19, 6242.
- <sup>119</sup> (a) S. Yang, W. Cai, G. Liu, H. Zeng, P. Liu, *J. Phys. Chem. C*, **2009**, 113, 6480. (b) H. Muto, K. Yamada, K. Miyajima, F. Mafune, *J. Phys. Chem. C*, **2007**, 111, 17221. (c) P. Liu, W. Cai, H. Zeng, *J. Phys. Chem. C*, **2008**, 112, 3261. (d) S. Hashimoto, T. Uwada, H. Masuhara, T. Asahi, *J. Phys. Chem. C*, **2008**, 112, 15089.
- <sup>120</sup> (a) K. Wegner, B. Walker, S. Tsantilis, S. E. Pratsinis, *Chem. Eng. Sci.*, **2002**, 57, 1753. (b) C. C. Chen, C. C. Yeh, *Adv. Mater.*, **2000**, 12, 738.
- <sup>121</sup> R. Sardar, J. W. Park, J. S. Shumaker-Parry, *Langmuir*, **2007**, 23, 11883.
- <sup>122</sup> L. Longenberger, G. Mills, *J. Phys. Chem.*, **1995**, 99, 475.
- <sup>123</sup> T. Sakai, P. Alexandridis, *Chem. Mater.*, **2006**, 18, 2577.
- <sup>124</sup> I. Pastoriza-Santos, L. M. Liz-Marzan, *Nano Letters*, **2002**, 2, 903.
- <sup>125</sup> L. K. Kurihara, G. M. Chow, P. E. Schoen, *NanoShuchued Mater.*, **1995**, 5, 607.
- <sup>126</sup> I. Sondi, D. V. Goia, E. Matijevic, *J Colloid Interf. Sci.*, **2003**, 260, 75.
- <sup>127</sup> Y. Yin, Z. Y. Li, Z. Zhong, B. Gates, Y. Xia, S. Venkateswaran, *J Mater. Chem.*, **2002**, 12, 522.
- <sup>128</sup> S. H. Hu, T. Y. Liu, H. Y. Huang, D. M. Liu, S. Y. Chen, *Langmuir*, **2008**, 24, 239.
- <sup>129</sup> F. Y. Cheng, C. H. Su, Y. S. Yang, C. S. Yeh, C. Y. Tsai, C. L. Wu, M. T. Wu, D. B. Shieh, *Biomaterials*, **2005**, 26, 729.
- <sup>130</sup> C. L. Lin, C. F. Lee, W. Y. Chiu, *J. Colloid Interf. Sci.*, **2005**, 291, 411.
- <sup>131</sup> (a) Z. L. Liu, X. Wang, K. L. Yao, G. H. Du, Q. H. Lu, Z. H. Ding, J. Tao, Q. Ning, X. P. Luo, D. Y. Tian, D. J. Xi, *Mat. Sci.*, **2004**, 39, 2633. (b) H. S. Lee, W. C. Lee, *J. Appl. Phys.*, **1999**, 85, 5231. (c) L. Liz, M. A. L. Quintela, J. Mira, J. Rivas, *J. Mater. Sci.*, **1994**, 29, 3797. (d) V. Chhabra, P. Ayyub, A. N. Maitra, S. Chattopadhyay, *Mater. Lett.*, **1996**, 26, 21. (e) S. Bandow, K. Kimure, K. Kimura, K. Kon-on, A. Kitahara, *Jpn. J. Appl. Phys.*, **1987**, 26, 713.

- <sup>132</sup> (a) R. E. Rosensweig, *Scientific American*, **1992**, 247, 136. (b) Magnetic Fluids and Applications Handbook. B. Berkovski, Begell House: New York, **1996**.
- <sup>133</sup> (a) A. M. Gadalla, H. Yu, *J. Mater. Res.*, **1990**, 5, 1233. (b) T. G. Cattenom, P. Morales, *Mater. Lett.*, **1993**, 18, 151. (c) W. W. Yu, J. C. Falkner, C. T. Yavuz, V. L. Colvin, *Chem. Commun.*, **2004**, 20, 2306.
- <sup>134</sup> S. Franger, P. Berthet, J. Berthon, *J. Solid State Electr.*, **2004**, 8, 218.
- <sup>135</sup> M. Wu, Y. Xiong, Y. Jia, H. Niu, H. Qi, J. Ye, Q. Chen, *Chem. Phys. Lett.*, **2005**, 401, 374.
- <sup>136</sup> P. Berger, N. B. Adelman, K. J. Beckman, D. J. Campbell, A. B. Ellis, G. C. Lisensky, *J. Chem. Edu.*, **1999**, 76, 943.
- <sup>137</sup> (a) B. Karakaya, W. Claussen, K. Gessler, W. Saenger, S. A. D. Schlüter, *J. Am. Chem. Soc.*, **1997**, 119, 3296. (b) W. Stocker, B. Karakaya, B. L. Schürmann, J. P. Rabe, A. D. Schlüter, *J. Am. Chem. Soc.*, **1998**, 120, 7691. (c) Z. S. Bo, J. P. Rabe, A. D. Schlüter, *Angew. Chem. Int. Ed.*, **1999**, 38, 2370.
- <sup>138</sup> Z. N. Bao, K. R. Amundson, A. J. Lovinger, *Macromolecules*, **1998**, 31, 8647.
- <sup>139</sup> T. Sato, D. L. Jiang, T. Aida, *J. Am. Chem. Soc.*, **1999**, 121, 10658.
- <sup>140</sup> (a) A. G. MacDiarmid, *Synth. Met.*, **1997**, 84, 27. (b) R. H. Lee, H. S. Lai, J. J. Wang, R. J. Jeng, J. J. Lin, *Thin Solid Films*, **2008**, 517, 50.
- <sup>141</sup> A. P. H. J. Schenning, R. E. Martin, M. Ito, F. Diederich, C. Boudon, J. P. Gisselbrecht, M. Gross, *Chem. Commun.*, **1998**, 1013.
- <sup>142</sup> T. Kaneko, T. Horie, M. Asano, T. Aoki, E. Oikawa, *Macromolecules*, **1997**, 30, 3118.
- <sup>143</sup> H. Sirringhaus, P. J. Brown, R. H. Friend, M. M. Nielsen, K. Bechgaard, B. M. W. Langeveld-Voss, A. J. H. Spiering, R. A. J. Janssen, E. W. Meijer, P. Herwig, D. M. de Leeuw, *Nature*, **1999**, 401, 685.
- <sup>144</sup> J. F. Morin, M. Leclerc, D. Ades, A. Siove, *Macromol. Rapid Commun.*, **2005**, 26, 761.
- <sup>145</sup> (a) K. Müllen, F. Meghdadi, E. J. W. List, G. Leising, *J. Am. Chem. Soc.*, **2001**, 123, 946. (b) C. H. Chou, C. F. Shu, *Macromolecules*, **2002**, 35, 9673.
- <sup>146</sup> (a) D. W. Lee, T. M. Swager, *Synlett.*, **2004**, 149. (b) H. Korri-Youssoufi, A. Yassar, *Biomacromolecules*, **2001**, 2, 58. (c) A. Satrijo, T. M. Swager, *J. Am. Chem. Soc.*, **2007**, 129, 16020.
- <sup>147</sup> (a) S. Kumaraswamy, T. Bergstedt, X. Shi, F. Rininsland, S. Kushon, W. S. Xia, K. Ley, K. Achyuthan, D. McBranch, D. G. Whitten, *Proc. Natl. Acad. Sci. U.S.A.*, **2004**, 101, 7511. (b) M. R. Pinto, K. S. Schanze, *Proc. Natl. Acad. Sci. U.S.A.*, **2004**, 101, 7505.
- <sup>148</sup> (a) B. Karakaya, W. Claussen, K. Gessler, W. Saenger, S. A. D. Schlüter, *J. Am. Chem. Soc.*, **1997**, 119, 3296. (b) W. Stocker, B. Karakaya, B. L. Schürmann, J. P. Rabe, A. D. Schlüter, *J. Am. Chem. Soc.*, **1998**, 120, 7691. (c) Z. S. Bo, J. P. Rabe, A. D. Schlüter, *Angew. Chem. Int. Ed.*, **1999**, 38, 2370. (d) Z. N. Bao, K. R. Amundson, A. J. Lovinger, *Macromolecules*, **1998**, 31, 8647. (e) T. Sato, D. L. Jiang, T. Aida, *J. Am. Chem. Soc.*, **1999**, 121, 10658. (f) A. P. H. J. Schenning, R. E. Martin, M. Ito, F. Diederich, C. Boudon, J. P. Gisselbrecht, M. Gross, *Chem. Commun.*, **1998**, 1013. (g) T. Kaneko, T. Horie, M. Asano, T. Aoki, E. Oikawa, *Macromolecules*, **1997**, 30, 3118. (h) R. D. McCullough, *Adv. Mater.*, **1998**, 10, 93. (i) J. V. Grazuleviciusa, P. Strohrrieglb, J. Pielichowski, K. Pielichowski, *Prog. Polym. Sci.*, **2003**, 28, 1297.
- <sup>149</sup> (a) M. D. McGehee, A. J. Heeger, *Adv. Mater.*, **2000**, 12, 1655. (b) D. T. McQuade, A. E. Pullen, T. M. Swager, *Chem. Rev.*, **2000**, 100, 2537.
- <sup>150</sup> (a) K. Faid, M. Leclerc, *Chem. Commun.*, **1996**, 2761. (b) C. Y. Yang, P. J. Mauricio, K. Schanze, W. H. Tan, *Angew. Chem. Int. Ed.*, **2005**, 44, 2572.

- <sup>151</sup> (a) K. W. Lee, L. K. Povlich, J. Kim, *Adv. Funct. Mater.*, **2007**, 17, 2580.
- <sup>152</sup> (a) A. O. Patil, Y. Ikenoue, F. Wudl, A. J. Heeger, *J. Am. Chem. Soc.* **1987**, 109, 1858. (b) P. Pickup, *J. Electroanal. Chem.*, **1987**, 225, 273. (c) S. Shi, F. Wudl, *Macromolecules*, **1990**, 23, 2119. (d) T. I. Wallow, B. M. Novak, *J. Am. Chem. Soc.*, **1991**, 113, 7411. (e) A. D. Child, J. R. Reynolds, *Macromolecules*, **1994**, 27, 1975. (f) R. Matthias, S. Arnulf-Dieter, W. Gerhard, *Polymer*, **1989**, 30, 1054. (g) B. Balanda, M. B. Ramey, J. R. Reynolds, *Macromolecules*, **1999**, 32, 3970.
- <sup>153</sup> J. Bieleman, Additives for Coatings, WILEY-VCH, Weinheim, **2000**.
- <sup>154</sup> H. J. Spinelli, *Adv. Mater.*, **1998**, 10, 1215.
- <sup>155</sup> (a) K. H. Kuo, Y. H. Peng, W. Y. Chiu, T. M. Don, *J. Polym. Sci. A: Polym. Chem.*, **2008**, 46, 6185. (b) S. Creutz, R. Jerome, *Langmuir*, **1999**, 15, 7145.
- <sup>156</sup> (a) N. A. D. Burke, H. D. H. Stover, F. P. Dawson, *Chem. Mater.*, **2002**, 14, 4752. (b) Y. Kang, T. A. Taton, *Macromolecules*, **2005**, 38, 6115. (c) M. Nuopponen, H. Tenhu, *Langmuir*, **2007**, 23, 5352. (d) Y. M. Chen, H. C. Lin, R. S. Hsu, B. Z. Hsieh, Y. A. Su, Y. J. Sheng, J. J. Lin, *Chem. Mater.*, **2009**, 21, 4071.
- <sup>157</sup> (a) H. J. Spinelli, H. L. Jakubauskas, P. F. McIntyre, J. G. King, US Patent 6306521B1, **2001**. (b) C. Auschra, A. Muhlebach, E. Eckstein, US Patent 7199177B2, **2007**.
- <sup>158</sup> C. J. Hawker, A. W. Bosman, E. Harth, *Chem. Rev.*, **2001**, 101, 3661.
- <sup>159</sup> G. Moad, E. Rizzardo, S. H. Thang, *Aust. J. Chem.*, **2005**, 58, 379.
- <sup>160</sup> J. Wang, K. Matyjaszewski, *J. Am. Chem. Soc.*, **1995**, 117, 5614.
- <sup>161</sup> X. Yan, F. Liu, Z. Li, G. Liu, *Macromolecules*, **2001**, 34, 9112.
- <sup>162</sup> F. Zeng, Y. Shen, S. Zhu, R. Pelton, *Macromolecules*, **2000**, 33, 1628.
- <sup>163</sup> Z. Chen, H. Cui, K. Hales, Z. Li, K. Qi, D. Pochan, K. Wooley, *J. Am. Chem. Soc.*, **2005**, 127 8592.
- <sup>164</sup> (a) J. Merrington, P. Hodge, S. Yeates, *Macromol. Rapid Commun.*, **2006**, 27, 835. (b) C. Auschra, E. Eckstein, A. Muhlebach, M. Zink, F. Rime, *Prog. Org. Coat.*, **2002**, 45, 83. (c) D. Nguyen, H. S. Zondanos, J. M. Farrugia, A. K. Serelis, C. H. Such, B. S. Hawkett, *Langmuir*, **2008**, 24, 2140.
- <sup>165</sup> Y. F. Lan, New Method of Dispersing Carbon Nanotubes. Master Thesis, National Chung Hsing University, Taichung, Taiwan, **2006**.
- <sup>166</sup> G. L. Hwang, S. J. Tsai, J. J. Lin, Y. F. Lan, New Method of Dispersing Carbon Nanocapsule by Geometric Shape Inhomogeneity Factor. US Patent 7,625,952, **2010**.
- <sup>167</sup> R. S. Hsu, W. H. Chang, J. J. Lin, *ACS Applied Materials & Interfaces*, **2010**, 2, 1349.
- <sup>168</sup> Y. F. Lan, J. J. Lin, Y. C. Hsu New method of dispersing pigments by layered clays. Application No.: USPTO 20090145333, **2009**.
- <sup>169</sup> (a) Y. F. Lan, R. H. Lee, J. J. Lin, *J. Phys. Chem. B*, **2010**, 114, 1897. (b) Y. F. Lan, B. Z. Hsieh, H. C. Lin, Y. A. Su, Y. N. Chan, J. J. Lin, *Langmuir*, **2010**, 26, 10572.
- <sup>170</sup> (a) M. D. Gawryla, L. Liu, J. C. Grunlan, D. A. Schiraldi, *Macromol. Rapid Commun.*, **2009**, 30, 1669. (b) Y. Q. Zhao, K. T. Lau, Z. Wang, Z. C. Wang, H. Y. Cheung, Z. Yang, H. L. Li, *Polymer Composites*, **2009**, 30, 702. (c) L. Liu, J. C. Grunlan, *Adv. Funct. Mater.*, **2007**, 17, 2343.
- <sup>171</sup> V. C. Tung, L. M. Chen, M. J. Allen, J. K. Wassei, K. Nelson, R. B. Kaner, Y. Yang, *Nano Lett.*, **2009**, 9, 1949.
- <sup>172</sup> D. S. Yu, L. Dai, *J. Phys. Chem. Lett.*, **2010**, 1, 467.
- <sup>173</sup> H. Wang, X Xiang, F. Li, *An official publication of the American Institute of Chemical Engineers (AIChE Journal)*, **2010**, 56, 768.
- <sup>174</sup> T. J. Pinnavaia, *Science*, **1983**, 220, 365.

- 
- <sup>175</sup> (a) G. Qi, Y. Yang, H. Yan, L. Guan, Y. Li, X. Qiu, C. Wang, *J. Phys. Chem. C*, **2009**, 113, 204. (b) T. Saito, M. Okamoto, R. Hiroi, M. Yamamoto, T. Shiroy, *Macromol. Mater. Eng.*, **2006**, 291, 1367. (c) L. A. Utracki, M. Sepehr, E. Boccaleri, *Polym. Adv. Technol.*, **2007**, 18, 1. (d) C. W. Chiu, C. C. Chu, S. A. Dai, J. J. Lin, *J. Phys. Chem. C*, **2008**, 112, 17940.
- <sup>176</sup> Y. N. Chan, T. Y. Juang, Y. L. Liao, S. A. Dai, J. J. Lin, *Polymer*, **2008**, 49, 4796.
- <sup>177</sup> (a) V. Rives, M. A. Ulibarri, *Coord. Chem. Rev.*, **1999**, 181, 61. (b) V. Rives, *Mater. Chem. Phys.*, **2002**, 75, 19.
- <sup>178</sup> R. Roto, G. Villemure, *J. Electroanal. Chem.*, **2006**, 588, 140.
- <sup>179</sup> (a) R. H. Lee, H. S. Lai, J. J. Wang, R. J. Jeng, J. J. Lin, *Thin Solid Films*, **2008**, 517, 500. (b) R. H. Lee, G. H. Hsiue, R. J. Jeng, *Polymer*, **1998**, 40, 13.
- <sup>180</sup> C. C. Chu, M. L. Chiang, C. M. Tsai, J. J. Lin, *Macromolecules*, **2005**, 38, 6240.
- <sup>181</sup> (a) N. Grossiord, O. Regev, J. Loos, J. Meuldijk, C. E. Koning, *Anal. Chem.*, **2005**, 77, 5135. (b) J. Yu, N. Grossiord, C. E. Koning, J. Loos, *Carbon*, **2007**, 45, 618.
- <sup>182</sup> (a) D. Baskaran, J. W. Mays, M. S. Bratcher, *Chem. Mater.*, **2005**, 17, 3389.
- <sup>183</sup> G. L. Hwang, S. J. Tsai, J. J. Lin, Y. F. Lan, New Method of Dispersing Carbon Nanocapsule by Geometric Shape Inhomogeneity Factor. US Patent 7,625,952, **2010**.
- <sup>184</sup> R. S. Hsu, W. H. Chang, J. J. Lin, *ACS Applied Materials & Interfaces*, **2010**, 2, 1349.
- <sup>185</sup> R. Traiphol, P. Sanguansat, T. Sriksirin, T. Kerdcharoen, T. Osotchan, *Macromolecules*, **2006**, 39, 1165.
- <sup>186</sup> Y. F. Lan, B. Z. Hsieh, H. C. Lin, Y. A. Su, Y. N. Chan, J. J. Lin, *Langmuir*, **2010**, 26, 10572.
- <sup>187</sup> T. Q. Nguyen, I. B. Martini, J. Liu, B. J. Schwartz, *J. Phys. Chem. B*, **2000**, 104, 237.
- <sup>188</sup> R. B. Grubbs, J. M. Dean, F. S. Bates, *Macromolecules*, **2001**, 34, 8593.
- <sup>189</sup> Fu, S. H.; Fang, K. J. *J. Dispersion Sci. Technol.*, **2006**, 27, 971.